TECHNISCHE UNIVERSITÄT DRESDEN

Aus dem Zentrum für Translationale Knochen-,Gelenk- und Weichgewebeforschung
Direktor: Herr Prof. Dr. Michael Gelinsky

Traditional Chinese Medicine extracts exert angiogenic and protective effects towards human endothelial progenitor cells: from cellular function to molecular pathway

Dissertation

zur Erlangung des akademischen Grades *Doctor of Philosophy (Ph.D.)*

vorgelegt der Medizinischen Fakultät Carl Gustav Carus

der Technischen Universität Dresden

von

Yubo Tang

Born on the 22th of April 1984 in China

Dresden 2014

Thesis Reviewers

Prof. Dr. Michael Gelinsky

Prof. Dr. Klaus-Peter Günther

Head of PhD Committee

Prof. Dr. Richard Funk

Date of Defense: 26.05.2014

Summary

Despite intense research efforts, the repair of large bone defects is still not satisfactory and remains a major challenge in Orthopaedic Surgery. In this context bone tissue engineering has emerged as a promising strategy. However, one of the fundamental principles underlying tissue engineering approaches is that newly formed tissue must maintain sufficient vascularization to support its growth. Thus an active blood vessel network is an essential pre-requisite for scaffold constructs to integrate within existing host tissue. Currently, great efforts are made to address this problem employing transplantation of vascular cells and loading of appropriate biological factors.

Endothelial progenitor cells (EPCs) are a heterogeneous subpopulation of bone marrow mononuclear progenitor cells with potential for differentiation to the endothelial lineage and thus vasculogenic capacity. However, clinical studies reported that with the increase of age, increased susceptibility to apoptosis and accelerated senescence may contribute to the numerical and functional impairments observed in EPCs, which may lead to a reduced angiogenic capacity and an increased risk of vascular disease. Hence attention has increasingly been paid to enhance mobilization and differentiation of EPCs for therapeutic purposes.

A large body of evidence indicates that in Traditional Chinese Medicine (TCM) a plethora of herbs and herbal extracts are effective in the treatment of vascular diseases such as chronic wounds, diabetic retinopathy and rheumatoid arthritis. Thus, it seems rational to explore these medicinal plants as potential sources of novel angiomodulatory factors.

In this thesis we demonstrated that treatment with TCM herbal extracts promote cell growth, cell migration, cell-matrix and capillary-like tube formation of BM-EPCs. Among these TCM extracts, Salidroside (SAL) and Icariin (ICAR) incubation increased VEGF and nitric oxide secretion, which in turn mediated the enhancement of angiogenic differentiation of BM-EPCs. A mechanic evaluation provided evidence that SAL stimulates the phosphorylation of Akt, mammalian target of rapamycin (mTOR) and ribosomal protein S6

kinase (p70S6K), as well as phosphorylated ERK1/2, which is associated with the cell migration and tube formation. Furthermore, a pilot *in vivo* study showed that SAL has the potential to enhance bone formation in a murine femoral critical-size bone defects model.

Another new finding of the present study is that hydrogen peroxide (H_2O_2)-induced cytotoxicity is counteracted by TCM extracts. We found that SAL, Salvianolic acid B (SalB) and ICAR significantly abrogated H_2O_2-induced cell apoptosis, reduced the intracellular level of reactive oxygen species (ROS) and nicotinamide adenine dinucleotide phosphate-oxidase (NADPH) expression, and restored the mitochondrial membrane potential of BM-EPCs. Our data suggest that this protective effect of SalB is mediated by the activation of mTOR, p70S6K, 4EBP1, and by the suppression of MKK3/6-p38 MAPK-ATF2 and ERK1/2 signaling pathways after H_2O_2 stress. In addition, the investigation also demonstrates that ICAR owns the ability to inhibit apoptotic and autophagic programmed cell death via restoring the loss of mTOR and attenuation of ATF2 activity upon oxidative stress.

Based on the outcomes of the present work, we propose SAL, SalB and ICAR as novel proanigiogenic and cytoprotective therapeutic agents with potential applications in the fields of systemic and site-specific tissue regeneration including ischaemic disease and extended musculoskeletal tissue defects.

Trotz intensiver Forschung stellt die Behandlung von großen Knochendefekten die regenerative Medizin vor eine große Herausforderung. Zahlreiche Knochenersatzmaterialien sowie Methoden zur Regeneration von Knochengewebe durch Tissue Engineering haben sich in der Praxis als wirksame Strategie herausgebildet. Um größere Knochendefekte langfristig erfolgreich durch regenerierbare Implantate ersetzen zu können, muss neu gebildetes Gewebe jedoch ausreichend durch ein Gefäß-/ Kapillarnetz vaskularisiert werden, um eine ausreichende Versorgung des Gewebes zu gewährleisten. Daher wird die Entwicklung vaskularisierter Knochenimplantate als ein aussichtsreicher Ansatz für den Ersatz großer Knochendefekte angesehen. Die Transplantation von Gefäßzellen in Kombination mit Faktoren die die Knochenregeneration stimulieren, stellt ein vielversprechendes Konzept dar.

Endotheliale Vorläuferzellen (EPCs) sind eine heterogene Subpopulation von mononukleären Vorläuferzellen aus dem Knochenmark mit dem Potenzial zur Differenzierung in die endotheliale Linie. Klinische Studien zeigten, dass mit der Zunahme des Alters, eine erhöhte Anfälligkeit für programmierten Zelltod (Apoptose) und eine beschleunigte Alterung im Zusammenhang mit in EPCs beobachteten numerischen und funktionalen Störungen steht. Dies führt zu einer verminderten angiogenen Kapazität und kann zu einem erhöhten Risiko von Gefäßkrankheit beitragen. Daher hat sich die verstärkte Aufmerksamkeit bezahlt gemacht, die Mobilisierung und Differenzierung von EPCs für therapeutische Zwecke zu verbessern.

Eine große Anzahl von Studien hat gezeigt, dass sich in der traditionellen chinesischen Medizin (TCM) eine Vielzahl von Kräutern und Kräuterextrakten bei der Behandlung von vaskulären Erkrankungen, wie chronischen Wunden, diabetischer Retinopathie und rheumatoider Arthritis bewährt haben. Diese Heilpflanzen als potentielle Quellen für neuartige angiomodulatorische Faktoren zu erforschen, stellt ein innovatives Konzept dar.

In dieser Arbeit wurde gezeigt, dass die Behandlung mit TCM das Zellwachstum, die Zellmigration, eine Zell-Matrix-und Kapillar-ähnlichen Gefäßverzweigungen von EPCs

fördert. Eine Inkubation mit Salidrosid (SAL) und Icariin (ICAR) erhöhte die Vascular Endothelial Growth Factor (VEGF)- und Stickoxid-Sekretion, das wiederum eine Verstärkung der angiogenen Differenzierung von EPCs vermittelte. Mechanische Untersuchungen belegten, dass SAL die Phosphorylierung der Proteinkinase B (Akt), dem Zielgen von Rapamycin (mTOR) und der ribosomalen Protein S6 Kinase (p70S6K) sowie der mitogen-aktivierten Proteinkinasen ERK1/ 2 stimulierte. Darüber hinaus zeigten erste *in-vivo*-Experimente, dass SAL deutlich die Knochenbildung in kritischen Knochendefekten von immundefizienten Mäusen steigerte.

Eine weitere neue Erkenntnis der vorliegenden Studie ist, dass Wasserstoffperoxid (H_2O_2) -induzierter Zytotoxizität durch TCM entgegengewirkt werden kann. SAL, Salvianolsäure B (SalB) und ICAR minimierten signifikant die H_2O_2 -induzierte Apoptose, reduzierten die Bildung intrazellulärer reaktiver Sauerstoffspezies (ROS) und die Expression von Nicotinamidadenindinucleotidphosphat-Oxidase (NADPH) in EPCs. Die Ergebnisse belegen, dass die protektive Wirkung von SalB durch die Aktivierung von mTOR, p70S6K, 4EBP1 und durch die Unterdrückung der MKK3/6-p38 MAPK - ATF2 und ERK1/2 Signalwege nach H_2O_2 Stress vermittelt wird. Die Untersuchungen zeigten des Weiteren, dass ICAR die Fähigkeit besitzt apoptotisch und autophagisch induzierten programmierten Zelltod zu inhibieren, indem es den Verlust von mTOR ausgleicht und eine ATF2 Aktivität, induziert durch oxidativem Stress, minimiert.

Basierend auf den Ergebnissen der vorliegenden Studie etablierten sich SAL, SalB und ICAR als neuartige proangiogene und zellschützende therapeutische Mittel. Möglichen Anwendungen könnten sich in den Bereichen der systemischen und ortsspezifischen Geweberegeneration einschließlich ischämischer Erkrankungen und Muskel-Skelett ausgedehnten Gewebedefekten finden.

Table of contents

List of figures and tables

Table 1. List of antibodies.

Table 2. The expression pattern of cell surface markers of CD133, CD34, KDR, VE-Cadherin, E-selectin and vWF was determined by flow cytometry at 7 d and 14 d culture.

SAL Salidroside

SalB Salvianolic acid B

ICAR Icariin

PUER Puerarin

BM-EPCs bone marrow derived-endothelial progenitor cells

ECs endothelial cells

ROS reactive oxygen species

NADPH oxidase nicotinamide adenine dinucleotide phosphate-oxidase

MMP mitochondrial membrane potential

mTOR mammalian target of rapamycin

p70S6K ribosomal protein S6 kinase

MKK 3/6 mitogen activated protein kinase kinase 3/6

MAPK mitogen activated protein kinase

SAPK/JNK stress-activated protein kinase/Jun-amino-terminal kinase

ATF2 activating transcription factor 2

4EBP1 eukaryotic translation Initiation Factor 4E Binding Protein 1

PARP Poly (ADP-ribose) polymerase

DPI diphenyleneiodonium

DHE **d**ihydroethidium

L-NAME N^G-nitro-L- arginine methyl ester.

DCF Dichloro-dihydro-fluorescein

3-MA 3-methy-ladenine

NO nitric oxide

LDH lactate dehydrogenase

VEGF vascular endothelial growth factor

bFGF basic fibroblast growth factor

KDR Kinase insert domain receptor

VE-cadherin vascular endothelial cadherin

vWF von Willebrand factor

PECAM-1 Platelet endothelial cell adhesion molecule

Nox4 NADPH oxidase 4

STAT-3 signal transduction and activators of transcription-3

eNOS Endothelial nitric oxide synthase 3

GAPDH glyceraldehyde-3-phosphate dehydrogenase

1. INTRODUCTION

1.1 Current concepts and future directions for repair of bone defect

Bone regeneration is a complex, well-orchestrated biological process that comprised of a series of events of bone induction and conduction, involving a number of cell types, intracellular and extracellular molecular-signaling pathways, with a definable temporal and spatial sequence, in an effort to optimize skeletal repair and restore skeletal function (Cho et al., 2002; Einhorn, 1998). Multiple factors regulate this cascade of events by affecting different sites in the osteoblast and chondroblast lineage through various processes such as migration, proliferation, chemotaxis, differentiation, inhibition, and extracellular protein synthesis (Colnot et al., 2005).

Bone possesses the intrinsic regeneration capacity as part of the repair process in response to injury, during skeletal development or continuous remodeling throughout adult life (Dimitriou et al., 2011). However, there are complex clinical conditions requires bone regeneration in large quantity, such as for skeletal reconstruction of large bone defects created by trauma, infection, tumor resection and congenital malformation, or cases in which the regenerative process is compromised, including avascular necrosis, atrophic non-unions and osteoporosis (Dimitriou et al., 2011; Jimi et al., 2012).

At present, the gold standard for the reconstruction of large bone defects is the use of autogenous bone grafts. While autogenous bone graft is the most effective clinical method, surgical stress to the part of the bone being extracted and the quantity of extractable bone limit this method. One alternative to autograft is allograft, whose surfaces support bone formation and allow structural restoration of the skeleton. However, allograft bone lacks viable osteoprogenitor cells and has low levels of growth factors.

With the ongoing research in all related fields, treatment strategies should aim to address all prerequisites for optimal bone healing, including osteoconductive matrices,

osteoinductive factors, osteogenic cells and mechanical stability, following the ‘diamond concept’ suggested for fracture healing (Giannoudis et al., 2007).

1.2 The role of angiogenesis in bone healing

Angiogenesis is the formation of new blood vessels occurring in an adult through migration and proliferation of endothelial cells (ECs), and tubular structures formation, which plays a role in many physiological processes (i.e. remodeling of ischemic muscle, wound healing, fracture repair) as well as in pathological process such as rheumathoid arthritis and metastases (Albrecht-Schgoer et al., 2012; Harris et al., 2013; Mobasheri, 2013). Intravital microscopy and angiographic analysis in bone chamber models indicate that angiogenesis temporally precedes osteogenesis, as predicted by Trueta’s early work (Trueta and Buhr, 1963). In bone, vasculature is essential for cartilage resorption and angiogenesis temporally precedes osteogenesis: the origin of bone is the artery carrying calcium and phosphate ions. Osteogenesis takes place near newly formed vessels that mediate delivery of osteoprogenitor cells, secrete mitogens for osteoblasts, and transport nutrients and oxygen. Inadequate or inappropriate bone vascularity is associated with decreased bone formation and bone mass. Risk factors for impaired bone healing include: poor blood supply, poor apposition of fractured bone ends, interposition of soft tissues or necrotic bone between bone fragments, inadequate immobilization, infection, drug use (e.g. corticosteroid therapy or nicotine), advanced age, and systemic disorders, such as diabetes or poor nutrition (Einhorn, 1995). Negative effects on the vascular system might be the mechanism whereby many other risk factors delay or impair bone healing (Glowacki, 1998).

In the mature established vasculature, the endothelium plays a pivotal role in the maintenance of homeostasis of the surrounding tissue providing the communicative network to neighbouring tissues to respond to requirements as needed. Furthermore, the vasculature provides the necessary factors such as growth factors, hormones, cytokines, chemokines and metabolites needed by the surrounding tissue and acts, when needed, as a barrier to limit the

movement of molecules and cells. A fully functional vascular network within bone-engineered constructs is crucial and remains a major challenge in bone tissue engineering (Grellier et al., 2009). After a bone construct is implanted *in vivo*, induction of initial vascularization is important: in particular, the survival of osteogenic cells in the interior of the scaffold is often threatened by the limited extent of initial vascularization (Kneser et al., 1999; Kneser et al., 2006). The implanted construct requires ongoing vascularization to ensure survival and integration, since it takes weeks for the host's blood circulation to establish sufficient supply to the implant (Jain, 2003; Kaigler et al., 2006; McCarthy, 2006). Several strategies have been proposed to address this problem. For example, the addition of vascular cells such as ECs might offer several advantages over seeding of osteogenic cells alone (Unger et al., 2007).

However, as the bone development and remodeling depend on complex interactions between bone-forming osteoblasts and other cells present within the bone microenvironment, particularly ECs that may be pivotal members of a complex interactive network acted on bone, the mode of communication between the bone cells and vascular cells, at the molecular level, has yet to be fully elucidated.

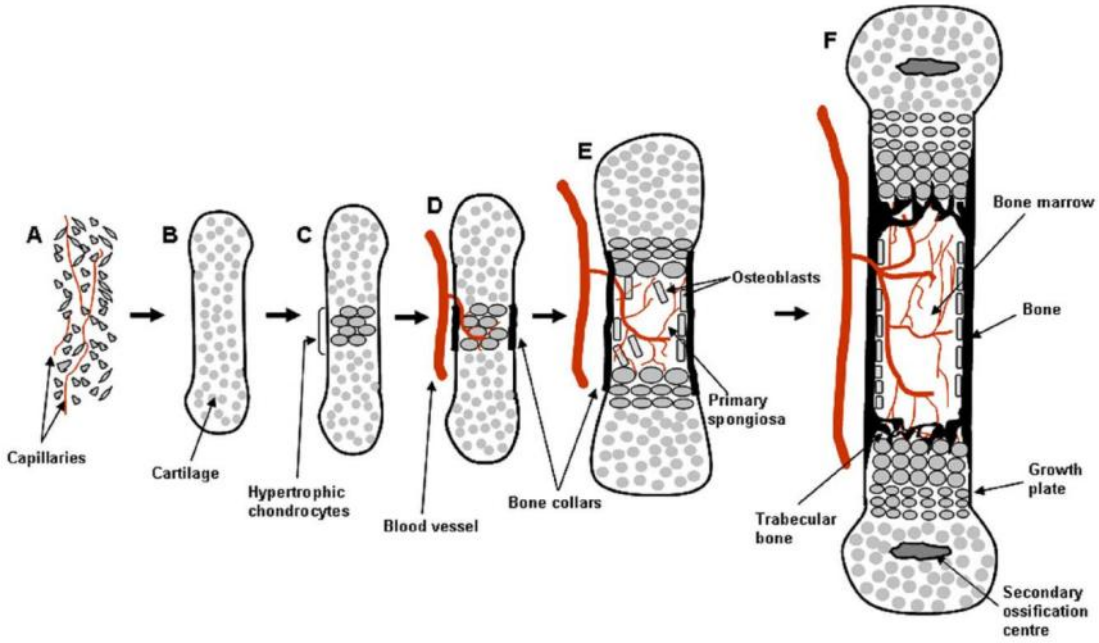

Figure 1. A schematic diagram of endochondral bone formation. (A) Mesenchymal cells condense and (B) differentiate into chondrocytes forming an avascular cartilage model of the future bone. (C) At the centre of condensation the chondrocytes cease proliferating and become hypertrophic. (D) Perichondral cells adjacent to the hypertrophic chondrocytes differentiate into osteoblasts forming a bone collar. The hypertrophic cartilage regulates the formation of mineralised matrix; the release of angiogenic factors to attract blood vessels and undergoes apoptosis. (E) The coordination of osteoblasts and vascular invasion form the primary spongiosa. The chondrocytes continue to proliferate with concomitant vascularization resulting in a coordinated process that lengthens the bone. Osteoblasts of the bone collar will eventually form cortical bone; while osteoblasts precursors located in the primary spongiosa will eventually form trabecular bone. (F) At the ends of the bone, secondary ossification centres develop through cycles of chondrocyte hypertrophy, vascular invasion and osteoblast activity. Columns of proliferating chondrocytes form in the growth plate beneath the secondary ossification centre. Finally, expansion of stromal cells and hematopoietic marrow starts to take place in the marrow space (Adapted from Kronenberg, 2003 and Horton, 1990).

1.3 Bone regeneration induced by angiogenic factors

With improved understanding of fracture healing and bone regeneration at the molecular level, a number of key molecules that regulate this complex physiological process have been identified, and are already in clinical use or under investigation to enhance bone repair.

1.3.1 Vascular endothelial growth factor

Previous studies have shown that endogenous VEGF is important for endochondral bone formation (Gerber et al., 1999; Haigh et al., 2000; Zelzer et al., 2002). VEGF is expressed before blood vessels are detected in developing mouse bones, and this expression is tightly associated with cells involved in bone formation (osteoblasts) (Zelzer et al., 2002). Inhibition of VEGF leads to expansion of the hypertrophic zone, loss of metaphyseal blood vessels and impaired trabecular bone formation in developing mice (Gerber et al., 1999; Haigh et al., 2000) and monkeys (Ryan, 1999). Thus, during development, VEGF is essential for blood vessel invasion of hyaline cartilage, growth late morphogenesis, and cartilage remodeling.

It has been shown that both osteoblasts and hypertrophic chondrocytes express high levels of VEGF, thereby promoting the invasion of blood vessels and transforming the avascular cartilaginous matrix into a vascularized osseous tissue (Keramaris et al., 2008). VEGF promotes both vasculogenesis, i.e. aggregation and proliferation of mesenchymal stem cells (MSCs) into a vascular plexus, and angiogenesis, i.e. growth of new vessels from already existing ones (Kanczler and Oreffo, 2008; Street et al., 2002). Hence, VEGF plays a crucial role in the neoangiogenesis and revascularization at the fracture site.

Given the importance of VEGF in normal bone repair, treatment with exogenous VEGF might be expected to promote angiogenesis and bone formation after injury- a hypothesis that is supported by several studies. Local administration of exogenous VEGF, in

the absence of a scaffold or progenitor cells, enhances bone formation in mouse femur fractures and rabbit radial critical-sized defects (Street et al., 2002).

1.3.2 The transforming growth factor superfamily

This superfamily includes most factors known to induce cartilage and bone formation during development, including TGF-βs, BMPs, growth and differentiation factors (GDFs) and activins. By virtue of shared receptors and structural homology, many of the members of this large family have overlapping activities, including stimulation of mesenchymal stem cell differentiation into chondrocytes or osteoblasts. However, their distinct expression pattern during bone repair, the developmental phenotypes observed when the genes are mutated or deleted and their activities when added exogenously in animal models or humans suggest subtly distinct roles in the process of bone repair.

Transforming growth factor-β

TGF-β, the prototypical member of this superfamily, is one of the most abundant cytokines present in bone matrix and exerts a dual role on osteoblastic bone formation. TGF-β stimulates early osteoblast differentiation by promoting recruitment and proliferation of osteoblast precursors and the expression of matrix proteins; on the other hand, it inhibits late osteoblast differentiation and mineralization (Alliston et al., 2001; Janssens et al., 2005; Maeda et al., 2004; Tang et al., 2009). TGF-β is a potent chemotactic stimulator of mesenchymal stem cells (MSCs) and it enhances proliferation of MSCs, preosteoblasts, chondrocytes and osteoblasts (Lieberman et al., 2002). It also induces the production of extracellular proteins such as collagen, proteoglycans, osteopontin, osteonectin, and alkaline phosphatase (Sandberg et al., 1993). Its main role is thought to be during mchondrogenesis and endochondral bone formation (Barnes et al., 1999). TGF-β may also initiate signaling for BMP synthesis by the osteoprogenitor cells, while it may inhibit osteoclastic activation and promote osteoclasts apoptosis (Mundy, 1996).

Bone morphogenetic proteins

Several BMPs have been found to induce ectopic bone, due, at least partly, to stimulation of mesenchymal and osteoprogenitor cell proliferation and differentiation (Barnes et al., 1999; Reddi, 2001). Early pre-clinical studies indicated that BMP-2 stimulates bone formation in critical size defects, fractures and spinal fusions (Egermann et al., 2006). In a rabbit ulna model, BMP-2 in a collagen sponge accelerates repair (Bouxsein et al., 2001) and overcomes the inhibitory effects of chronic glucocorticoid therapy on bone repair (Luppen et al., 2002). In rabbit tibial fractures, BMP-2 accelerates repair only in non-stable fractures, not in stable fractures (Bax et al., 1999). Injection of BMP-2 locally over the surface of calvariae of mice induces periosteal bone formation without a prior cartilage phase (Chen et al., 1997).

1.3.3 Fibroblast growth factor

Fibroblast Growth Factors (FGFs) belong to a family of polypeptides that regulate several important cellular processes. FGFs bind to high affinity FGF receptors (FGFR), leading to FGFR dimerization, phosphorylation of intrinsic tyrosine residues and activation of several signal transduction pathways (Beenken and Mohammadi, 2009). In the skeleton, FGF/FGFR signaling is an important regulator of prenatal and postnatal skeletal development. Cellular and genetic studies in mice and humans have revealed that FGFs control chondrogenesis and osteoblastogenesis by modulating the recruitment and activity of chondroblasts and cells of the osteoblast lineage (Dailey et al., 2005; Marie, 2003; Ornitz, 2005). During bone healing, FGFs are synthesized by monocytes, macrophages, mesenchymal cells, osteoblasts and chondrocyte. FGFs are identified during the early stages of fracture healing and they play a critical role in angiogenesis and MSC mitogenesis. α-FGF mainly effects chondrocyte proliferation and is probably important for chondrocyte maturation, whilst ß-FGF is expressed by osteoblasts and is generally more potent than

α-FGF (Lieberman et al., 2002). In a canine tibial osteotomy model, a single injection of FGF-2 was associated with an early increase in callus size (Nakamura et al., 1998).

1.4 Angiogenic potential of endothelial progenitor cells

In the early embryo, mesodermal stem cells in the bone marrow (BM) differentiate to form haemangioblasts, the common precursor of haematopoietic stem cells and endothelial-lineage angioblasts (Adams and Alitalo, 2007; Sirker et al., 2009). During vasculogenesis these immature but lineage-committed angioblasts, termed endothelial progenitor cells (EPCs), migrate and congregate into clusters, called blood islands, forming the primary vascular plexus from which a complex microcirculation arises (Paleolog, 2005; Risau, 1997). In contrast, adult vascular growth occurs primarily through angiogenesis whereby new capillaries develop endogenously from fully-differentiated endothelial cells (ECs) within existing vessels. Circulating EPCs share phenotypic characteristics with embryonic EPC (Hristov and Weber, 2004) and incorporate into sites of neovascularisation, suggesting a role for EPCs in angiogenic renewal (Iwami et al., 2004; Zhang et al., 2006a). *In vitro*, EPCs differentiated into endothelial lineage cells, and in animal models of ischemia, heterologous, homologous, and autologous EPCs were shown to incorporate into sites of active neovascularization. This finding was followed by diverse identifications of EPCs by several groups (Gunsilius et al., 2001; Lin et al., 2000; Peichev et al., 2000) using equivalent or different methodologies. Recently, similar studies with EPCs isolated from human cord blood have demonstrated their analogous differentiation into ECs *in vitro* and *in vivo* (Murohara et al., 2000; Nieda et al., 1997). These findings, together with other recent studies, are consistent with the notion of postnatal "vasculogenesis", which is de novo vessel formation by in situ incorporation, differentiation, migration, and/or proliferation of BM-derived EPCs.

EPCs express endothelial-specific markers, including VEGF, vascular endothelial growth factor receptor 2 (VEGFR2), PECAM-1 (CD31), CD133, VE-cadherin, E-selectin and von Willebrand factor (vWF), which have various roles in cell-cell adhesion, vascular permeability and the modulation of other cellular responses during angiogenesis (Asahara et al., 1997; Michaud et al., 2006). Indeed, EPCs are implicated in angiogenesis stimulated by conditions such as coronary artery disease and myocardial infarction, confirmed by clinical observations of EPC mobilisation in such patients and incorporation into foci of pathological neovascularisation (Ding et al., 2007; Kawamoto and Asahara, 2007).

Several studies have demonstrated that bone marrow-derived EPCs (BM-EPCs) functionally contribute to vasculogenesis during wound healing (Gill et al., 2001), limb ischemia (Iwaguro et al., 2002; Kalka et al., 2000), postmyocardial infarction (Edelberg et al., 2002; Shintani et al., 2001), endothelialization of vascular grafts (Bhattacharya et al., 2000; Gill et al., 2001; Shi et al., 1998), or physiological cyclic organogenesis of endometrium (Asahara et al., 1999) under the influence of appropriate cytokines, growth factors and/or hormones through the autocrine, paracrine, and/or endocrine systems.

Chemical stimuli may, at least in part, drive the response of EPCs during angiogenesis. These stimuli can be released from surrounding tissues, i.e. from within the microenvironment, or from the endothelial cells themselves. Indeed, it has been shown in hypoxic wounds of diabetic patients that EPCs in the BM respond by following chemokine gradients, resulting in their homing to sites of hypoxia where they can participate in neovascularisation (Gallagher et al., 2007). Consequently, the microenvironment in which progenitor cells are cultured is critical to their ability to maintain their progenitor status, i.e. to self-renew and give rise to differentiated cell types as and when recruited to do so.

Nevertheless, current approaches to angiogenic therapies are problematic. Endogenous approaches most likely rely on the recruitment of circulating EPCs, and the delivery of a single pro-angiogenic substance is insufficient to elicit the complete and prolonged response necessary for effective angiogenesis (Milkiewicz et al., 2006; Williams et al., 2006).

Exogenous therapies involve administration of allogeneic donor EPCs, which with poor HLA matching leads to increased immune rejection resulting in reduced transplantation efficiency (Garmy-Susini and Varner, 2005; Shantsila et al., 2007). Furthermore, clinical studies reported that with the increase of age, increased susceptibility to apoptosis and accelerated senescence may contribute to the numerical and functional impairments observed in EPCs (Hoetzer et al., 2007; Kushner et al., 2009), which ultimately lead to the increased risk of vascular diseases and the prolonged and often complicated recovery from acute vascular events (Dimmeler and Zeiher, 2004; Scheubel et al., 2003). What's more, the reduced levels of EPCs and functional impairment of endothelium are often indicated in patients with diabetes and cardiovascular disease (De Vriese et al., 2000; Vasa et al., 2001). Therefore, attention has increasingly been paid to enhance mobilization and differentiation of EPCs.

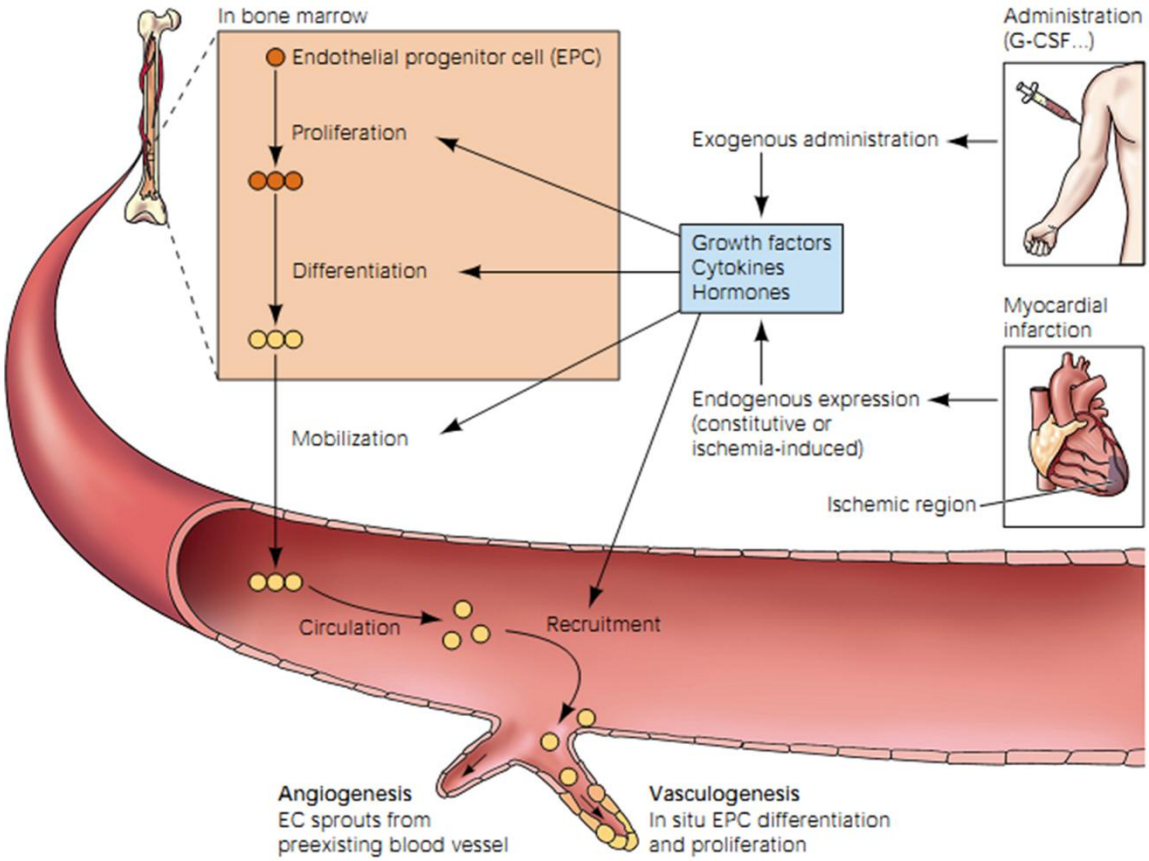

Figure 2. Kinetics of endothelial progenitor cells for neovascularization. Endothelial progenitor cells (EPCs) circulate in adult human peripheral blood and are mobilized from bone marrow by cytokines, growth factors, and ischemic conditions. Vascular injury is repaired by both angiogenesis and vasculogenesis mechanisms. Circulating EPCs contribute to repair of injured blood vessels mainly via a vasculogenesis mechanism. (Adapted from Murasawa, 2005).

1.5 Interaction of endothelium and bone

In the context of the intricate relationship between angiogenesis and osteogenesis, communication between MSC and EC is one of the most important cellular interactions that orchestrates bone formation (Brandi and Collin-Osdoby, 2006; Carano and Filvaroff, 2003). Several mechanisms are involved: interaction between membrane molecules of two adjacent cells (adherens and tight junctions); gap junction communications which form direct cytoplasmic connections; and secretion of diffusible factors from cells, or from the extracellular matrix (Grellier et al., 2009). It has been demonstrated that ECs co-cultured with MSCs are able to establish microcapillary-like structures in a three dimensional spheroids (Rouwkema et al., 2006). Previous studies indicated that ECs could effect certain levels of osteogenesis, releasing bone morphogenetic proteins (Kaigler et al., 2005) and controlling the transcription factor Osterix for bone cell differentiation (Klinkner et al., 2006).

The intercellular signaling pathways of ECs have also been implicated in the functions of the osteoclastic lineage. For the recruitment of osteoclasts to areas of bone resorption, osteoclast precursors need to adhere and migrate through the endothelium in a tightly regulated mechanism similar to that of the systematic process of transendothelial migration of leukocytes and monocytes (Imhof and Dunon, 1997). It has been hypothesized that the endothelium may direct osteoclast precursor to specific areas of bone to help tightly control the resorptive process (Parfitt, 2000). Therefore, alterations in the micro-vascular supply network will ultimately affect the tightly regulated resorption sequence resulting in

decreases in bone formation, regeneration and repair as well as altered osteointegration of orthopaedic and dental implants (Burkhardt et al., 1987; Glowacki, 1998).

Bone ECs display their own distinctive characteristics, with a capacity to respond to bone regulators such as cytokines, estrogen and PTH (Streeten and Brandi, 1990; Streeten et al., 1989). In addition, bone endothelial cells secrete high levels of hormone B-type Natriuretic peptide (Bordenave et al., 2002) and express stromal cell-derived factor-1 (SDF-1) (Imai et al., 1999).

VEGF lead to an upregulation of BMP-2 in microvascular endothelial cells (Bouletreau et al., 2002) demonstrating the intricate signaling pathways affecting the interactive relationship of endothelial cells and cells of the osteoblastic lineage. The *in vivo* overexpression of HIF-1α showed striking and progressive increases in bone volume, and the amount of bone in the axial skeleton was directly proportional to the amount of skeletal vasculature (Wang et al., 2007). This study has established that the upregulation of HIF-1α and VEGF in osteoblasts specifically promoted bone formation secondarily to angiogenesis, clarifying the importance of osteoblast-derived VEGF in the coupling of angiogenesis to osteogenesis. Moreover, hypoxia lead to an upregulation of BMP-2 in microvascular endothelial cells (Bouletreau et al., 2002) demonstrating the intricate signaling pathways affecting the interactive relationship of endothelial cells and cells of the osteoblastic lineage.

1.6 Endothelial death due to oxidative stress

The endothelium is located between the blood stream and the vessel wall which is the largest organ in the body. The endothelium regulates vascular homoeostasis through local elaboration of mediators that modulate vascular tonus and growth, as well as platelet adhesion, inflammation, fibrinolysis (Vane et al., 1990). The endothelium regulates vascular homoeostasis through local elaboration of mediators that modulate vascular tonus and growth, as well as platelet adhesion, inflammation, fibrinolysis (Vane et al., 1990). Vascular

endothelial cells normally perform several key homeostatic functions such as keeping blood fluid, regulating blood flow thereby modulating tissue macromolecule and fluid exchange. Endothelial dysfunction was first characterized in humans in 1986 by Ludmer et al, who demonstrated that atherosclerotic coronary arteries contracted in response to intracoronary infusion of acetylcholine, while normal coronaries showed dilatation (Ludmer et al., 1986). Endothelial dysfunction is frequently present in common chronic degenerative disorders, such as diabetes, hypertension and coronary artery disease (Brunner et al., 2005). The initial state of endothelial dysfunction is also considered as an early stage of atherosclerosis, finally leading to clinical manifestations like coronary artery disease. Multiple risk factors can cause endothelial injury or death including oxidative (Yamada et al., 2010), endoplasmic reticulum (Kim et al., 2007; Matsushita et al., 2011), and genotoxic stress (Basuroy et al., 2013), as well as activated pathways of injury mediated by the innate and adaptive immune systems.

Interestingly, vascular endothelium is specifically sensitive to oxidative stress, and this is one of the mechanisms that causes endothelial dysfunction in frequent cardiovascular diseases and disorders, including atherosclerosis and acute coronary syndromes (Anderson et al., 1995; Libby, 2001). Notably, both the endothelium and the outer adventitial layer themselves initiate potent oxidative stress reactions in case of injury (Sorescu et al., 2002).The mechanisms by which oxidative stress mediates alterations in vascular cell function are complex. Oxidative stress increases vascular endothelial permeability and promotes inflammatory response - a condition that is coupled with alterations in endothelial signal transduction and redox-regulated transcription factors (Beswick et al., 2001; Lee et al., 2004; Orr et al., 2007). In addition, there is growing pathophysiological evidence that overproduction and accumulation of reactive oxygen species (ROS) leads to cell injury mediated by specific cellular macromolecules (lipids, proteins, and nucleic acids) that activate proatherogenic mechanisms (Fleury et al., 2002; Venkatesh et al., 2009). Oxidative stress-induced apoptosis is suggested to be dependent on mitochondrial dysfunction including mitochondrial derived-ROS. Thus, antioxidant therapy can be effective in

preventing oxidative stress-induced cell injury. However, the limited success of currently available antioxidant therapeutic agents (e.g. metalloporphyrins and catalytic antioxidants) expedites the development of innovative drugs.

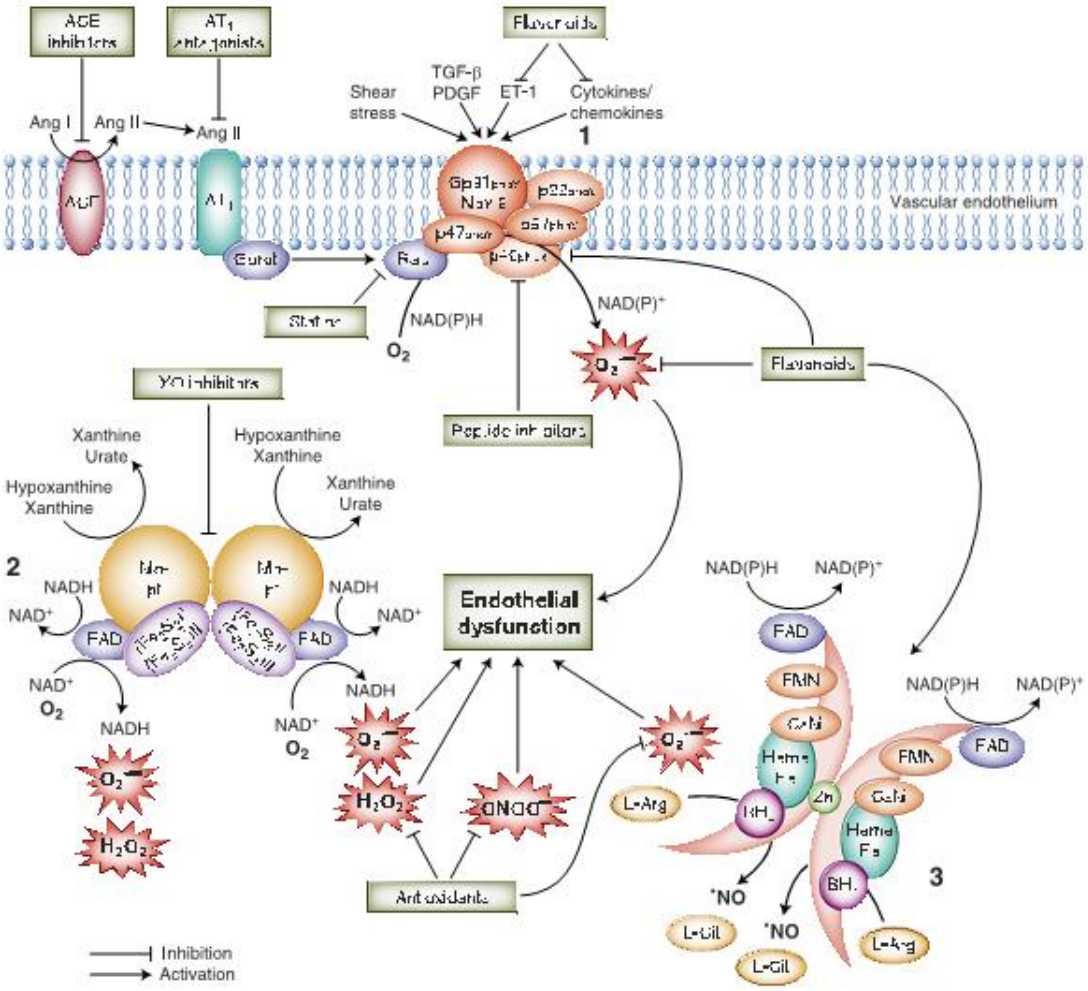

Figure 3. Molecular sources of vascular oxidative stress and pharmacologic intervention strategies. Vascular enzymes such as NADPH oxidase 2 (1), xanthine oxidase (2), and uncoupled endothelial nitric oxide synthase (3) can promote the production of reactive oxygen species (ROS) considerably. Eventually, these processes contribute to the development of endothelial dysfunction and vascular damage. Established and novel cardiovascular drugs, as well as dietary flavonoids, can attenuate cellular ROS concentrations via direct or indirect mechanisms. ACE: angiotensin-converting enzyme; Ang: angiotensin; AT1: Ang II type 1; CaM: calmodulin; ET-1: endothelin 1; FAD: flavindenine dinucleotide;

FMN: flavinmononucleotide; L-Arg: L-arginine; L-Cit: L-citrulline; PDGF: platelet -derived growth factor; TGF-β: transforming growth factor-β. (Adapted from Weseler, 2010)

1.7 ROS, antioxidant and signaling

Reactive oxygen species (ROS), a heterogeneous population of biologically active intermediates, are generated as by-products of the aerobic metabolism and exhibit a dual role in biology. When produced in controlled conditions and in small amount, ROS may function as signaling intermediates, contributing to critical cellular functions such as proliferation, differentiation, and cell growth. However, ROS overproduction and, particularly, the formation of specific reactive species, inflicts cell death and tissue damage by targeting vital cellular components such as DNA, lipids, and proteins, thus arising as key players in disease pathogenesis.

The most potent pathway for generating ROS is catalyzed by the phagocyte oxidase (Phox) complex, which is expressed by neutrophils and macrophages. In addition to Phox, ECs also express homologous nonphagocyte NADPD-dependent oxidase (Nox) complexes. Rather than contribute to EC barrier function and vascular remodeling (Rhee et al., 2000), endogenous Nox enzymes have also been considered to cause EC dysfunction in the pathogenesis of hypertension, atherosclerosis, cardiac hypertrophy, and heart failure (Keaney, 2005). Increasing evidence supports the idea that ROS generated from mitochondria significantly contribute to EC dysfunction and the progression of atherosclerosis (Nishikawa et al., 2000).

The maintenance of intracellular redox homeostasis is dependent on a complex web of antioxidant molecules. These antioxidants include low molecular weight molecules such as glutathione, present in millimolar concentrations within cells, as well as an array of protein antioxidants that each has specific subcellular localizations and chemical reactivities. One important and emerging theme is that antioxidant proteins are not merely passive disposers

of intracellular oxidants but rather active participants in redox signaling. One of the earliest descriptions of this trend emerged from the interaction between thioredoxin (Trx) and the apoptosis signal-regulating kinase (ASK-1) (Saitoh et al., 1998). It had been previously known that agents such as TNF that activate ASK1 also stimulate ROS production. The link between ROS production and the subsequent activation of ASK1-dependent signaling appears to involve a redox-dependent interaction between ASK1 and Trx (Yamamoto et al., 2003).

Vascular cell dysfunction can be caused by dysbalance between mitogen activated protein kinase (MAPK) signaling and the redox state of vascular ECs. Different members of the MAPK family, such as extracellular signal-regulated kinases (ERKs), c-Jun N-terminal kinases (JNKs), and p38 mitogen-activated protein kinases (p38 MAPK) play important roles in the coordination of ROS-induced cellular stress responses (Matsuzawa and Ichijo, 2008). Both duration and magnitude of toxicant exposure is suggested to be proportional to the state of MAPK activation thereby being determinative for the cell's fate (Dickinson et al., 2002). As ROS are generated mainly as byproducts of mitochondrial respiration, mitochondria are thought to be the primary target of oxidative damage. Increasing evidence indicates that mitochondrial damage and dysfunction contribute to the pathological processes underlying the vascular disease (Ballinger et al., 2002; Knight-Lozano et al., 2002; Mercer et al., 2010). Mitochondrial dysfunction may lead to the activation of a series of caspases, and the subsequent events of apoptosis, e.g. the cleavage of poly (ADP-ribose) polymerase (PARP), a downstream substrate of activated caspases, protects DNA from oxidative damage. Dysregulation of any of these phenotypes in human ECs alters cell function thereby predisposing to vascular pathology.

ROS are also known to affect proteins, such as NF-κB, Akt, ERK, CREB, and the EGF-receptor, in a manner which is thought to have a positive role in cell survival or proliferation (Bowie and O'Neill, 2000; Fantz et al., 2001; Huang et al., 2001; Salsman et al., 2001; Suzaki et al., 2002). If damage to DNA or other cellular constituents is too great to repair, organisms have evolved mechanisms to promote apoptosis.

1.8 ROS regulate autophagy

Autophagy is a self-digesting mechanism responsible for removal of long-lived proteins, damaged organelles, and malformed proteins during biosynthesis by lysosome (Baehrecke, 2005; Kondo et al., 2005). A body of evidence demonstrates that autophagic process is meant for regulating diverse cellular functions including growth, differentiation, response to nutrient deficit and oxidative stress, cell death, and macromolecule and organelle turnover (Klionsky et al., 2005; Massey et al., 2004).

Autophagy begins with an isolation membrane, also known as a phagophore that is likely derived from lipid bilayer contributed by the endoplasmic reticulum (ER) and/or the trans-Golgi and endosomes (Axe et al., 2008; Simonsen and Tooze, 2009), although the exact origin of the phagophore in mammalian cells is controversial. This phagophore expands to engulf intracellular cargo, such as protein aggregates, organelles and ribosomes, thereby sequestering the cargo in a double-membraned autophagosome (Mizushima, 2007). The loaded autophagosome matures through fusion with the lysosome, promoting the degradation of autophagosomal contents by lysosomal acid proteases. Lysosomal permeases and transporters export amino acids and other by-products of degradation back out to the cytoplasm, where they can be re-used for building macromolecules and for metabolism (Mizushima, 2007).

Conserved from yeast to humans, autophagy occurs at low basal levels to maintain cellular homeostasis through cytoplasmic and organelle turnover. For example, an animal model of Atg5-deficient mice, although nearly normal at birth, they cannot survive the early neonatal starvation period: they have reduced circulating amino acids and decreased cardiac ATP (Hamacher-Brady et al., 2006). Under most circumstances, autophagy mechanism constitutes a stress adaptation pathway that protects cell survival. An apparent paradox is that autophagy is also considered a form of nonapoptotic programmed cell death called “programmed cell death type two” (PCD II) or “autophagic” cell death, which is characterized by morphologic and molecular features that are distinct from apoptosis (PCD I)

(Maiuri et al., 2007). This type of cell death has been defined by morphological criteria, but it is now clear that the mere presence of autophagosomes in dying cells is not sufficient to distinguish “cell death with autophagy” from “cell death by autophagy”.

Certain cellular stresses can induce autophagy formation, such as oxidative stress. ROS are essential for autophagosome formation under starvation conditions through targeting cysteine protease HsAtg 4, an autophagy-related gene, leading to cell survival. However, little is known about the role of ROS in autophagy-induced cell death.

High levels of ROS induce cell death, which often involves apoptosis through caspase activation (Pelicano et al., 2004). The NF-kB transcription factor could repress ROS-mediated autophagy. One study showed that tumor necrosis factor a-induced autophagy through ROS production in the absence of NF-kB activation but with NF-kB activation autophagy is repressed (Djavaheri-Mergny et al., 2007). Autophagy was involved in this pathway by the finding that siRNA knockdown of two proteins known to regulate autophagy, beclin1 and Atg7, reduced cell death (Ichimura et al., 2000; Liang et al., 1999). In another study, autophagy was implicated in the death of lipopolysaccharide (LPS)-activated macrophages. Treatment of these cells with the caspase inhibitor Z-VAD blocked classic apoptosis but nevertheless induced cell death in a caspase-independent pathway, suggested to involve autophagy (Xu et al., 2006). In addition, Bcl-2 directly associates with Beclin-1-suppressing autophagy (Luo and Rubinsztein, 2010). Bcl-2 also contributes to the regulation of the type III PI3-K and autophagy through attenuating ROS production. Hence, Beclin-1 regulates autophagy through integration of signals from many pathways in response to ROS (Lipinski et al., 2010). Therefore, ROS can regulate autophagy, depending on the severity of oxidative stress, suggesting regulation of intracellular redox status that controls autophagy (Yang et al., 2008).

A role for autophagy in response to ROS is highlighted by the accumulation of oxidized proteins in aged cells under normal growth conditions, where autophagic pathways are compromised in age-related disorders, such as Alzheimer’s disease and diabetes mellitus

with a decrease in autophagy (Donati et al., 2001). Although autophagy is largely considered nonselective, preferential autophagy of damaged or excess organelles, such as peroxisomes (Farre and Subramani, 2004), endoplasmic reticulum (ER) (Bernales et al., 2006; Kruse et al., 2006) and mitochondria (Lemasters, 2005), can occur and there is accumulating evidence for selective autophagic processes in response to ROS.

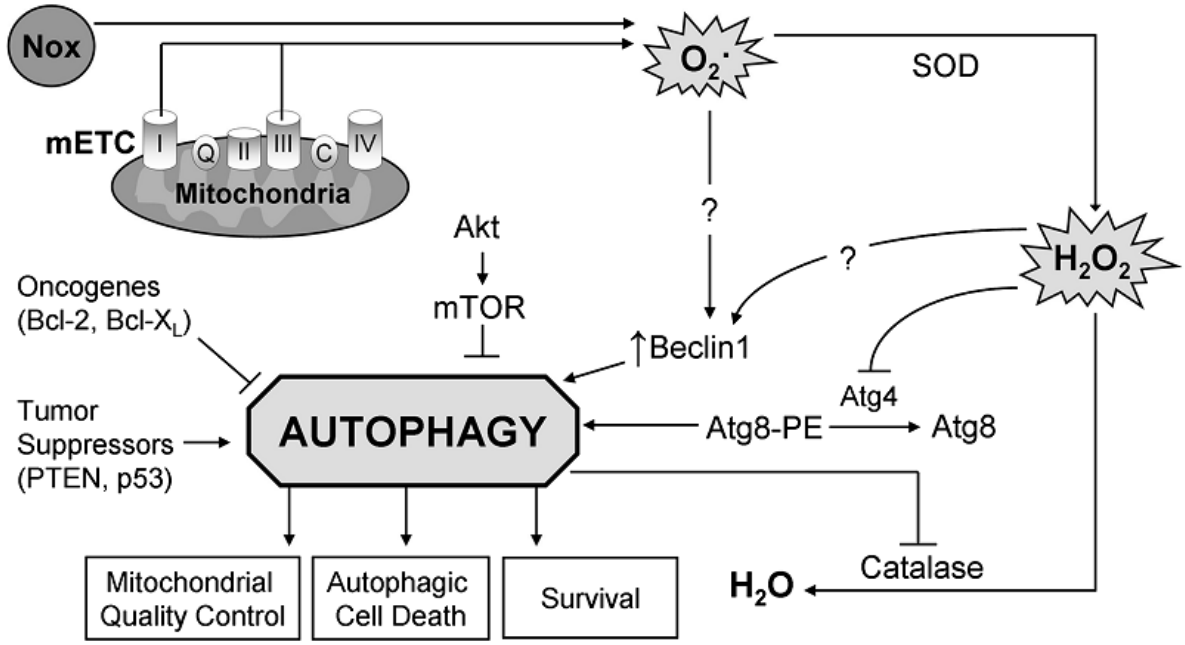

Figure 4. Regulation of autophagy by ROS in normal cells. Intracellular ROS are generated by Nox (cytoplasmic) or by the mitochondrial. ROS can increase expression of Beclin-1 by an unknown mechanism, leading to autophagy. H_2O_2 can directly inactivate the cysteine protease Atg4, blocking the delipidation of Atg8 to induce autophagy. Selective autophagic degradation of catalase serves as a positive-feedback loop, causing accumulation of ROS, which further enhances autophagy. Other regulators of autophagy include the Akt/mTOR pathway, oncogenes Bcl-2/Bcl-xL, and tumor suppressors PTEN/p53. (Adapted from Azad, 2009)

1.9 Crosstalk between autophagy and apoptosis

Both autophagy and apoptosis are important for the development and prevention of human diseases. They have been shown to act in synergy and also to counter each other. In a

clinical setting, one cannot predict the outcome of inhibition or activation of one death program without considering the effect on the other. Under certain conditions, autophagy and apoptosis are two independent processes, whereas in other situations, the activation of autophagy inhibits apoptosis (Platini et al., 2010) or autophagy occurs upstream of apoptosis (Eisenberg-Lerner et al., 2009). Several Atg proteins have been implicated in apoptosis. For instance, death-associated protein kinase (DAPK) has been proposed to convert autophagy from a cell survival mechanism to one of the initiation of cell death (Bialik and Kimchi, 2010). Caspase 3 cleaves the human Atg4 family member Atg4D to generate a truncated product, △N63 Atg4D that, when overexpressed, induces autophagy-independent apoptosis (Betin and Lane, 2009). Furthermore, regulators of apoptosis, such as Bcl-2 family members (Bcl-2 and Bcl-xL) (Betin and Lane, 2009), CASP8 and FADD-like apoptosis regulator (CFLAR) can regulate autophagy, and proteins involved in autophagy, such as Atg5, beclin 1 and Atg4D, can also have a role in apoptosis (Fimia and Piacentini, 2010). Caspases also cleave Beclin 1 at Asp149 during apoptosis resulting in the inhibition of autophagy (Djavaheri-Mergny et al., 2010; Luo and Rubinsztein, 2010; Wirawan et al., 2010). It remains to be investigated whether other Atg proteins are also cleaved during apoptosis.

In mammalian cells, Bcl-2 family members in the outer mitohondrial membrane modulate autophagy. Bcl-2 downregulation increases autophagy in a caspase-independent manner in human leukemic HL60 cells (Saeki et al., 2000), and Bcl-2 overexpression inhibits both autophgy and caspase-independent death in growth factor-deprived neural progenitor cells and in serum- and potassium-deprived cultured cerebellar granule cells (Canu et al., 2005). Recent evidence suggests that Bcl-2 inhibits autophagy through a direct interaction with Beclin 1 and that the interaction between them may function as a rheostat that maintains autophagy at levels that are compatible with cell survival rather than cell death (Pattingre et al., 2005). In contrast, Bcl-2 or Bcl-xL overexpression potentiates autophagy and autophagy gene-dependent death in MEFs treated with the proapoptotic stimulus etoposide (Shimizu et al., 2004). The basis for the opposite effects of Bcl-2 family

members on autophagy in different settings is unclear. Furthermore, it is not yet clear that Bcl-2 proteins function at the mitochondrion to regulate autophagy, since autophagy is inhibited by Bcl-2 targeted to endoplasmic reticulum but not by Bcl-2 targeted to mitochondria (Pattingre et al., 2005).

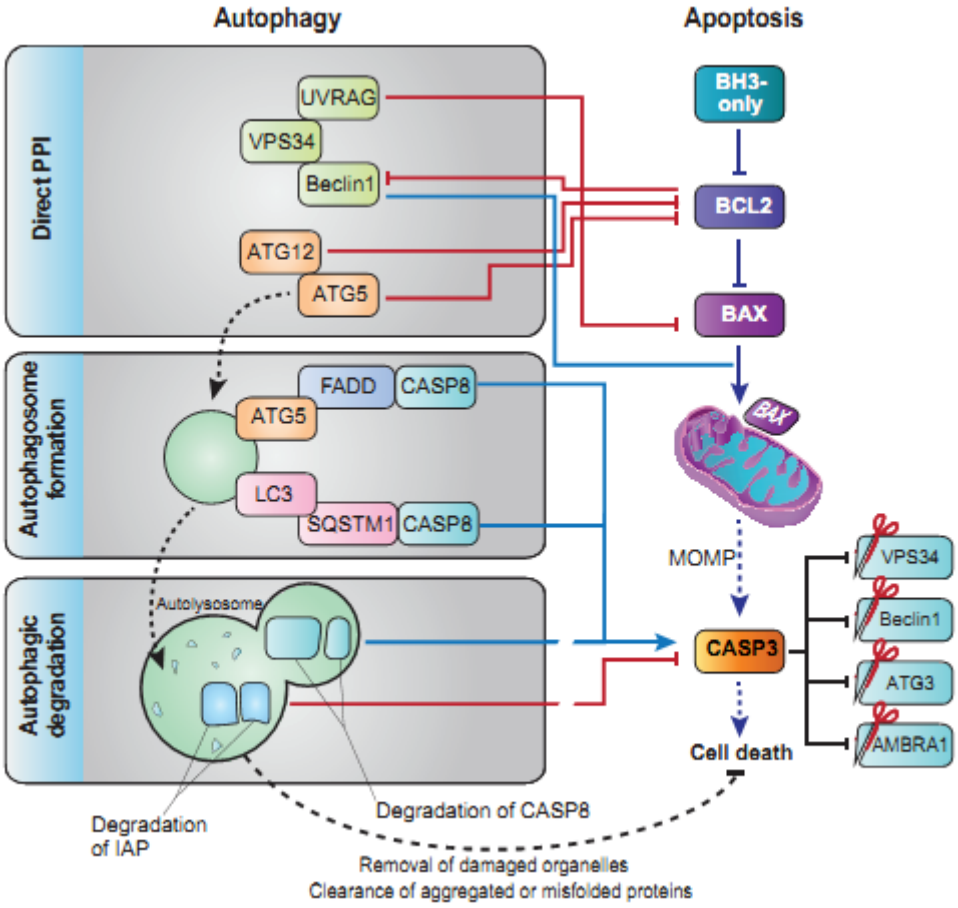

Figure 5. Overview of the molecular mechanisms underlying the autophagy-apoptosis crosstalk. There are three mechanistic paradigms of apoptosis that regulated by autophagy: (1) specific autophagy proteins; (2) autophagosomes as platforms for caspase activation; (3) autophagic degradation. Stimulatory interactions are depicted in blue, whereas inhibitory interactions are depicted in red. PPI, protein–protein interaction; MOMP, mitochondrial outer-membrane permeabilization. (Adapted from Rubinstein, 2012)

1.10 Therapeutic potential of Tranditional Chinese Medicine

A large body of evidence indicates that in traditional Chinese medicine (TCM) a plethora of herbs and herbal extracts are effective in the treatment of vascular diseases such as chronic wounds, diabetic retinopathy and rheumatoid arthritis (Shu et al., 2010; Zhai et al., 2013). Thus, it seems rational to explore these medicinal plants as potential sources of novel angiomodulatory factors. Rhodiola is a widely used TCM herb that has been shown to improve cognitive function, reduce mental fatigue, promote free radical mitigation, and enhance learning and memory (Darbinyan et al., 2000; De Bock et al., 2004; Shevtsov et al., 2003; Spasov et al., 2000). Rhodiola extracts exert anti-arrhythmic activity, show anti-inflammatory and neuroprotective effects, and prevent ischemia-reperfusion-induced ventricular tachycardia (Maslov et al., 2009; Qu et al., 2012; Sun et al., 2012). Salidroside (SAL), the major phenylpropanoid glycoside and pharmacological active constituent derived from Rhodiola, possesses potent anti-apoptotic effects in various cell types, e.g. neurons and cardiomyocytes as well as in preclinical disease models, e.g. acute myocardial infarction in rats (Qu et al., 2012; Zhong et al., 2010). Furthermore, SAL attenuated early ischemic brain injury, improved acute behavioral dysfunctions caused by focal cerebral ischemia, and protected against cerebrovascular injuries (Shi et al., 2012).

Salvianolic acid B (SalB), a pure water-soluble compound extracted from Danshen, is known for its broad pharmacological potential, including neuro- and cardioprotective properties by inhibiting the lipid peroxidation and superoxide anion production (Chen et al., 2000; Tang et al., 2002). SalB may furthermore suppress platelet aggregation, inhibit tumor necrosis factor-α-induced matrix metalloproteinase-2 upregulation, improve coronary microcirculation and cerebral blood flow, as well as inhibit myocardial ischemia (He et al., 2008; Li et al., 2004; Pan et al., 2011; Zhang and Wang, 2006). Sal B also regulates vascular homeostasis by exerting a number of vasoprotective effects, including the stimulation of vasodilation, suppression of smooth muscle cell proliferation, and inhibition of inflammatory responses (Chen et al., 2011; Pan et al., 2012; Shou et al., 2012). However,

the molecular mechanisms responsible for the putative antioxidant action mediated by SalB are poorly understood.

Icariin (ICAR) is a major flavonoid isolated from the traditional oriental herbal medicine Epimedium koreanum Nakai, has been proven to exert a broad range of biological efficacy on osteoporosis, cardiovascular diseases, and immunological function regulation (He et al., 1995; Xin et al., 2003; Yin et al., 2005). It has been reported that ICAR possessed a vasodilatory effect on the coronary vessels of animals, which is involved in the inhibiting of Ca^{2+}channels, and has cardioprotective effects during ischemia and reoxygenation (Zhang et al., 2000). ICAR also has the ability to prevent endothelial cells from damage induced by H_2O_2 through increasing the NO content and decreasing of caspase expression (Wang and Huang, 2005). Therefore, the discovery of molecules that regulate autophagy may be of great significance in the development of drugs for the treatment.

Puerarin (PUER) is the main isoflavone glucoside extracted from Puerariae Radix, which comes from the kudzu root (Pueraria lobota (Wild.) Howe). Puerarin is widely prescribed for patients with cardio-cerebrovascular diseases in China and it has been reported to have therapeutic effects on hypertension (Zhang et al., 2011b), cerebral ischemia (Gao et al., 2009), myocardial ischemia (Zhang et al., 2006b), diabetes mellitus (Hsu et al., 2003), arrhythmia (Zhang et al., 2011a), and arteriosclerosis (Yan et al., 2006). Puerarin also improves endothelial function by inhibiting cellular factors, such as adhesive molecules (Hu et al., 2010) and C-reactive protein (Yang et al., 2010), and stimulating endothelial nitric oxide synthase phosphorylation and nitric oxide production via activation of an estrogen receptor-mediated phosphatidylinositol 3-kinase/Akt- and calmodulin-dependent kinase II/AMP-activated protein kinase- dependent pathway. The molecular mechanism underlying these pharmacological benefits are also believed to involve the decreases in the plasma levels of free fatty acids, matrix metalloproteinases-9, interleukin-6, and tumor necrosis factor-α, and the inhibition in inflammation and stabilization in the atherosclerotic plaque (Xiao et al., 2011; Yang et al., 2010; Yao et al., 2012).

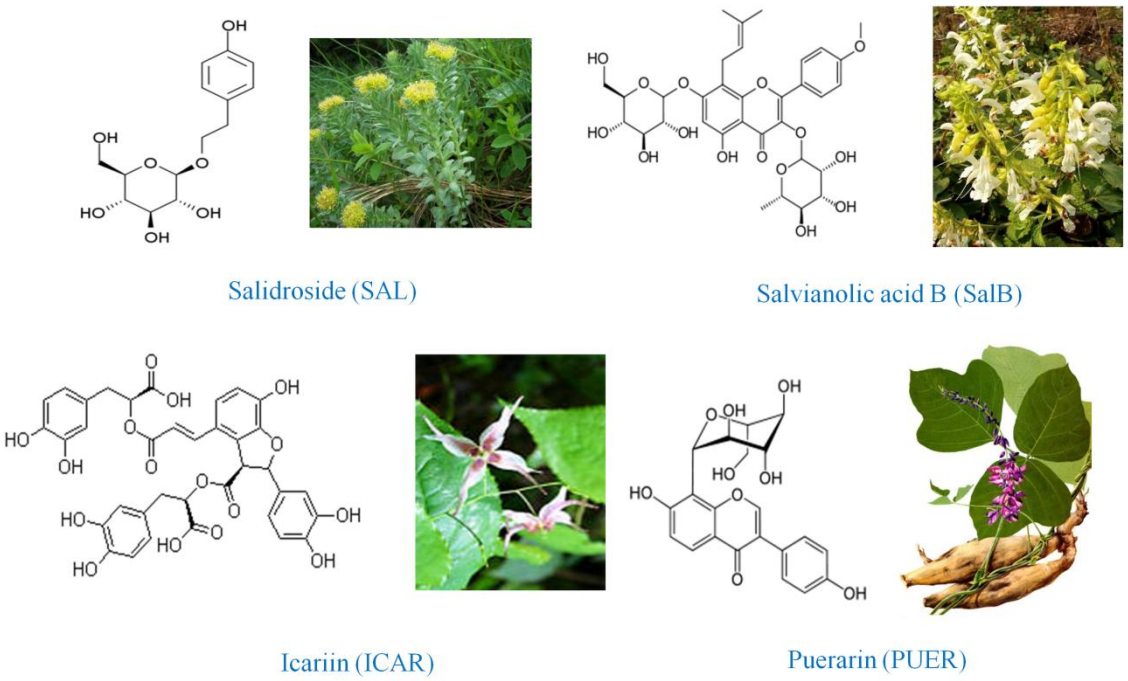

Figure 6. Chemical structure of Salidroside (SAL), Salvianolic acid B (SalB), Icariin (ICAR), Puerarin (PUER).

2. MATERIALS AND METHODS

2.1 Materials

2.1.1 Cell derivation

Informed consent for bone marrow collection was obtained from healthy volunteers (8 donors, age range 20-51 years, mean age 28.6 years) and all procedures were performed in accordance with the guidance and approval of the local institutional review board (approval no. EK263122004).

2.1.2 Antibodies

Table 1. List of antibodies.

ANTIGEN	COMPANY	CAT.NR.	APPLICATION	DILUTION
Phospho-Akt	Cell signaing	#4060	WB	1 to 1000
Akt	Cell signaing	#4691	WB	1 to 1000
Phospho-mTOR	Cell signaing	#5536	WB	1 to 1000
mTOR	Cell signaing	#2983	WB	1 to 1000
Phospho-p70S6K (Thr389)	Cell signaing	#9234	WB	1 to 1000
Phospho-p70S6K (Ser371)	Cell signaing	#9208	WB	1 to 1000
p70S6K	Cell Signalling	#2181	WB	1 to 1000
PCNA	Cell Signalling	#13110	WB	1 to 1000
Phospho-4EBP1	Cell signaing	#2855	WB	1 to 1000

4EBP1	Cell signaing	#9644	WB	1 to 1000
Phospho-ERK1/2	Cell signaing	#4370	WB	1 to 2000
Phospho-JNK	Cell signaing	#4668	WB	1 to 1000
Phospho-p38 MAPK	Cell Signaling	#4511	WB	1 to 1000
ERK1/2	Cell signaling	#4695	WB	1 to 1000
JNK	Cell Signaling	#9258	WB	1 to 1000
p38 MAPK	Cell Signaling	#9212	WB	1 to 1000
Bcl-xL	Cell Signaling	#2764	WB	1 to 1000
Bax	Cell Signaling	#2774	WB	1 to 1000
CD34	eBioscience	25-0349-42	Flow cytometry	1 to 1000
CD133	Miltenyi Biotec	130-098-826	Flow cytometry	1 to 1000
KDR	Miltenyi Biotec	130-098-905	Flow cytometry	1 to 1000
E-seclectin	BD Biosciences	551145	Flow cytometry	1 to 500
vWF	Abcam	Ab9378	Flow cytometry	1 to 250
VE-cadherin	BD Biosciences	560411	Flow cytometry	1 to 500
Cleaved-caspase 3	Cell Signaling	#9664	WB	1 to 1000
Cleaved-PARP	Cell Signaling	#5625	WB	1 to 1000
Phospho-MKK3/6	Cell Signaling	#9236	WB	1 to 1000
MKK3	Cell Signaling	#5674	WB	1 to 1000
Phospho-ATF2	Cell Signaling	#5112	WB	1 to 1000
ATF2	Cell Signaling	#9226	WB	1 to 1000
Cytochrome c	Cell Signaling	#4280	WB	1 to 500
LC3B	Sigma Aldrich	#9664	WB	1 to 1000

p62/SQSTM1	NOVUS	NBP1-48320	WB	1 to 4000
Beclin1	Cell Signaling	#3761	WB	1 to 1000
ß-actin	Cell Signaling	#4970	WB	1 to 2000
GAPDH	Sigma Aldrich	T9026	WB	1 to 5000
HRP-conjugated secondary antibody	Cell Signaling	#7074	WB	1 to 2000
DyLight® 594 conjugated secondary antibody	Abcam	Ab96921	IF	1 to 800

2.1.3 Buffers and culture medium

For Biochemistry:

1×RIPA (Radioimmunoprecipitation) Lysis Buffer

0.1% PMSF in DMSO

0.15 % protease inhibitor cocktail in DMSO

0.1% sodium orthovanadate in water

in 1× lysis buffer

5× Protein loading buffer

50% 500 mM Tris-HCl（pH6.8）

4% ß-Mercaptoethanol

5 mg/ml Bromophenol Blue

100 mg/ml Sodium dodecyl sulphate

50% Glycerol

10 × TBE (Tris/Borate/EDTA) buffer

0.5 M Tris

0.5 M Boric Acid

20 mM EDTA

pH 8.0

in ddH_2O

10 × TBS-T (Tris buffered saline-Tween)

1.5 M NaCl

0.5 M Tris-HCl

1% Tween

pH 7.6

in ddH_2O

1 ×Electrophoresis buffer

25 mM Tris-HCl

250 mM Glycine

3.5 mM Sodium dodecyl sulphate

in ddH_2O

1 ×Transfer buffer

25 mM Tris-HCl

192 mM Glycine

20% Methanol

in ddH_2O

Stripping buffer

700 μM ß-Mercaptoethanol

2% Sodium dodecyl sulphate

62.5 mM Tris-HCl（PH 6.7）

in ddH_2O

Blocking buffer

5% non-fat powder milk

in TBS-T

Antibody incubation buffer

1% non-fat powder milk

in TBS-T

10×Ponceau S buffer

2% Ponceau S

30% Trichloroacetic acid

30% Sulfosalicylic acid

in ddH_2O

10% Resolving gel (10mL)

30% Acrylamide 3.3 mL

1.5 M Tris-HCl (PH 8.8) 2.5 mL

10% Sodium dodecyl sulphate 0.1 mL

10% Ammonium persulfate 0.1 mL

TEMED 4 μL

ddH_2O 4 mL

4% Stacking gel (4 mL)

30% Acrylamide 536 µL

0.5 M Tris-HCl (PH 6.8) 1 mL

10% Sodium dodecyl sulphate 40 µL

10% Ammonium persulfate 40µL

TEMED 4 µL

ddH_2O 2.4 mL

For cell culture:

Culture media

Endothelial Cell Growth Medium

Fetal Calf Serum 0.02 mL/mL

Epidermial Growth Factor (recombinant human) 5 ng/mL

Basic Fibroblast Growth Factor (recombinant human) 10 ng/mL

Insulin-like Growth Factor (Long R3 IGF) 20 ng/mL

Vascular Endothelial Growth Factor 165 (recombinant human) 0.5 ng/mL

Ascorbic Acid 1 µg/mL

Heparin 22.5 µg/mL

Hydrocortisone 0.2 µg/mL

100 U/ml of penicillin/streptomycin

10× PBS (Phosphate buffered saline)

1.37 M NaCl

27 mM KCl

80 mM Na_2HPO_4

17.6 mM KH_2PO_4

pH 7.4

in ddH_2O

Cryoprotectant solution

10% DMSO

90% fetal bovine serium

For immunofluorescence:

Permeabilization-blocking buffer

5% Normal Goat Serum

0.2% Triton-X-100

in PBS

Antibody incubation buffer

3% Normal Goat Serum

0.1% Triton-X-100

in PBS

2.1.4 Chemicals, dyes and kits

Endothelial Cell Growth Medium 2 was purchased from PromoCell. Salidroside (SAL), Salvianolic acid B (SalB), Icariin (ICAR) and Puerarin (PUER) were obtained from Tauto Biotec. PicoGreen dsDNA Quantitation Kit was obtained from Life Technologies. Human basic fibroblast growth factor (bFGF) and VEGF ELISA kit were purchased from Peprotech. Nitric oxide colorimetric assay kit was obtained from Biovision. Hoechst 33258, DAPI and

Alexa Fluor 488® phalloidin were obtained from Invitrogen. RNeasy Mini kit was obtained from Qiangen. Matrigel™ Basement Membrane Matrix and human fibronectin were obtained from BD Biosciences. 2',7'-Dichlorofluorescin diacetate, diphenyleneiodonium chloride (DPI), Rhodamine 123, N^G-nitro-L-arginine methyl ester (L-NAME), acridine orange, specific siRNAs targeting human 4EBP1 (MISSION® siRNA, SASI_Hs02_00336903), specific siRNAs targeting human ATF2 (MISSION® siRNA, SASI_Hs01_00147372), negative control siRNA, and MISSION® siRNA Transfection Reagent were purchased from Sigma Aldrich. Ficoll-Paque PLUS 1.077, hydrophobic PVDF membrane, ECL Plus Western Blotting Detection Reagents were obtained from GE healthcare life sciences. Specific primer-probe sets for VEGF, KDR, VE-cadherin, vWF, PECAM-1, Nox4, STAT-3, eNOS and GAPDH, High Capacity cDNA Reverse Transcription Kit and Two Step TaqMan® Fast Universal PCR Master Mix were purchased from Applied Biosystems. LY294002, U0126, SP600125 were obtained from Cell Signaling. SB2003580 was ordered from Calbiochem. Rapamycin was ordered from Santa Cruz. LIVE/DEAD viability/cytotoxicity kit was purchased from Invitrogen. Cytotox 96® non-radioactive cytotoxicity assay kit was purchased from Promega. Annexin V-FITC apoptosis detection kit was obtained from Miltenyi. Dihydroethidium (DHE) was ordered from Cayman Chemical. NADP/NADPH Assay kit was obtained from AAT Bioquest.

2.2 Methods

2.2.1 Isolation and cultivation of human bone marrow-derived endothelial progeinitor cells (BM-EPCs)

Bone marrow sample was diluted with equal volume of DPBS, then the diluted sample was carefully layered onto the Ficoll-Paque PLUS. Centrifuge at 400×g for 20 min with the brake off. The mononuclear cells were carefully harvested from the interface between the Ficoll-Paque PLUS and sample buffer using a sterile pasteur pipette, and transfered to sterile centrifuge tubes. Cells were washed with an equal volume of DPBS twice to remove

the Ficoll-Paque PLUS residue. After washing, the isolated mononuclear cells were cultivated in flasks coated with human fibronectin (25 μg/mL) and induced by EGM-2 medium at 37℃ with 5% CO_2 in humidified air at a density of 3-5×10^6/cm^2. After 3 d in culture, non-adherent cells were removed by washing with phosphate-buffered saline (PBS), new medium was applied and the cultivation was maintained through 7 d.

2.2.2 Characterization of BM-EPCs

Quantitative fluorescence-activated cell sorting (FACS) was performed on a vantage SE flow cytometer to detect the surface marker of CD34, CD133, KDR, VE-cadherin, E-selectin, vWF on the cells at 7 and 14 d. The Weibel-Palade body in cells was visualized by transmission electron microscopy (TEM). Immunofluorescence staining was performed using FITC-UEA-I and Dil-acLDL.

2.2.3 Analysis of cellular proliferation

BM-EPCs were seeded at a density of 6×10^3 cells per well in 96-well plates, cultured with EGM-2 for 24 h followed by a starvation period of 24 h in EGM-2 without fetal bovine serum (FBS). Then medium was replaced by fresh non-FBS EGM-2 containing different concentrations of TCM extracts and cells were incubated for an additional period of 1, 2, and 4 d. After the samples were washed once with PBS and lysed in PBS containing 0.1% Triton X-100 for 50 min, DNA content was determined using the Quant-iT PicoGreen dsDNA Assay Kit according to the manufacturer's instructions. Fluorescence was measured using a fluorescence microplate reader (SpectraFluorPlus, Tecan, Männedorf, Switzerland) at 480/520 nm wavelength. Triplicates were used for each experimental unit.

2.2.4 Cell migration (chemotaxis) assay

Here we have adopted two methods to investigate the TCM extracts-induced migratory activity of human BM-EPCs in a transwell assay (6.5 mm diameter, 8 μm pore size filters). First, cells were cultivated for 7 d with EGM-2, trypsinized and counted. A fraction of 8×10^4 cells in 200 μL non-FBS EBM-2 were seeded into the upper chamber while 700 μL of culture medium containing 1% FBS and different concentrations of TCM extracts were placed in the lower chamber. The EPCs were allowed to migrate for 4 h at 37 ℃ in the tissue culture incubator. Second, BM-EPCs that were treated with TCM extracts for 48 h were trypsinized, washed and resuspended in EBM-2 without FBS. A fraction of 1×10^5 cells in 200 μL EBM-2 were added to the top chamber of a transwell and 700 μL EBM-2 with 5% FBS were added to the bottom chamber. Cells were allowed to migrate for 2 h. To quantify the number of migrated EPCs on the membrane, the upper side of the membrane was washed carefully with cold PBS and the remaining cells on this side were removed with a cotton swab. Transwell membranes were stained with Alexa Fluor 488® phalloidin in PBS and the migrated cells were examined using an inverted fluorescence microscope (Apotome, Carl Zeiss, Germany). All experiments were performed in at least triplicate with cells counted in 10 random fields of view.

2.2.5 Cell adhesion assay

Cell-matrix adhesion assay

Cell-matrix adhesion assay using human BM-EPCs was performed as was previously published (Tang et al., 2011). Briefly, 96-well plates were coated with 25 μg/mL human fibronectin for 1 h. Human BM-EPCs at 1×10^4 cells per well in EGM-2 were plated onto fibronectin-coated 96-well culture plates and incubated for 30 min at 37 ℃. After washing twice with PBS, adherent cells were fixed with 4% paraformaldehyde, stained with Hoechst 33258, and visualized under a fluorescence microscope. Additionally, adherent cells were

lysed with Triton X-100 and the DNA content was determined using the Quant-iT PicoGreen dsDNA Assay Kit. Representative results of five independent experiments were shown.

Cell-cell adhesion assay

To characterize the possible effect of TCM extracts on cell-cell adhesion, EPCs were grown overnight to a confluent monolayer in EGM-2 and labeled with Hoechst 33258. In addition, EPCs from the same donor were treated with TCM extracts for 48 h and fluorescence-labeled with calcein acetoxymethyl (AM) for 1 h at 37 ℃ followed by washing with PBS. These cells were then plated onto the established cell monolayer (acceptor cells). Attachment and spreading of the plated cells were monitored and recorded after 20 min by fluorescence microscopy. Quantification of intercellular adhesion was performed by counting the number of cells per microscopic field of view that remained attached after three gentle washing steps with PBS.

2.2.6 Matrigel-based capillary-like tube formation assay

The effect of TCM extracts on morphogenesis and tube formation capacity of BM-EPCs was investigated using the capillary tube formation assay on Matrigel basement membrane matrix. Briefly, ECMatrix™ solution was thawed on ice overnight, mixed with 10× ECMatrix™ diluents and placed in a 96-well tissue culture plate (50 μL per well) at 37 ℃ for 1 h to allow the matrix solution to solidify. A fraction of 1.2×10^4 cells per well were seeded on a Matrigel-precoated 96-well plate. Tube formation was observed under an inverted light microscope. Five independent fields were assessed for each well and the average numbers of tubes per 40× magnified field were determined.

2.2.7 Enzyme-linked immunosorbent assay (ELISA)

Cell culture supernatants were harvested 24 h and 48 h after stimulation with TCM extracts and frozen for later analysis. The levels of vascular endothelial growth factor (VEGF) secreted by BM-EPCs into the medium were measured by a commercially available ELISA kit. Briefly, capture antibody was diuted and added to a ELISA plate well and incubated overnight at room temperature (RT). After washing the plate for 4 times, immediately added 100 μL of standard or sample to each well in triplicate, incubated at RT for 2 h. The plate was aspirated and washed for 4 times. Detection antibody was added to each well and incubated at RT for 2 h. After washing for 4 times, substrate solution was added and incubated at RT for color development. The absorbance at 405 nm was measured with a microplate reader.

2.2.8 Measurement of nitric oxide production of BM-EPCs

Accumulated nitrite (NO_2^-) generated from cell-released nitric oxide (NO) in culture supernatants was determined using a spectrophotometric assay based on the Griess reaction. In brief, adherent cells were stimulated with TCM extracts for 2, 5, 8 and 10 d and cell culture supernatants were collected to demonstrate any time dependent effect. Supernatants were converted to nitrite by nitrate reductase followed by the Griess reagent (1% sulfanilamide - 0.1 % N-1-naphthyl-ethylenediamine dihydrochloride in 2.5% phosphoric acid) to convert nitrite to a deep purple azo compound. For determination of this compound the absorbance at 540 nm was measured with a microplate reader and all samples were tested in triplicate.

2.2.9 Cellular viability and lactate dehydrogenase release assay

BM-EPCs were treated with TCM extracts or basal medium for 48 h followed by incubation with 1 mM H_2O_2 for 6 h to induce oxidative stress. Cell numbers were

determined by DNA quantification as described above. Cells incubated without TCM extracts (in EBM-2 only) served as control group.

Lactate dehydrogenase (LDH) is a stable cytosolic enzyme present in all cell types. The cellular viability can be measured in terms of LDH released from dead cells into the supernatant upon rupture of cell membrane. For this purpose, CytoTox 96® Non-Radioactive cytotoxicity assay kit was employed according to the manufacturer's instructions. Briefly, 100 µL of lysis solution were added into wells containing the untreated control cells prior to the assay to induce maximum LDH release. To define the LDH content 50 µL supernatant with 50 µL of substrate solution were mixed in 96-well plates. After 30 min incubation at RT under absence of light, the enzymatic reaction was stopped with 50 µL stop solution. The absorbance was measured spectrophotometrically at 490 nm using a microplate reader. The percentage of cytotoxicity was calculated according to the following equation:

$$\text{percentage of cytotoxicity} = \frac{\text{Absorbance of experimental samples}}{\text{Absorbance of maximun LDH release}} \times 100\%.$$

2.2.10 Assessment of intracellular ROS and superoxide production

Intracellular ROS measurement by dichlorofluorescein (DCF)

The assessment of ROS involves the use of 2',7'-dichloro-fluorescein diacetate, which is a stable non-fluorescent molecule that readily crosses cell membranes and is hydrolyzed by intracellular esterases to form non-fluorescent DCFH. DCFH is then rapidly oxidized in the presence of ROS into highly fluorescent DCF. Cells were incubated in fresh EBM-2 containing 20 µM DCFH-DA for 30 min at 37℃. After removal of the DCFH-DA-containing medium, ROS formation was stimulated by H_2O_2 (final concentration: 1 mM) for 6 h at 37℃. Prior to and 6 h after H_2O_2 addition, the fluorescence levels of the samples were measured using a fluorescence microplate reader with the excitation and emission wavelengths set at 488 and 525 nm, respectively.

Superoxide measurement by dihydroethidium (DHE)

Superoxide generation causes oxidation of DHE into ethidium bromide, which binds to DNA in the nucleus and fluoresces red. EPCs were treated with H_2O_2 in the presence or absence of TCM extracts as described above. The medium was then replaced by PBS containing DHE (10 μM) followed by incubation for 30 minutes at 37℃. The intensity of DHE fluorescence was acquired by fluorescence microplate readings and images were collected using a fluorescence microscope and analyzed by Zeiss Imaging System.

2.2.11 Determination of NADPH oxidase activity

NADP and NADPH were measured using an Amplite Fluorimetric NADP/NADPH Assay kit. Cells treated with TCM extracts as well as untreated cells were lysed with 0.5% Triton-X100 for 10 min at RT and then mixed with 50 μL NADPH reaction mixture to a total volume of 100 μL per well. After incubation for 90 min at RT absorbance was monitored at 575 nm using the microplate reader.

2.2.12 Measurement of mitochondrial membrane potential

Measurement of the mitochondrial membrane potential (ΔΨm) was performed by loading cells with 5 μM Rhodamine123, a cationic lipophilic fluorochrome that can be taken up by mitochondria in proportion to the ΔΨm. After 20 min incubation in the dark, the cells were washed twice with PBS immediately followed by fluorescence reading at 507/529 nm (ex/em).

2.2.13 Calcein AM/ Ethidium homodimer-1 cellular viability assay

Cell viability was determined using a calcein-AM/Ethidium homodimer-1 (EthD-1) dual-staining assay kit (Invitrogen). This assay relies on the intracellular esterase activity within living cells, through which the calcein-AM, a cell permeable fluorogenic esterase substrate, hydrolyzes to the green fluorescent product calcein. Dead cells are stained by the cell-impermeant indicator EthD-1, which is a high-affinity nucleic acid stain that is weakly fluorescent until bound to DNA and emits red fluorescence. The cell cultures were treated with or without 1 mM H_2O_2 for 6 h after TCM extracts stimulation. After treatment, the culture medium was removed, and cells were rinsed with warm PBS very gently as not to stir cells. Subsequently 2 μM calcein-AM and 4 μM EthD-1 in 100 μL PBS were added to each culture well and incubated at 37℃ for 30 min, and fluorescence signals of the cells were observed under a Zeiss fluorescence microscope.

2.2.14 Apoptosis assay with flow cytometry analysis

BM-EPCs were seeded in six-well plates and allowed to attach for 24 h. After 48 h of treatment with SAL and 6 h of induction by H_2O_2 as described above, cell apoptosis was detected by annexin V-FITC apoptosis detection kit following the manufacturer's instructions. Briefly, the cells were gently trypsinized, washed with PBS, re-suspended in binding buffer and incubated with annexin V-FITC and PI at RT in the dark for 10 min, and then measured immediately by Flow Cytometer (BD™ LSRII, Heidelberg, Germany). The analysis of the data was performed using FlowJo Software (Tree Star, Inc., Ashland, OR, USA).

2.2.15 Immunofluorescence

To confirm the results of the apoptosis assay, immunofluorescence stain for Bax and Bcl-xL was used. The cells were fixed with 4% paraformaldehyde for 20 min at RT and

washed three times in PBS buffer. Fixed cells were blocked by incubation in PBS with 5% normal goat serum and 0.2% triton X-100 at RT for 30 min. Then the cells were incubated with primary antibody overnight at 4 ℃. After cells were washed three times with PBS, they were incubated with red-fluorescent Alexa Fluor 594 secondary antibody for 1 h at 37 ℃. Finally, these cells were stained with DAPI at RT for 10 min. The stained cells were washed three times with PBS. The results were visualized using fluorescence microscopy (Apotome, Carl Zeiss, Oberkochen), with fluorescence filter set at 488 nm (green) and 570 nm (red).

2.2.16 Acridine orange staining

Acidic intracellular compartments were visualized by acridine orange staining. After treatment, cells were washed with PBS and stained with 10 mg/mL acridine orange for 15 min at 37 ℃. Microscopic images were collected using the fluorescence microscope. Depending on their acidity, autophagic lysosomes appeared as orange/red fluorescent cytoplasmic vesicles, while the nuclei were stained green.

2.2.17 Small interference RNA transfection

Specific siRNAs targeting human ATF2 and 4EBP1 were obtained from Sigma-aldrich. The cells were transiently transfected with a negative control siRNA or ATF2 (or 4EBP1) siRNA using the MISSION® siRNA Transfection Reagent. Cellular levels of the proteins specific for the siRNA transfection were checked by qRT-PCR and Western blot, the cells were then prepared for further experiments at 48 h after transfection.

2.2.18 RNA isolation, cDNA synthesis and quantitative real-time polymerase chain reaction (qRT-PCR) procedure

Total RNA was isolated by using RNeasy Mini Kit. Total RNA (300 ng) from each sample was subjected to reverse transcription using a cDNA reverse transcription kit. For the reverse transcription, typical 20 μL reactions contained 2 μL 10×RT Buffer, 0.8 μL 25×dNTP Mix, 2 μL 10×RT Random Primers, 1 μL MultiScribe Reverse Transcriptase, 1 μL RNase Inhibitor, 3.2 μL Nuclease-free H_2O, and 10 μL RNA sample. Thermal cycling conditions were: 25℃ for 10 min, 37℃ for 120 min and finally 85℃ for 5 min. The ABI Prism 7500 fast Sequence Detection System was used for the qRT-PCR. Typical 20 μL reactions contained 10 μL ABI fast Universal TaqMan Master Mix, 1 μL mixture of forward and reverse primers and TaqMan probe, 1 μL cDNA and 8 μL water. Each PCR run was performed in triplicate including negative control samples containing master mix, primers and probes as described above but no cDNA template. Thermal cycling conditions of the ABI 7500 fast were: 95℃ for 20 s for pre-denaturation, then 40 cycles of 95℃ for 3 s and finally 60℃ for 30 s each. Data were normalized to GAPDH expression and fold change was calculated by the $2^{-\Delta\Delta CT}$ method.

2.2.19 Western blot analysis

Whole-cell lysates of cell groups were analyzed by Western blot assays. Cells were washed twice with PBS, sonicated in radioimmunoprecipitation (RIPA) buffer and homogenized. Debris was removed by centrifugation at 12,000 g at 4℃ for 10 min and protein concentration was determined using the BCA Protein assay kit according to the manufacturer's instructions. Samples containing 30 μg of protein were separated by electrophoresis on sodium dodecyl sulfate (SDS) polyacrylamide gels and transferred to polyvinylidene difluoride membranes by electroblotting. The membranes were then blocked by incubating with 5% BSA in 20 mM Tris-HCl, 150 mM NaCl, pH 7.5 (TBS) buffer for 1 h followed by incubation with primary antibodies (see **Materials section, *2.1.2 Antibodies*** for

a detailed list and conditions), overnight at 4 ℃. After washing with TBS-T, membranes were incubated with horseradish peroxidase-conjugated secondary antibodies, diluted in incubation buffer, for 2 h at RT. After washing with TBS-T, luminescence was developed using an automated developer (Sysgen) and non saturated radiograms analyzed with Quantity One 4.6.2 software (Bio-Rad Laboratories, Hercules, CA, USA). GAPDH or ß-actin were used for internal normalization.

2.2.20 Animal study

For *in vivo* study, 2 mg SAL was embedded into 5 µL gel (25 mg/mL Fibrinogen and 25 IU/mL Thrombin, 1:1) to make the final concentration of 50 mg/kg body weight. The operations were performed under surgical aseptic conditions. Each immunodeficient mouse was placed in the prone position. The right rear extremity was extended and rotated inward at the hip joint. Exact locations of the hip and knee joints were detected by flexion and extension of the hip and of the knee. A 12-mm incision was then performed along the lateral upper leg, giving exposure to the greater trochanter. An incision was then made along the fascia lata, following a line from the greater trochanter to the knee joint. The quadriceps femoris muscle was mobilized anteriorly towards the knee and the hip using two spatulas. A sharp elevatorwas used to expose the distal femur and the first hole (diameter 0.45 mm) was drilled into the distal femur. The first pin was put into one of the lateral holes of the plastic body of the external fixation device and was subsequently orthogonally drilled into the distal femur, penetrating both the lateral and the medial cortex. The second hole was drilled through the remaining lateral hole on the plastic body and into the proximal femur or the lateral femoral neck as described above. The second pin was then placed through this hole. The inner two pins were then placed after drilling the inner two guide holes. After having fixed all four pins, two Gigli wires were placed around the femur and placed into the fixed saw guide on the body of the external fixator. A defect was cut using two Gigli wires while the body of the fixation device was stabilized with the help of two clamp. The Fibrinogel

(10 μL) containg SAL were laid on the mineralized collagen scaffold and embedded between the fixed pins. The clamps were then removed and the femur and surrounding structures were all guided back into their natural anatomic positions. Finally, the skin was closed with interrupted sutures. To investigate bone healing during the 6-week observation period, 20-mm data sets of all operated and six untreated contralateral femurs were scanned using μCT (SCANCO viva CT 75; SCANCO Medical AG, Bruttisellen, Switzerland). The defect volume reported is the difference of the bone volume of the control femurs, BMP-2 treated femurs, and the SAL treated femurs.

2.2.21 Statistical analysis

Numerical data are presented as the means ± standard deviation from at least three individual experiments with cells from different donors, unless otherwise indicated. All statistical analysis were performed using the SPSS 16.0 software package. Comparisons between two groups were performed using independent-samples *t*-test. Experiments with more than two groups were compared by ANOVA followed by the Tukey post-hoc test. P values of ≤ 0.05 were considered statistically significant

3. RESULTS

3.1 TCM extracts induce angiogenic differentiation in bone marrow derived-endothelial progenitor cells

3.1.1 Cultivation and identification of BM-EPCs

When mononuclear cells isolated from human bone marrow were cultured in endothelial cell growth medium on fibronectin-coated dishes, both adherent and non-adherent cells demonstrated round morphology with different sizes as assessed by light microscopy during the first 3 d, suggesting the presence of various subpopulations within the human mononuclear cell fraction. Approximately 20% of the mononuclear cells transferred to culture plates grew as adherent cells during the first week of culture with a tendency to form clusters or colonies (Figure 7A). When cultivated for 7 d, the adherent cells exhibited strong ability to take up Dil-acLDL and FITC-UEA-I, and the double positive rate was (95.1 ±4.0)% (Figure 7B), which were identified as differentiating EPCs. The Weibel-Palade body was observed in endochylema by TEM (Figure 7C). During the second week of culture, the cells changed toward a spindle-shaped endothelium-like morphology. Then, attached cells formed a cobblestone-like structure at d 14 (Figure 7A). In the culture process, the expression pattern of surface markers changed toward a more mature endothelial cell phenotype during the cultivation period of 2 weeks, which showed a significant increase when 14 d cultures were compared to 7 d cultures with regard to the expression of KDR (from 66.7% to 79.2%), E-selectin (from 7.8% to 46.4%), vWF (from 5.4% to 35.4%), and a marked decrease in expression of CD133 (from 18.5% to 3.8%), and CD34 (from 45.4% to 36.1%) (Table 1).

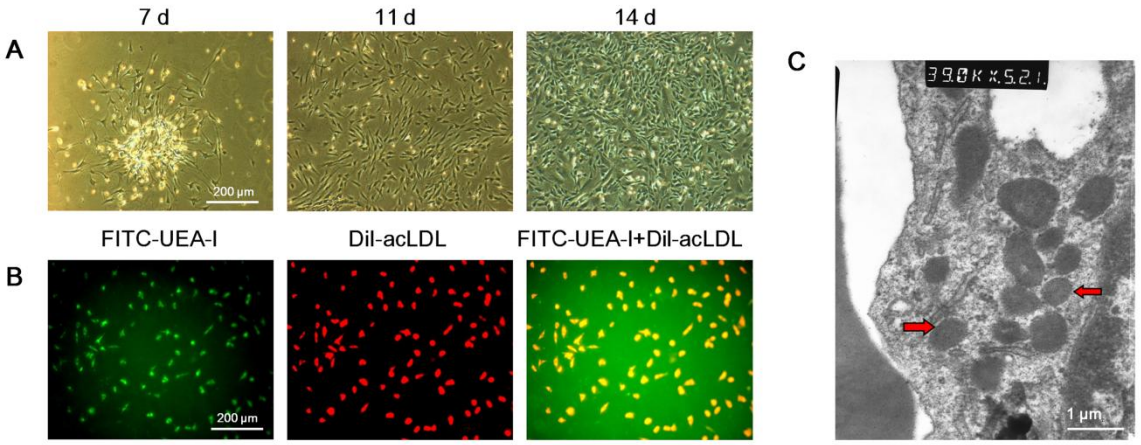

Table 2.

	CD133	CD34	KDR	VE-cadherin	E-selectin	vWF
7 d	18.5±2.8	45.4±7.8	66.7±7.2	26.5±5.3	7.8±1.3	5.4±1.0
14 d	3.8±0.7	36.1±3.9	79.2±5.1	32.1±4.3	46.4±8.3	35.4±6.2
P vaule	0.024	0.235	0.0452	0.398	0.001	0.001

Figure 7. Characterization of BM-EPCs. (A) The isolated mononuclear cells were cultivated in dishes coated with fibronectin and induced by EGM-2 at 37 ℃ with 5% CO_2 in humidified air. The morphology of the cells cultivated at 7 d, 11 d, and 14 d was observed under the inverted phase contrast microscope. (B) Cells cultivated at 7 d were washed with PBS two times, and stained with FITC-UEA-I and Dil-acLDL. (C) The Weibel-Palade body in cells was visualized by transmission electron microscopy (TEM).

Table 2. The expression pattern of cell surface markers of CD133, CD34, KDR, VE-Cadherin, E-selectin and vWF was determined by flow cytometry at 7 d and 14 d culture. Data are shown as mean ± SD.

3.1.2 SAL, ICAR and PUER promote the cellular proliferation of BM-EPCs

To assess the potent pro-angiogenic property of TCM extracts *in vitro*, we firstly examined the effect of TCM on cellular proliferation. Human BM-EPCs were treated with varying concentrations of SAL, SalB, ICAR and PUER for 24 h, 48 h and 96 h and cell number was assessed by DNA quantification with bFGF as a positive control. As shown in

Figure 8A, the cell number was apparently increased after the incubation with SAL for 48 h at the concentration of 20, 40, and 80 μM, with ICAR at 7.5, 15, 30 μM (Figure 8C), and with PUER at 40, 80 μM by both 24 and 48 h (Figure 8D). The protein expression of PCNA was also enhanced by 48 h incubation with SAL by 20, 40, and 80 μM (Figure 8E). But no significant effect was found at 24 h or 96 h treatment with SAL, compared to the control group. However, cell numbers were not significantly affected by SalB treatment (Figure 8B).

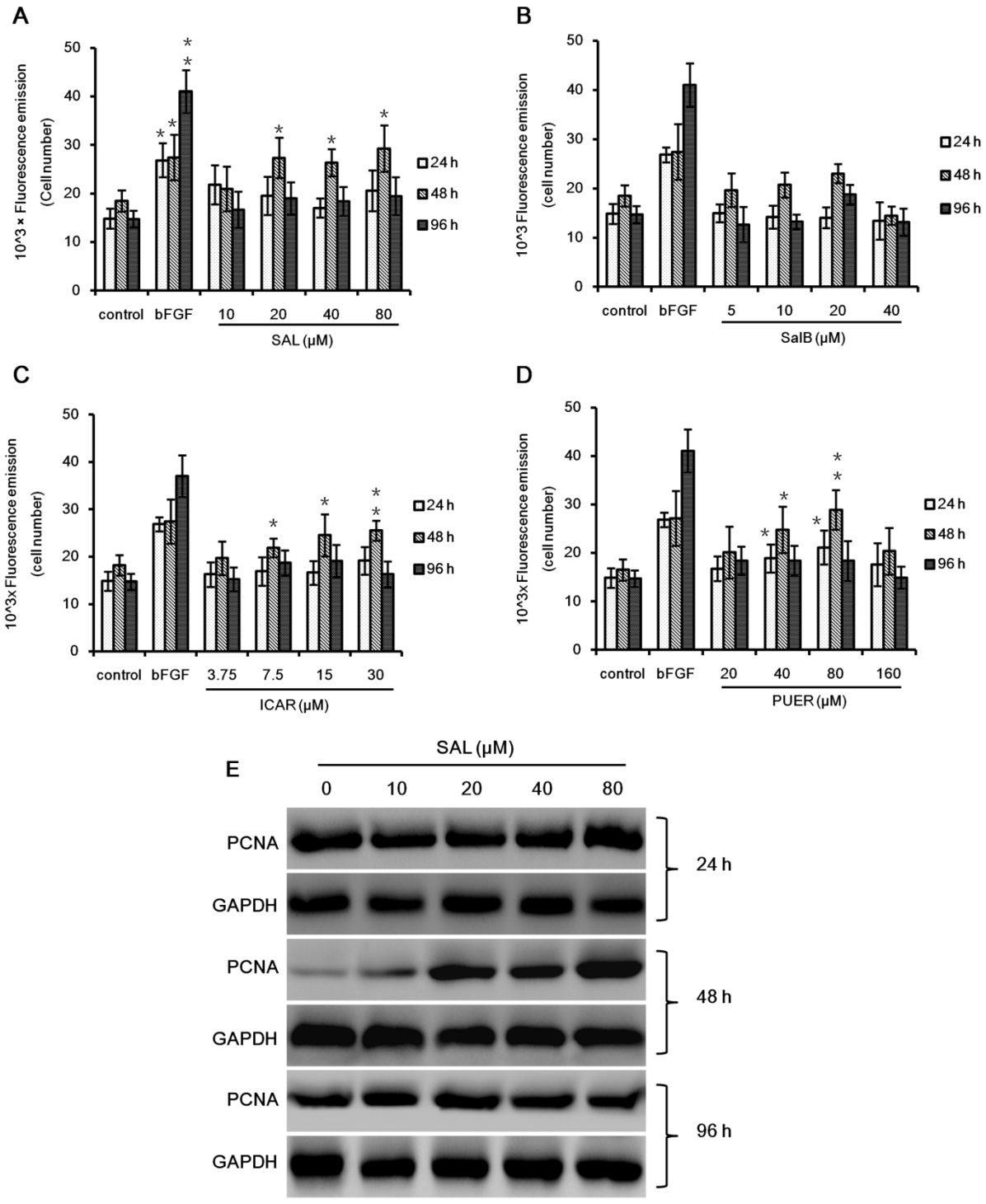

Figure 8. Effect of SAL, SalB, ICAR and PUER on cellular proliferation of BM-EPCs. (A-D) Cells were treated with indicated concentrations of TCM extracts for 24, 48, and 96 h followed by DNA quantification to determine cellular proliferation, n=6. (E) PCNA expression was measured by Western

blot. The immunoblots shown are representative of at least three independent experiments with comparable results. Data are shown as mean ± SD, $^{*}P < 0.05$, $^{**}P < 0.01$ versus control group.

3.1.3 SAL, SalB, ICAR and PUER enhance cell recruitment ability

EPCs that line the lumina of blood vessels are important players in blood vessel formation, and directed EPCs migration is a key component of the angiogenic process. To investigate the effects of TCM extracts-driven motility in BM-EPCs, transwell experiments were performed. When TCM extracts were added to the lower chamber compartment, cells showed a dramatically increased ability to migrate in response to all of them in a dose dependent manner. For SAL, the significant promotion effect was first occurred at 40 μM (2.59 ± 0.07-fold, $P < 0.01$) and peaked at 80 μM (3.05 ± 0.10-fold, $P < 0.01$) (Figure 9B, 9F). For SalB, the significant promotion effect was first occurred at 20 μM (1.80 ± 0.08-fold, $P < 0.05$), and peaked at 40 μM (1.92 ± 0.14-fold, $P < 0.01$) (Figure 9C, 9G). For ICAR, all of the three concentrations had remarkable effects on the chemotactic ability of BM-EPCs (7.5 μM, 2.79 ± 0.10-fold, $P < 0.01$; 15 μM, 4.15 ± 0.10-fold, $P < 0.01$; 30 μM, 4.95 ± 0.07-fold, $P < 0.01$) (Figure 9D, 9H). For PUER, the enhancing effect were occurred from 40 μM (1.82 ± 0.28-fold, $P < 0.05$), to 160 μM (3.05 ± 0.13-fold, $P < 0.01$) (Figure 9E, 9I).

Interestingly, for experiments involving pre-treatment of EPCs with TCM extracts which were used to measure the ability of TCM extracts to trigger innate cell recruitment ability, the results showed that cell migration increased significantly compared to the vehicle-treated control at a higher concentration of 80 μM SAL (Figure 9J, $P < 0.01$), and 15 μM and 30 μM of ICAR (Figure 9K, $P < 0.05$ and $P < 0.01$, respectively).

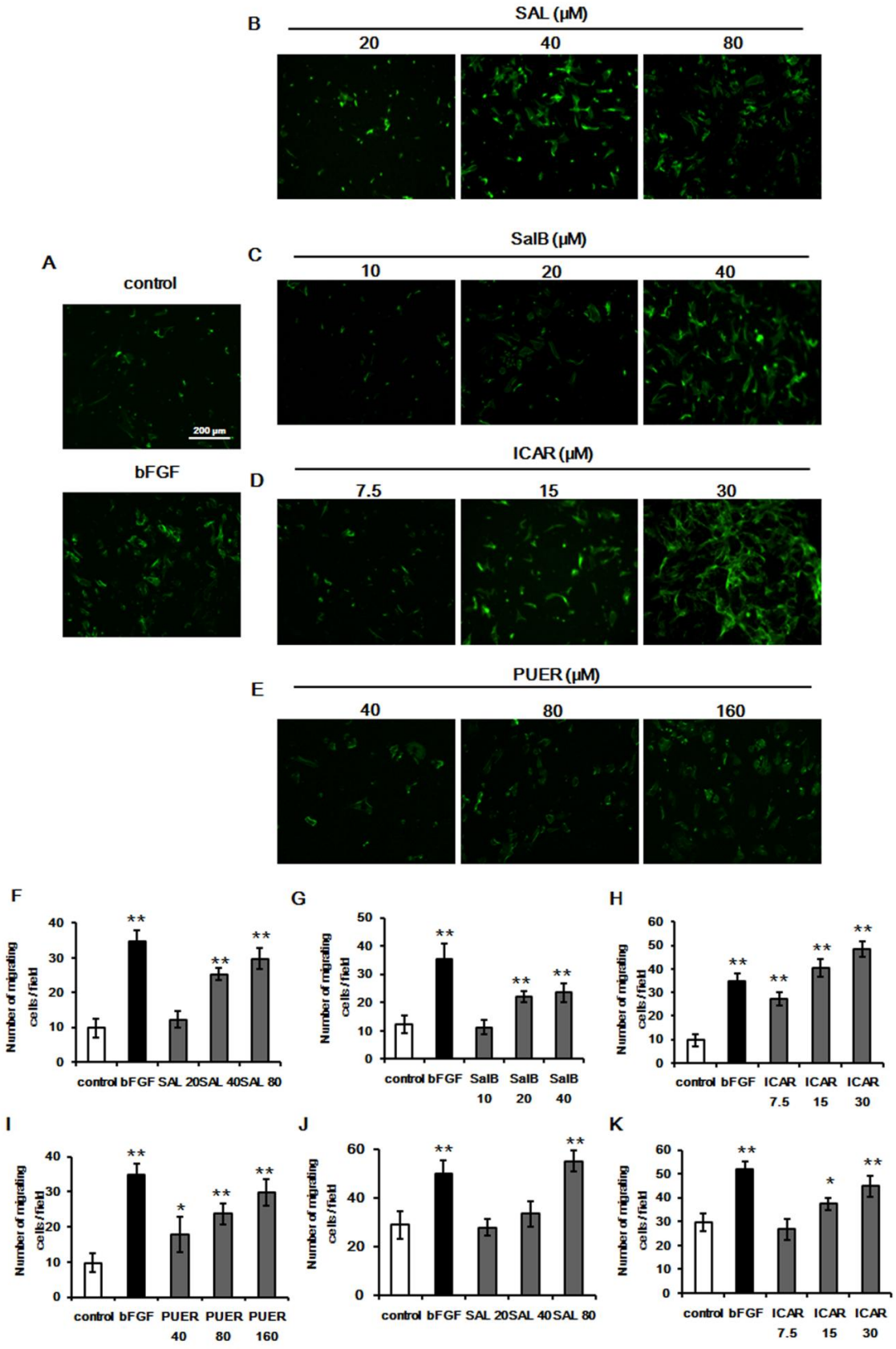
A
control
200 μm
bFGF
B
SAL (μM)
20
40
80
C
SalB (μM)
10
20
40
D
ICAR (μM)
7.5
15
30
E
PUER (μM)
40
80
160
F
Number of migrating cells / field
control bFGF SAL 20 SAL 40 SAL 80
G
control bFGF SalB 10 SalB 20 SalB 40
H
control bFGF ICAR 7.5 ICAR 15 ICAR 30
I
control bFGF PUER 40 PUER 80 PUER 160
J
control bFGF SAL 20 SAL 40 SAL 80
K
control bFGF ICAR 7.5 ICAR 15 ICAR 30

Figure 9. TCM extracts enhance cell migration capacity in a dose-dependent manner. (A-I) Transwell chemotaxis assay was performed on BM-EPCs with phosphate buffered saline (control), 50 ng/mL bFGF and indicated concentrations of TCM extracts in the lower chamber. To quantify the migrated EPCs on the membrane, the upper side of the membrane was washed and wiped with a cotton swab. Transwell membranes were stained with Alexa Fluor 488® phalloidin and the migrated cells were examined using an inverted fluorescence microscopy. The number of migrated cells was quantified by performing cell counts of 10 random fields, n=5. (J, K) BM-EPCs were treated in the absence or presence of indicated concentrations of SAL, ICAR and bFGF for 48 h, then seeded into the upper chamber of the transwell with culture medium containing 5% FBS in the lower chamber. Data are presented as mean ± SD, n=5, $^{*}P < 0.05$, $^{**}P < 0.01$ versus control group.

3.1.4 Effect of SAL, SalB, ICAR and PUER on cell adhesion to extracellular matrix (ECM) and cell-cell adhesion of BM-EPCs

To test whether TCM extracts affect cell-matrix adhesion we used human fibronectin as ECM. As shown in Figure 10B and 10F, SAL treated cells attached more readily to the ECM (1.95±0.14-fold and 1.98±0.10-fold increase at 40 and 80 μM) compared to the control ($P < 0.01$). Similarly, ICAR also promoted the cell-matrix adhesion at all of the three concentrations (7.5 μM, 1.70 ± 0.12-fold, $P < 0.01$; 15 μM, 2.40 ± 0.08-fold, $P < 0.01$; 30 μM, 2.78 ± 0.15-fold, $P < 0.01$, Figure 10D, 10H). In addition, PUER-treated cells showed an enhancing ability to adhere to the ECM at higher concentrations (1.91±0.09-fold and 2.19±0.14-fold increase at 80 and 160 μM, $P < 0.01$, Figure 10E, 10I). But there was no significant difference concerning the number of attached cells after 90 min adherence. However, SalB have shown no significant effect on the cell-matrix adhesion (Figure 10C, 10G).

To investigate whether TCM extracts could affect cell-cell adhesion of BM-EPCs, we examined the adherence of TCM extracts-stimulated cells to normal EPCs. In sharp contrast, a significant reduction in the adhesive properties was observed for SAL and ICAR-treated

BM-EPCs, which became apparent at 20 μM and peaked at 80 μM for SAL (Figure 10J-M), and showed effect at both 15 μM and 30 μM for ICAR (Figure 10L, 10N). Taken together, these results suggest that TCM extracts provoked the cell adhesive ability to ECM, while it diminished the capacity of cell-cell adhesion.

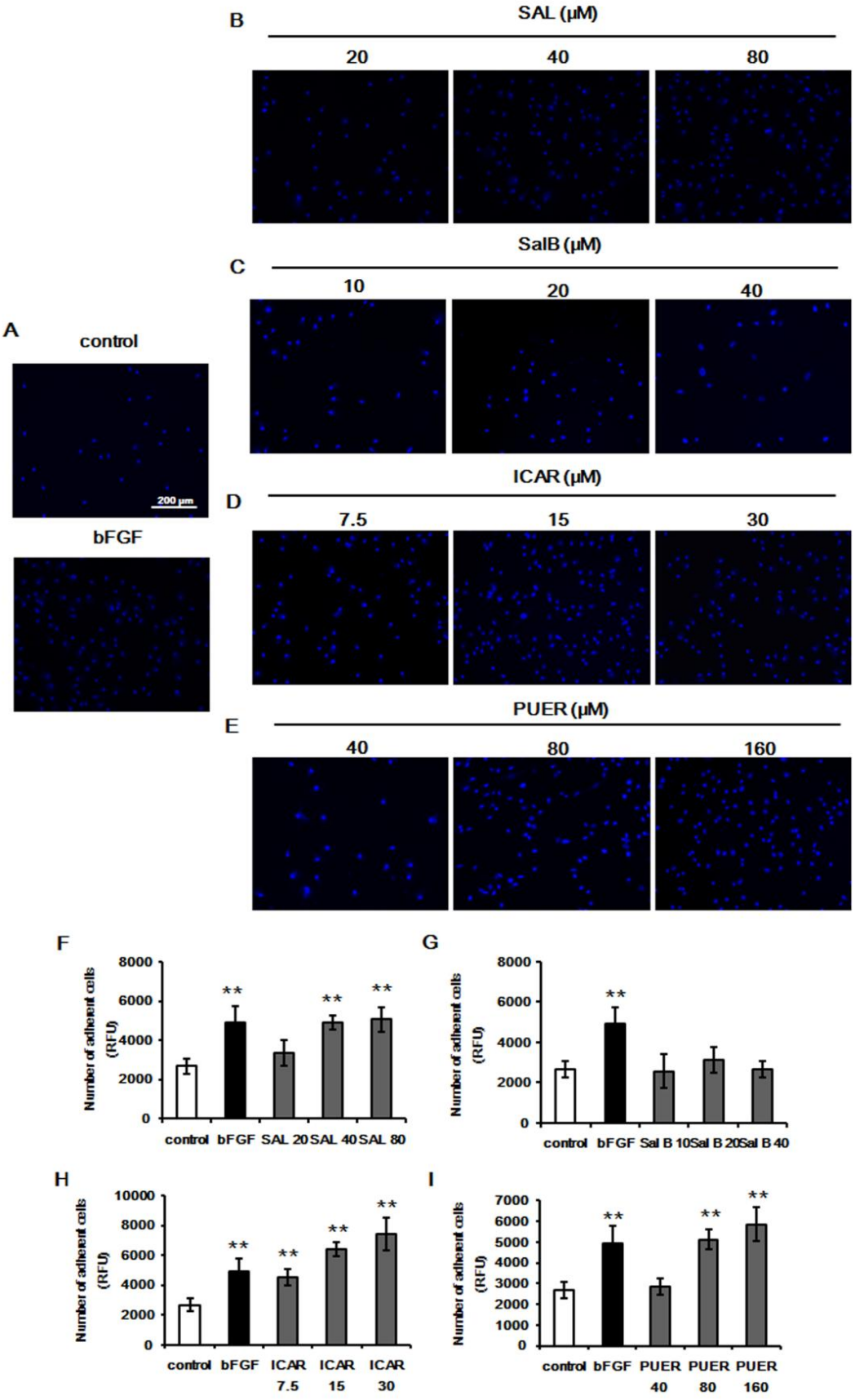
A
control
200 μm
bFGF
B
SAL (μM)
20
40
80
C
SalB (μM)
10
20
40
D
ICAR (μM)
7.5
15
30
E
PUER (μM)
40
80
160
F
Number of adherent cells (RFU)
8000
6000
4000
2000
0
control
bFGF
SAL 20
SAL 40
SAL 80
G
Number of adherent cells (RFU)
control
bFGF
Sal B 10
Sal B 20
Sal B 40
H
Number of adherent cells (RFU)
10000
8000
6000
4000
2000
0
control
bFGF
ICAR 7.5
ICAR 15
ICAR 30
I
Number of adherent cells (RFU)
7000
6000
5000
4000
3000
2000
1000
0
control
bFGF
PUER 40
PUER 80
PUER 160

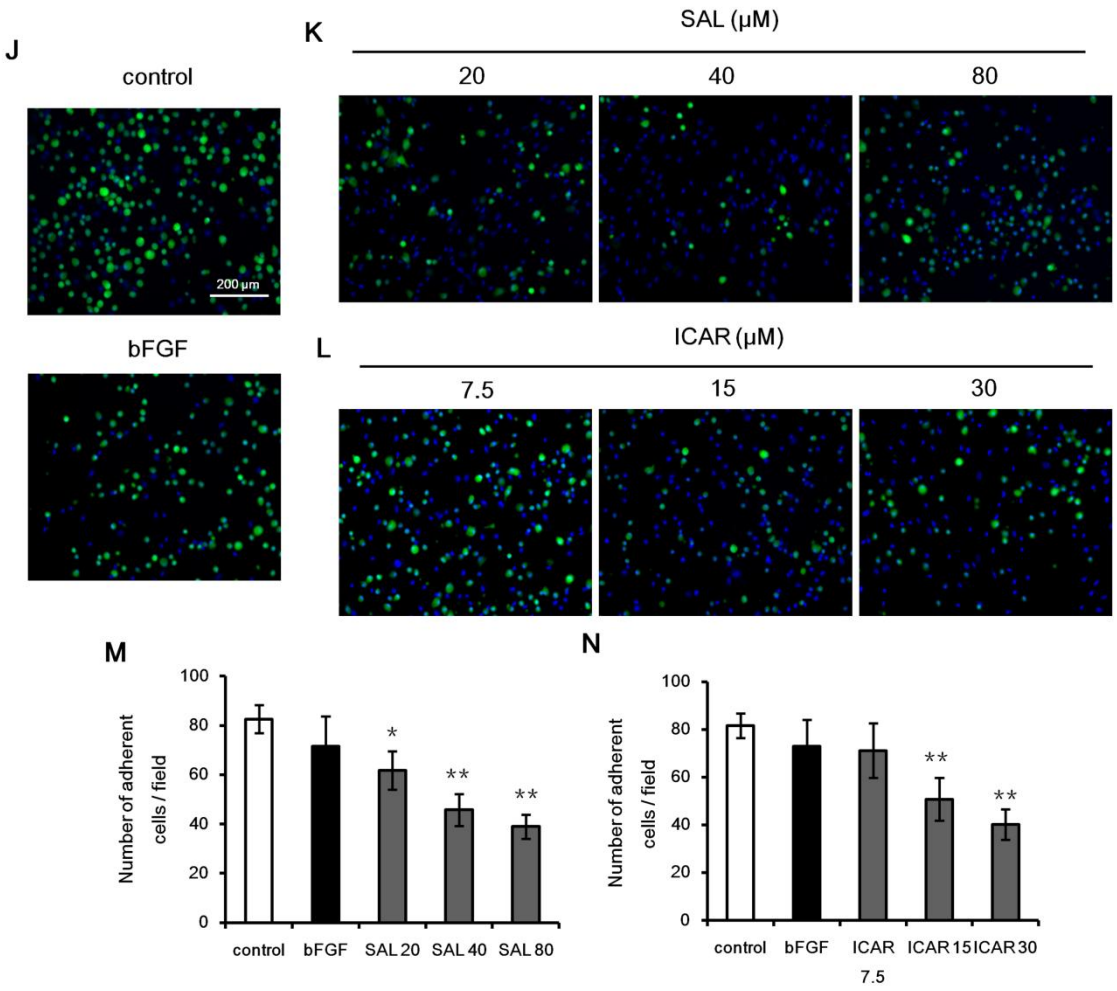

Figure 10. SAL, ICAR and PUER promote cell-matrix adhesion but SAL, ICAR inhibit cell-cell adhesion of BM-EPCs. (A-E) BM-EPCs were treated with indicated concentrations of TCM extracts or bFGF for 2 d. Cell adhesion to extracellular matrix was performed on fibronectin treated plates for 30 min followed by staining of adherent cells with Hoechst 33258 dye (nuclei, blue). (F-I) Quantification of attached cells was determined by DNA content using Quant-iT PicoGreen dsDNA Assay Kit. Data are presented as mean ± SD, n=5. (J-N) For the examination of cell-cell adhesion, BM-EPCs were grown overnight to a confluent monolayer in EGM-2 and labeled with Hoechst 33258 dye. Another set of BM-EPCs was treated with indicated concentrations of TCM extracts or bFGF for 48 h, fluorescence-labeled with calcein-AM for 1 h, and plated onto the established cell monolayer. Quantification of cell-cell adhesion was performed by counting the number of cells per microscopic field of view that remained attached after 20 min incubation. Data are presented as mean ± SD, n=5, $^{*}P < 0.05$, $^{**}P < 0.01$ versus control group.

3.1.5 Effect of SAL, SalB, ICAR and PUER on capillary tube formation of BM-EPCs *in vitro*

In vitro angiogenesis assay was used to investigate the ability of EPCs to participate in vascularization, which is the most important activity of EPCs. To determine whether TCM extracts affect the ability of BM-EPCs to form capillary-like tubes, cells were seeded on Matrigel and examined for tube formation microscopically. 18 h after plating onto the gel, more crosspoints and well formed connections were observed in the tubules formed by SAL-stimulated cells compared with control group (Figure 11A, 11B, 11F). The presence of 20, 40 and 80 μM SAL significantly increased the number of sprouting tubules by 250.1 ± 17.5%, 350.1 ± 18.8% and 525.4 ± 10.4% as compared with untreated BM-EPCs ($P < 0.01$). Moreover, 20 μM SalB significantly increased the number of sprouting tubules by 350 ± 13% as compared with untreated BM-EPCs. However, this effect was not observed at the concentration of 40 μM SalB (Figure 11C, 11G). Additionally, the presence of 7.5, 15 and 30 μM ICAR significantly increased the number of sprouting tubules by 225.4.4 ± 25.6%, 404.3 ± 19.9% and 598.1 ± 11.5% as compared with untreated BM-EPCs (Figure 11D, 11H). And PUER treatment also exerted enhanced capillary tube formation of the cells by 220.0 ± 21.8% and 263.4 ± 21.2% at 80 and 160 μM (Figure 11E, 11I). Thus TCM extracts strongly enhance the ability of EPCs to form tube-like structures

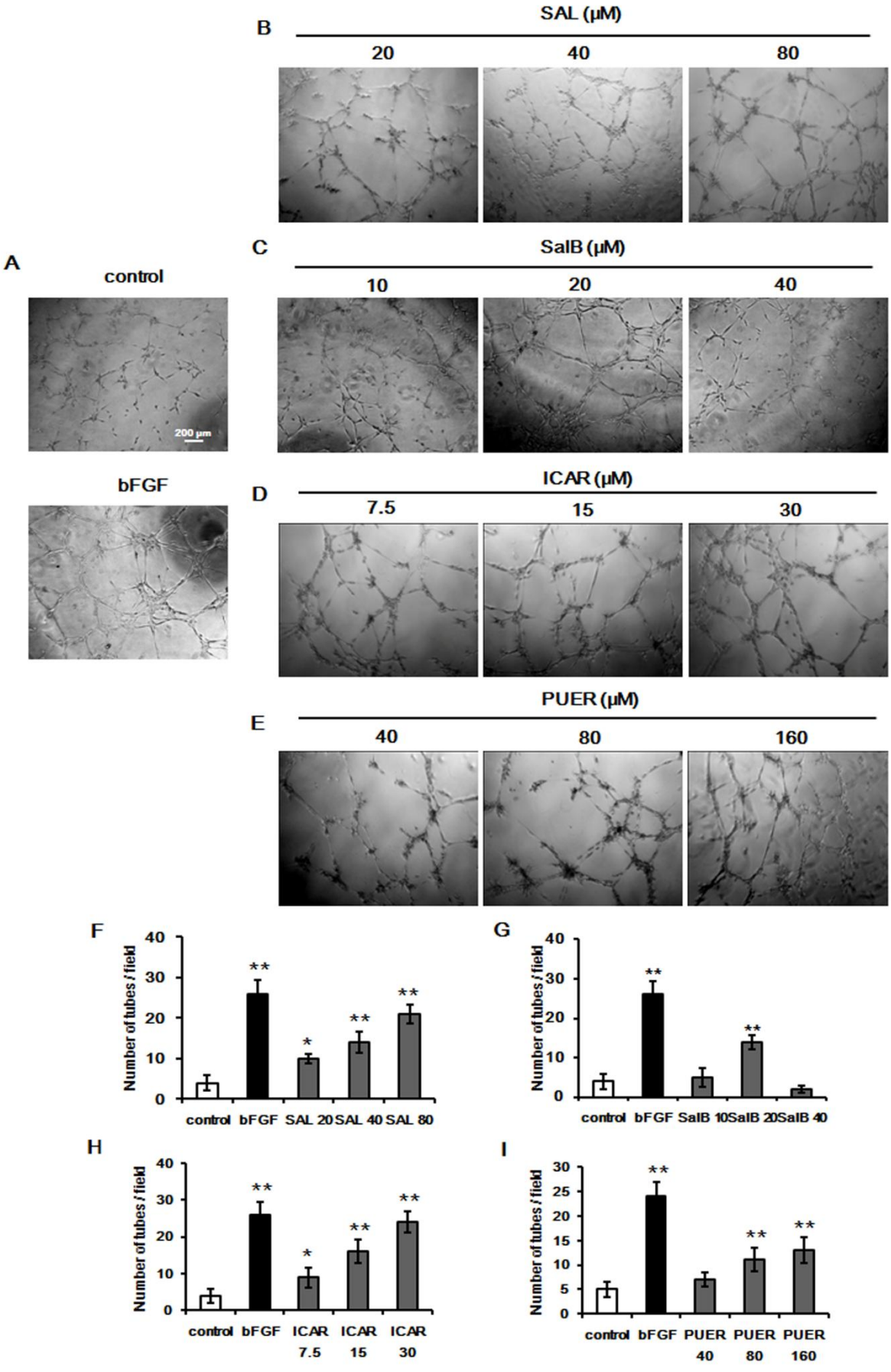
A
control
200 μm
bFGF
B
SAL (μM)
20
40
80
C
SalB (μM)
10
20
40
D
ICAR (μM)
7.5
15
30
E
PUER (μM)
40
80
160
F
Number of tubes / field
control
bFGF
SAL 20
SAL 40
SAL 80
G
Number of tubes / field
control
bFGF
SalB 10
SalB 20
SalB 40
H
Number of tubes / field
control
bFGF
ICAR 7.5
ICAR 15
ICAR 30
I
Number of tubes / field
control
bFGF
PUER 40
PUER 80
PUER 160

Figure 11. Effect of SAL, SalB, ICAR and PUER on capillary tube formation of BM-EPCs. (A-E) After TCM extracts treatment cells were grown on MatrigelTM for 18 h under normal growth conditions, capillary tube formation was observed by inverted light microscopy. (F-I) Five independent fields were assessed for each well and the average numbers of tubes/40× magnified field were determined. Data are expressed as mean ± SD, n=5, $^{*}P < 0.05$, $^{**}P < 0.01$ versus control group.

3.1.6 SAL and ICAR increase VEGF secretion and NO production in BM-EPCs

In the light of the important role of VEGF and NO in the regulation of angiogenesis and cell function, we treated EPCs with SAL or ICAR at different concentrations, and determined VEGF and NO production in the cell supernatants. Over a period of 24 h and 48 h incubation, SAL at both 40 μM and 80 μM enhanced the VEGF secretion by approximately 11.3% (24 h, 40 μM), 17.5% (24 h, 80 μM), 18.9% (48 h, 40 μM) and 21.0% (48 h, 80 μM) compared to respective controls (Figure 12A). ICAR enhanced the VEGF secretion in a time and concentration-dependent manner by 20.4% (24 h, 15 μM), 36.7% (24 h, 30 μM), 23.8% (48 h, 15 μM) and 30.0% (48 h, 30 μM) compared to respective controls (Figure 12B).

Moreover, NO production of BM-EPCs increased significantly when cells were stimulated by SAL or ICAR for 2, 5, 8, and 10 d (Figure 12C, 12D). These findings imply that the increased VEGF and NO production may play an important role in the enhanced tube formation ability of BM-EPCs induced by TCM extracts. Furthermore, we used N^{G}-nitro-L-arginine methyl ester (L-NAME) which is a selective inhibitor of NOS to examine the role of NO underlying the angiogenic effect of SAL. As shown in Figure 12E, L-NAME could significantly inhibit SAL-induced NO production after 2 d incubation. Furthermore, the promotion effect of SAL on migration and capillary tube formation ability on EPCs were suppressed by L-NAME (Figure 12F, 12G). The present study further supports the notion that endothelium-derived NO plays a key role in angiogenesis.

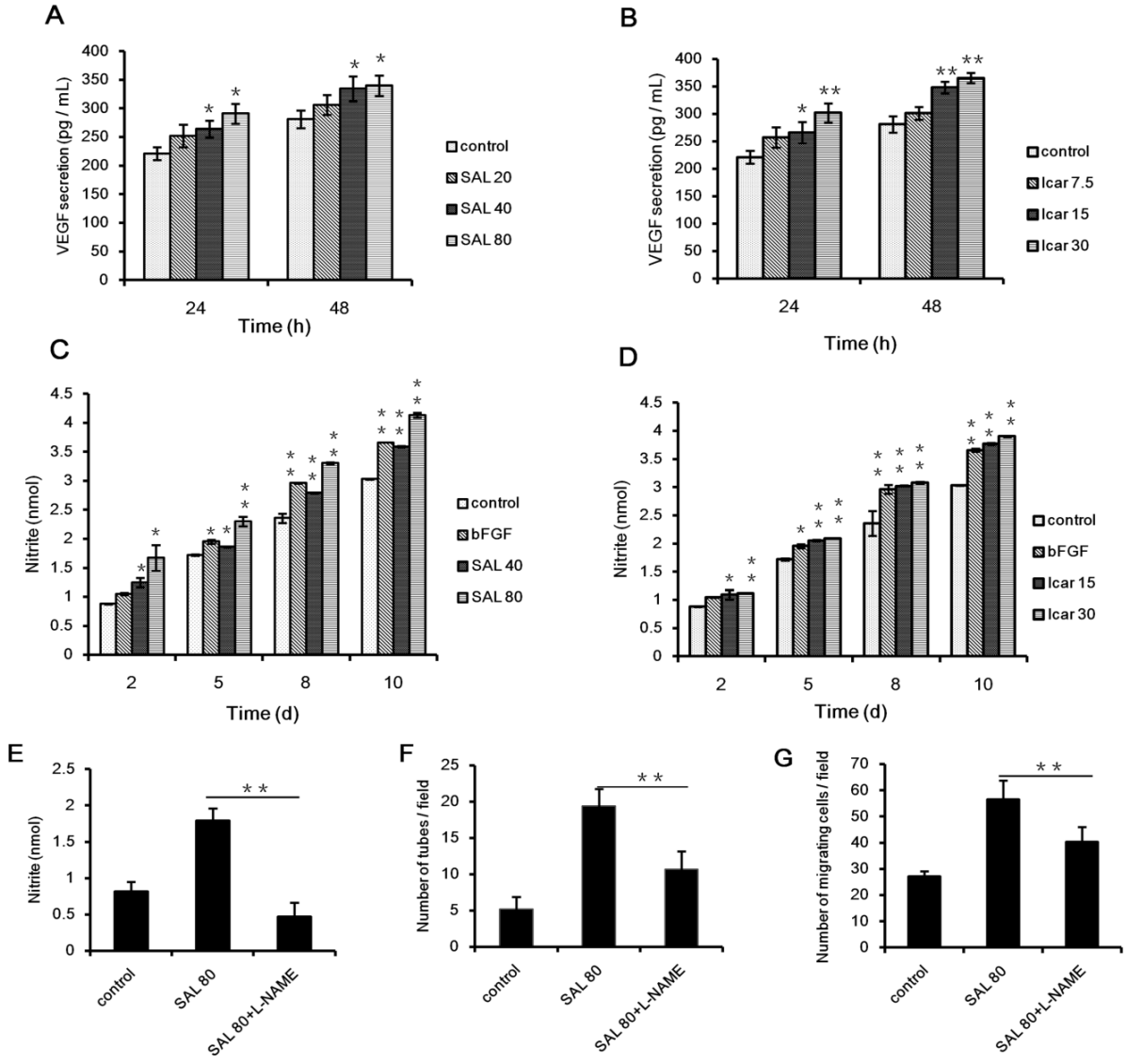

Figure 12. SAL and ICAR enhance the secretion of VEGF and the production of NO in BM-EPCs. Cells were cultured until confluency in 96-well plates and subsequently stimulated with indicated concentrations of TCM extracts. (A, B) Cell culture supernatants collected after 24 h and 48 h VEGF secretion was determined by ELISA, n=5. (C, D) To assess NO production, cell culture supernatants were collected 2, 5, 8, and 10 d after SAL or ICAR stimulation and analyzed by Griess assay, n=4. (E) Cell culture supernatants were collected 48 h after SAL stimulation with or without 10 μM L-NAME, NO levels were measured by Griess assay, n=3. (F, G) BM-EPCs were treated with 10 μM L-NAME and 80 μM SAL for 48 h. Cell migratory ability was evaluated by performing cell counts of 10 random fields,

n=4. Capillary-like tube formation were determined by assessing average numbers of tubes/40× magnified field, n=3. All data are presented as mean ± SD, $^{*}P < 0.05$, $^{**}P < 0.01$ versus control group.

3.1.7 SAL, SalB and ICAR induce angiogenic gene expression in BM-EPCs

To determine the underlying mechanism involved in the proangiogenic effects of TCM extracts, the expression of VEGF, KDR, eNOS, vWF, PECAM-1 and VE-cadherin were determined by quantitative RT-PCR. As shown in Figure 13A, the expression levels of VEGF, KDR, and eNOS significantly increased after 2 d (1.46 ± 0.24-fold, 1.96 ± 0.20-fold, 2.82 ± 0.37-fold) and 10 d (1.61 ± 0.15-fold, 1.66 ± 0.22-fold, 3.18 ± 0.42-fold) pretreatment with 80 μM SAL. While vWF gene expression was enhanced after 2 d (1.79 ± 0.22-fold) and 10 d (2.20 ± 0.29-fold) cultivation, PECAM-1 expression was increased only after 2 d (2.01 ± 0.18-fold) cultivation (Figure 13A). VE-cadherin expression was downregulated by 67.8% after 2 d and by 78.0% after 10 d with a similar trend for bFGF expression (Figure 13A). As shown in Figure 13B, the expression levels of VEGF, KDR, eNOS and PECAM-1 significantly increased after 2 d (2.27 ± 0.11-fold, 2.53 ± 0.06-fold, 2.27 ± 0.12-fold, 1.83 ± 0.10-fold) ($P < 0.01$) and 10 d (2.37 ± 0.06-fold, 1.51 ± 0.16-fold, 2.56 ± 0.15-fold, 1.84 ± 0.15-fold,) ($P < 0.01$) pretreatment with 20 μM SalB. In contrast, VE-cadherin expression was downregulated by 83.9% after 2 d and by 51.8% after 10 d. However, vWF gene expression was not affected by SalB administration. In Figure 13C, the expression levels of VEGF, KDR, and eNOS significantly increased after 2 d (2.80 ± 0.17-fold, 2.58 ± 0.16-fold, 3.68 ± 0.33-fold) and 10 d (3.11 ± 0.12-fold, 1.71 ± 0.14-fold, 3.66 ± 0.29-fold) pretreatment with 30 μM ICAR. PECAM-1 expression was increased only after 2 d (2.56 ± 0.06-fold, $P < 0.01$) cultivation, but reduced after 10 d treatment (0.42 ± 0.05-fold, $P < 0.01$). VE-cadherin expression was downregulated by 98.7% after 2 d and by 99.0% after 10 d with a similar trend for bFGF expression. But vWF gene expression was not affected by ICAR treatment (Figure 13C).

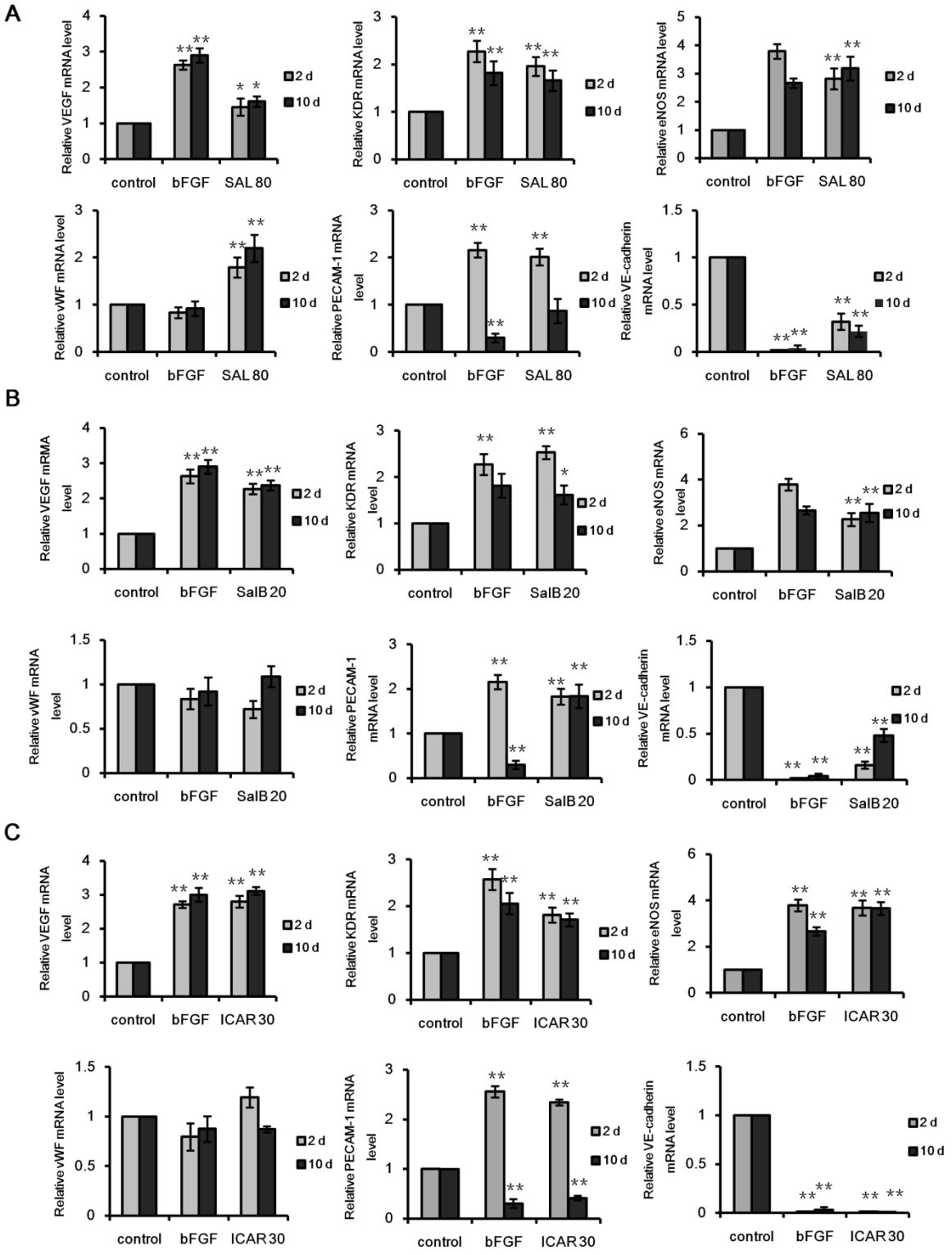

Figure 13. Gene expression analysis of SAL, SalB and ICAR-treated BM-EPCs. BM-EPCs were cultivated in endothelial basal medium with or without 80 μM SAL (A), 20 μM (B), 30 μM ICAR (C) for 2 and 10 d. Gene expression levels of VEGF, KDR, eNOS, VE-cadherin, vWF and PECAM-1 were

assessed via quantitative RT-PCR. Data were normalized to GAPDH expression and fold changes were calculated by the $2^{-\Delta\Delta CT}$ method, n=5, $^{*}P < 0.05$, $^{**}P < 0.01$ versus control group.

3.1.8 SAL and ICAR induce angiogenic differentiation via Akt/mTOR/p70S6K signaling pathways

Evaluating key pathway components involved in cellular function and angiogenesis we found that SAL effectively triggered the phosphorylation of mTOR signaling cascade, including Akt, mTOR, and p70S6K (Ser371) in BM-EPCs in a concentration-dependent manner (Figure 14A). Furthermore, we used the highly specific PI3-K inhibitor LY294002 to assess the role of the PI3-K/Akt pathway in angiogenesis. Unexpectedly, LY294002 inhibited not only Akt, but also notably phosphorylated mTOR (Figure 14B). Cell migration and tube formation ability were significantly decreased when SAL was co-administered with LY294002 (Figure 14D, 14E), suggesting that SAL promotes cell mobility and angiogenesis through activating the Akt/mTOR signaling pathway. To further define the roles of MAPK in the SAL-induced effects on BM-EPCs, we analyzed the expression of phosphorylated ERK1/2, p38 MAPK, and JNK following SAL treatment. As demonstrated in Figure 14A, the phosphorylation levels of ERK1/2 were increased after SAL treatment for 48 h. However, no significant changes of phosphorylation levels of p38 MAPK and JNK were observed after SAL treatment. Additionally, application of ERK 1/2 inhibitor U0126 also markedly reduced the phosphorylated expression of mTOR (Figure 14C) and blocked SAL-induced cell migration as well as angiogenesis (Figure 14D, 14E). This implies that, by interaction with mTOR, ERK1/2 is a potential target of SAL in BM-EPCs.

As shown in Figure 14F, treatment with ICAR (30 μM) alone significantly increased the expression of p-mTOR, p-p70S6K, and p-4EBP1 within 48 h. The phosphorylation of mTOR, p70S6K and 4EBP1 by ICAR was prevented with application of LY294002 (20 μM) (Figure 14G), illustrating again that phosphorylation of mTOR/p70S6K/4EBP1 was dependent upon activation of the PI 3-K pathway. Moreover, the promotion effect of ICAR

on migration and capillary tube formation ability were suppressed by rapamycin (Figure 14H, 14I), which imply a possible role of mTOR in the cell motility and angiogenesis ability. To further demonstrate the downstream protein that may regulate the effect of ICAR, we used specific siRNA to silence the 4EBP1 gene expression in EPCs. qRT-PCR and Western blot analysis were performed to ensure the adequate knocking down of 4EBP1 (Figure 14J). We observed that the tube formation induced by ICAR was suppressed markedly when 4EBP1 was silenced (Figure 14K). Interestingly, when 4EBP1 is downregulated, rapamycin inhibition of both basal and ICAR-stimulated cell motility was dramatically attenuated (Figure 14L).

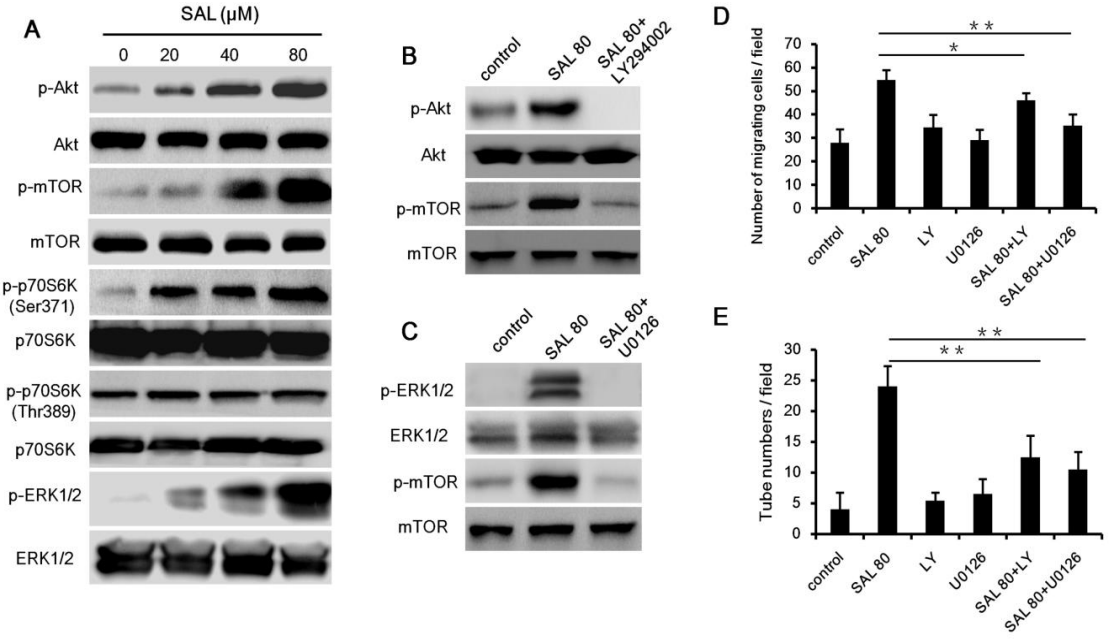

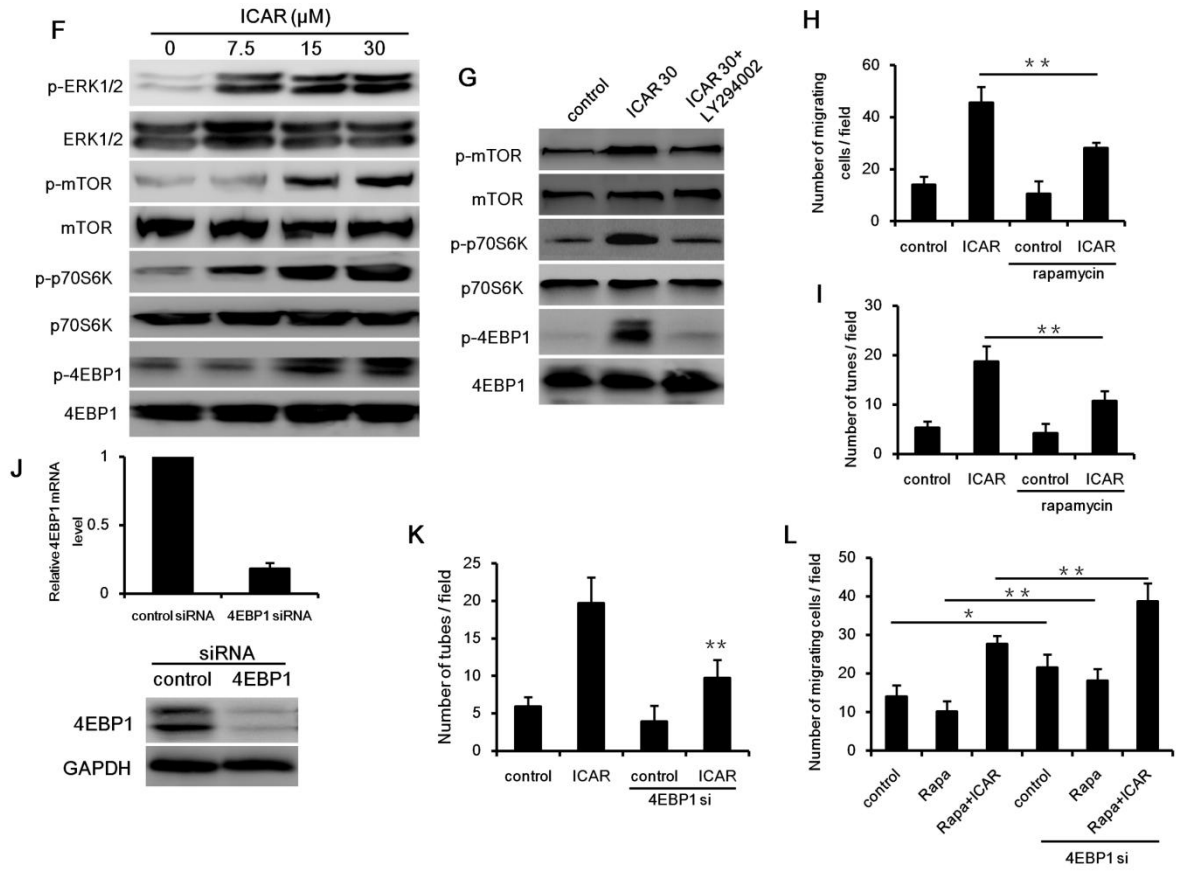

Figure 14. Signal pathway analysis of SAL and ICAR-treated BM-EPCs. (A, F) BM-EPCs were treated with or without TCM extracts for 48 h and then harvested. Total cell lysates were prepared and subjected to sodium dodecyl sulfate polyacrylamide gel electrophoresis, followed by Western blot analysis. The immunoblots shown are representative of at least three independent experiments with comparable results. (B, C, G) BM-EPCs were pretreated with 20 μM LY294002 or 10 μM U0126 for 90 min, then cultured with SAL or ICAR for 48 h. Protein expression was analyzed by Western blot analysis. (D, E, H, I) BM-EPCs were treated under the same conditions described above, cell migratory ability and capillary-like tube formation were determined by the methods as above, n=3. (J) BM-EPCs were transfected with 4EBP1-specific or non-specific siRNA. 48 h after transfection, mRNA and protein expression were measured to determine the efficiency of the silence. (K, L) BM-EPCs were incubated in the absence or presence of 4EBP1 siRNA for 48 h, then treated with rapamycin for 90 min, and stimulated by ICAR for 48 h, capillary-like tube formation and cell migration ability were determined by the methods as above, n=4. All data are presented as mean ± SD. $^{*}P < 0.05$, $^{**}P < 0.01$.

3.1.9 SAL augments bone healing *in vivo*

Therapeutic benefit of growth factor and SAL *in vivo* by embedding into the mineralized collagen scaffold were tested in femoral critical-size bone defect of immunodeficient mice. As shown in Figure 15E-G, after 6 weeks, the therapy with BMP-2 or SAL both resulted in an significant augment in total bone growth compared to the control group as corroborated by micro-CT.

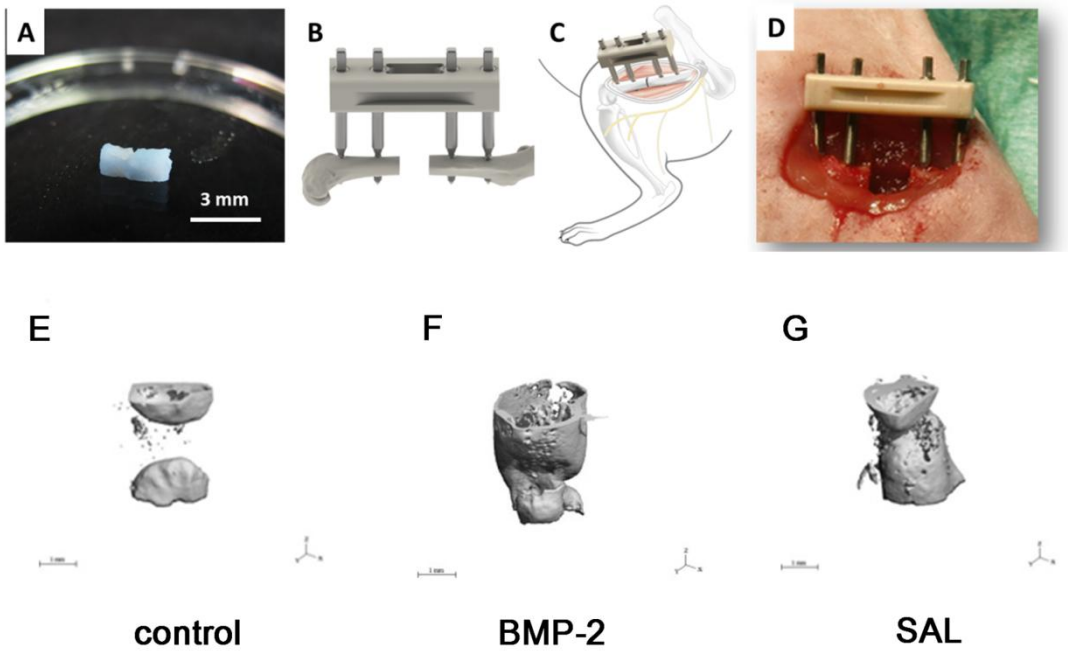

Figure 15. SAL augments bone healing *in vivo*. (A) Representative picture of the mineralized collagen scaffolds. (B-D) The external fixator that was used in the animal study and the murine defect model. (E, F, G) Representative μCT images of a murine bone defect after 6 weeks, that was treated with mineralized collagen scaffolds functionalized with SAL or BMP-2. In animals treated with SAL-functionalized implants, improved bone formation was observed (images kindly provided by Dr. Stefan Zwingenberger, Stiehler group).

3.2 TCM extracts prevent oxidative stress-mediated dysfunction in bone marrow derived-endothelial progenitor cell

3.2.1 SAL, SalB and ICAR inhibit cell death induced by H_2O_2

Although TCM extracts significantly enhanced the cell function *in vitro*, we wanted to investigate whether TCM extracts protect cell cultures from H_2O_2-induced apoptosis. To assess the consequences of TCM extracts treatment on the apoptotic effect induced by H_2O_2, BM-EPCs were double-stained with calcein-AM/EthD-1. While in the absence of H_2O_2 nearly all cells were alive, the addition of 1 mM H_2O_2 induced a significant level of apoptosis, as showed by contraction and nuclear membrane creasing. In contrast, very few cells preincubated with SAL, SalB or ICAR were EthD-1-positive. Cell retained good morphology without cytoplasm injury (Figure 16A), indicating a protective effect of SAL from H_2O_2 induced cell death.

As shown in Figure 16B, 48 h preincubation with 40 and 80 μM SAL dose-dependently attenuated the H_2O_2-induced cell death by 14.7% and 25.0%, respectively. Notably, cell death was also remarkably attenuated by 28.4% and 36.8% when pretreated with 10 μM and 20 μM SalB, respectively. And the pretreatment with ICAR at 15 and 30 μM reduced the cell death by 38.3% and 42.4%, respectively.

Furthermore, LDH levels in the cell culture supernatant significantly increased after exposure to 1 mM H_2O_2 (Figure 16C, 42.0 ± 1.5%, $P < 0.01$). The considerable adverse effect of H_2O_2 was significantly attenuated by pretreatment of BM-EPCs with 80 μM SAL (29.9 ± 1.1%), 10 μM (21.9 ± 1.3%) and 20 μM (19.4 ± 0.6) SalB, as well as 15 μM (28.4 ± 1.4%) and 30 μM (19.5% ± 2.1%) ICAR, but not in the control group. These results demonstrated that TCM extracts can obviously protect BM-EPCs against H_2O_2-induced cell damage (Figure 16C).

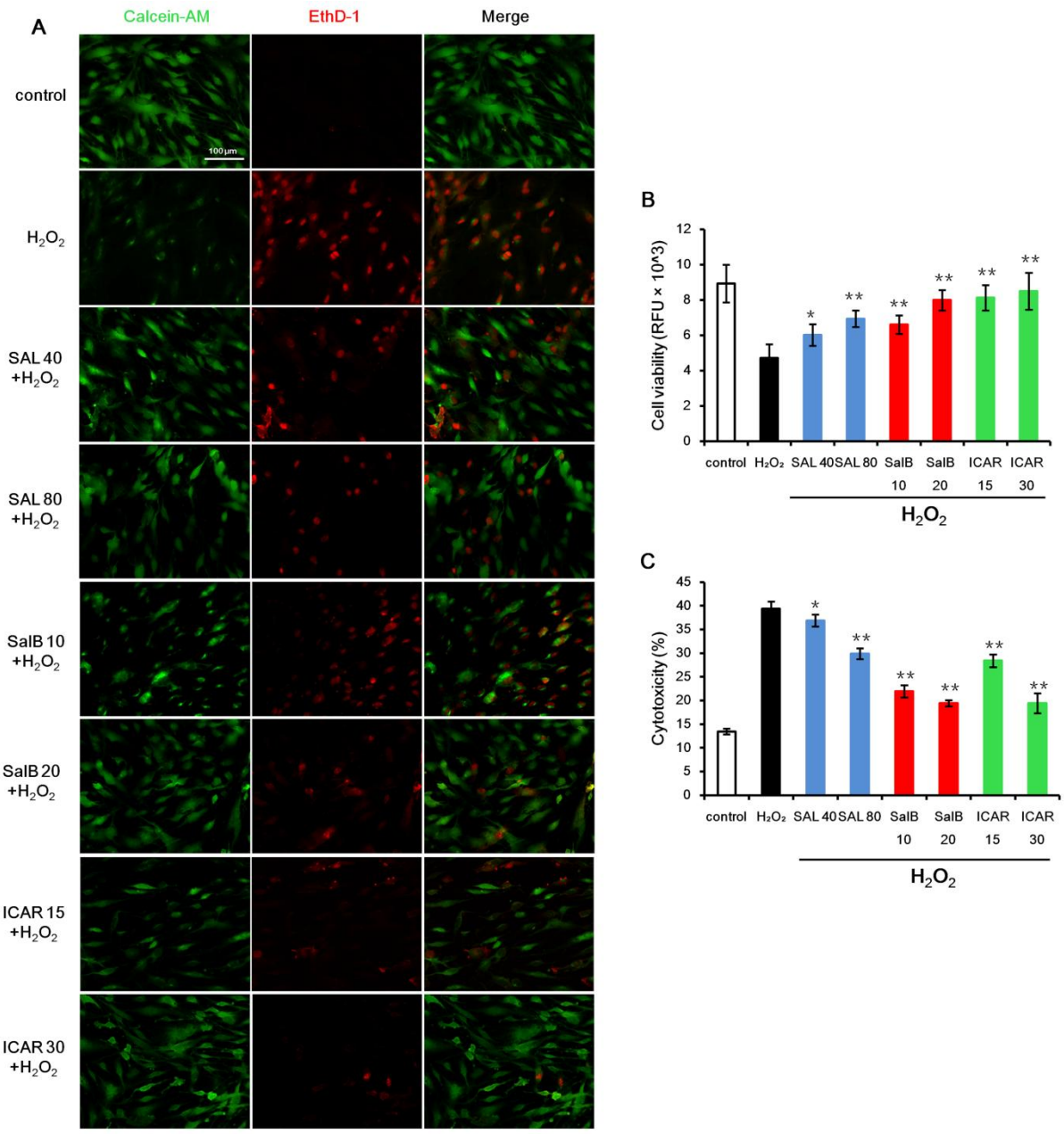

Figure 16. SAL, SalB and ICAR protect BM-EPCs from H_2O_2-induced cell damage. (A) Cells were pretreated with indicated concentrations of TCM extracts and stressed by 1 mM H_2O_2. Cell survival was monitored by calcein AM/EthD-1 double staining and analyzed qualitatively by fluorescence microscopy. Representative micrographs from each treatment group are shown. (B) After the treatment with TCM extracts and induction by 1 mM H_2O_2, BM-EPCs were washed with PBS and cellular viability was evaluated by quantification of DNA content, n=6. (C) Cell death was evaluated by LDH assay, n=4. All data are expressed as mean ± SD. $^{*}P < 0.05$, $^{**}P < 0.01$ versus H_2O_2 group.

3.2.2 SAL and SalB suppress H_2O_2-induced production of ROS and NADPH expression

As shown in Figure 17A and 17B, when compared with BM-EPCs incubated in EBM-2 alone, the addition of SAL to the cells did not affect the amount of ROS produced (104.8% ± 10.0% at 40 μM SAL and 97.5% ± 4.1% at 80 μM SAL, respectively). However, after exposure to 1 mM H_2O_2 for 6 h, fluorescence from the cells stained with DCFDA indicated that intracellular ROS had accumulated significantly in BM-EPCs (368.8% ± 8.3% control w/ H_2O_2 vs. control w/o H_2O_2), but pretreatment with SAL annihilated ROS production to nearly normal levels (160.2% ± 14.7% at 40 μM SAL and 147.3% ± 12.8% at 80 μM SAL, respectively).

The multimeric enzyme complex NADPH oxidase (Nox) is the major enzyme system generating superoxide in the vasculature. H_2O_2 markedly stimulatated NADPH oxidase activity suggesting that NADPH oxidase is an important source of H_2O_2-induced oxidative stress in BM-EPCs. Pretreatment with SAL (40 μM and 80 μM) significantly decreased H_2O_2-induced NADPH production by 23.1% ± 2.3% and 29.4% ± 1.0% respectively (Figure 17C). Hence SAL has a potent antioxidant activity on H_2O_2-induced ROS production and this may be mediated partly through inhibition of NADPH oxidase activity. To highlight the role of NADPH, diphenyliodonium (DPI) as an NADPH oxidase inhibitor was added to the cells for 90 min before H_2O_2 stimulation. DPI (10 μM) treatment significantly attenuated H_2O_2-induced generation of ROS and damage on cellular viability, and showed an enhanced effect when combined with 80 μM SAL (Figure 17D, 17E).

As shown in Figure 17F, 48 pretreatment with SalB (10 μM and 20 μM) also annihilated ROS production to nearly physiological levels (146.8% ± 5.9% and 109.1% ± 9.0% for 10 and 20 μM SalB, respectively) and decreased H_2O_2-induced NADPH production by 13.7% ± 1.2% and 37.0% ± 1.4%, respectively (Figure 17H). Additionally, compared to cells treated with H_2O_2, also NO generation was restored by SalB to a physiological level (Figure 17I). In an effort to confirm the protective effect of SalB

qRT-PCR revealed that mRNA expression levels of both both Nox4 and eNOS were considerably decreased by SalB ($P < 0.01$) (Figure 17J, 17K). Interestingly, treatment of BM-EPCs with 10 μM eNOS inhibitor L-NAME significantly prevented cell damage as demonstrated by decreased ROS generation (64.6% of H_2O_2 group, $P < 0.01$) and DHE level (74.0% of H_2O_2 group, $P < 0.05$) (Figure 17L, 17M), and enhanced the inhibitory effect of SalB. This finding indicates that the protective effect of SalB was at least partially dependent on the cells' ability to downregulate eNOS.

In order to evaluate the role of NADPH in this context, the NADPH oxidase inhibitor diphenyleneiodonium (DPI) was added prior to H_2O_2 stimulation. As shown in Figure 17N, 17O, DPI (10 μM) treatment significantly attenuated H_2O_2-induced Nox4 and eNOS expression, and undermined the suppressive effect exerted by SalB.

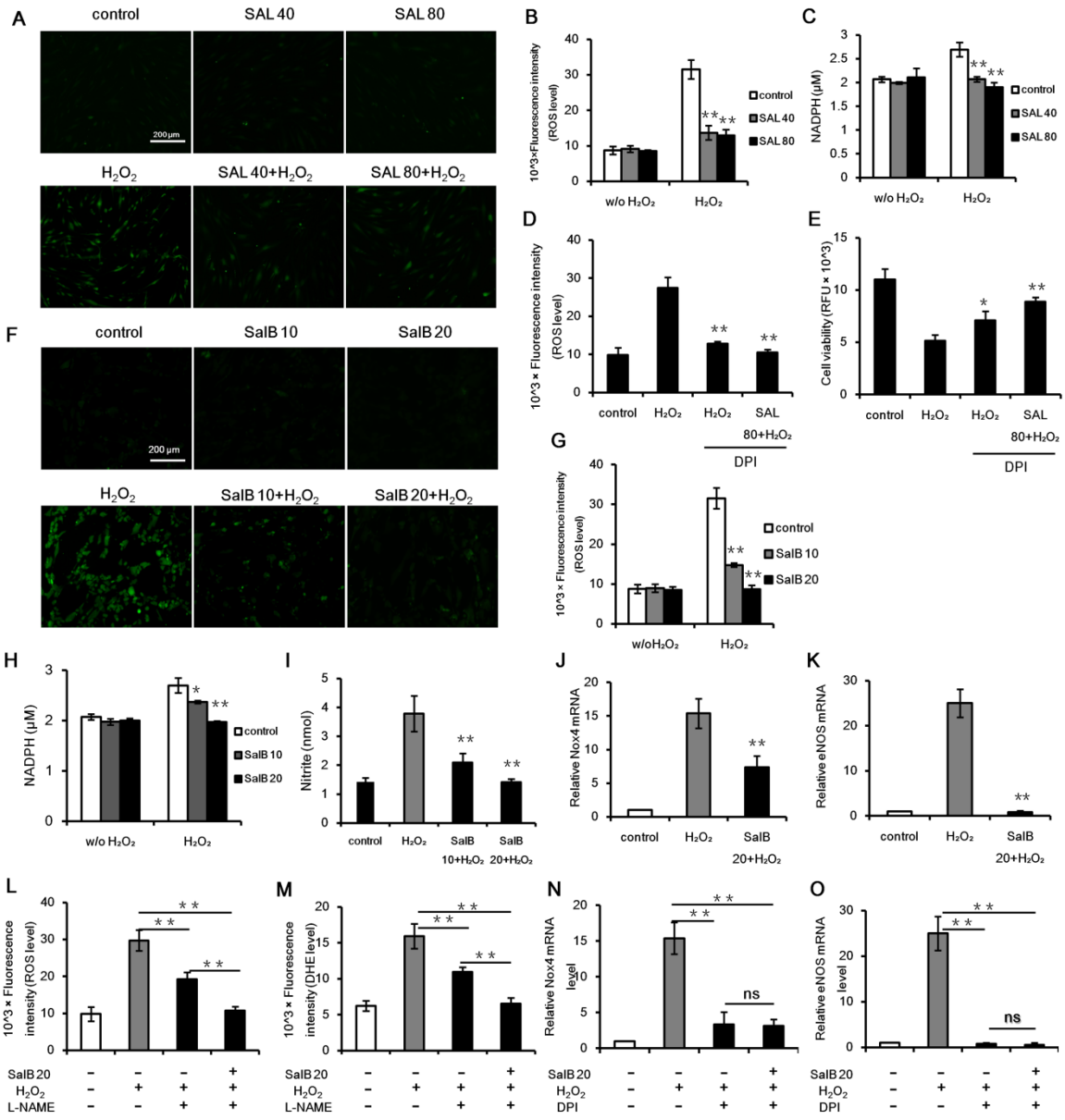

Figure 17. SAL and SalB suppress H_2O_2-induced production of ROS and NADPH expression. (A, F) Cells were pretreated with 40 and 80 μM SAL, or 10 and 20 μM SalB for 48 h, labeled with 30 μM DCFH-DA and subsequently stressed with H_2O_2 for 6 h prior to fluorescence microscopy. (B, G) Production of ROS was quantified by the amount of DCF formed in the BM-EPCs. The fluorescence intensity was measured using a microplate reader, n=6. (C, H) Cells were treated with 40 and 80 μM SAL, or 10 and 20 μM SalB for 48 h, followed by H_2O_2 treatment for 6 h. NADPH oxidase activity was measured colorimetrically using NADP/NADPH assay kit, n=5. (D, E) Cells were treated with 40 and 80 μM SAL for 48 h, and then stimulated with H_2O_2 for 6 h with pretreatment of 10 μM DPI. ROS was

quantified by DCF formation as described above (n=4), and cellular viability was evaluated by quantification of DNA content (n=3). (I) Cells were treated with 10 and 20 μM SalB for 48 h, and then stimulated with H_2O_2 for 6 h. Cell culture supernatants were collected and analyzed by Griess assay, n=4. (J, K) qRT-PCR was performed to measure Nox4 and eNOS mRNA expression levels in BM-EPCs in response to H_2O_2 stimulation with or without pretreatment by SalB over 48 h, n=4. (L, M) BM-EPCs were pretreated with SalB for 48 h, then incubated with 10 μM L-NAME for 90 min followed by 1 mM H_2O_2 for 6 h, ROS production and DHE level were assessed by fluorescence quantification, n=3. BM-EPCs were treated with 1 mM H_2O_2 in the absence or presence of 10 μM NOS inhibitor L-NAME, ROS production and mRNA level of Nox4 were assessed by DCF quantification (n=3) and by qRT-PCR, n=4. (N, O) BM-EPCs were pretreated with SalB for 48 h, then incubated with 10 μM DPI for 60 min followed by 1 mM H_2O_2 for 6 h, Nox4 and eNOS mRNA expression was quantified by qRT-PCR, n=4. All data are expressed as mean ± SD, $^{*}P < 0.05$, $^{**}P < 0.01$ versus H_2O_2 group.

3.2.3 SAL, SalB and ICAR protect mitochondrial function and inhibit mitochondrion-induced apoptosis

Furthermore, the mitochondrial function of the BM-EPCs was monitored using the fluorescent dye Rhodamine 123. After incubation with H_2O_2 for 6 h, the mean fluorescence intensity of Rhodamine 123 decreased to 65.5% compared to control cells, respectively (Figure 18A, 18B), representing a loss of MMP and a special oxidation of mitochondria. SAL (40 and 80 μM), SalB (10 and 20 μM), ICAR (15 and 30 μM) all alleviated mitochondrial injury remarkably, which restored the potential to nearly normal levels (Figure 18B). Moreover, the cells exposed to H_2O_2 exhibited enhanced DHE fluorescence when compared with control cells (Figure 18C). But the increase in DHE fluorescence in response to H_2O_2 was remarkably prevented by co-administration of SAL, SalB or ICAR (Figure 18A, 18C), which implied a suppression effect of superoxide radicals production imposed by TCM extracts. Furthermore, the method of Annexin V-FITC and PI double staining was employed to investigate the effect of SAL on H_2O_2-induced apoptosis. As

shown in Figure 18D, the apoptosis and necrosis rate were decreased significantly after cells were treated with both 40 and 80 μM SAL for 48 h.

Bcl-xL and Bax expression levels were detected to assess mitochondrial related apoptosis. The immunofluorescence data showed significantly increased Bax levels upon H_2O_2 stimulation and markedly attenuated levels of the apoptosis marker after 48 h SalB (10 and 20 μM) pretreatment (Figure 18E). On the other hand Bcl-xL expression was declined in H_2O_2-stressed BM-EPCs and restored in the presence of 10 and 20 μM SalB (Figure 18F). Immunoblot analysis supported this finding demonstrating that SalB reversed both H_2O_2-induced increased Bax/Bcl-xL ratio and oxidative stress activated cleaved PARP, cleaved caspase-3 protein expression, as well as cytochrome c release (Figure 18F). These findings suggest that SalB counteracts mitochondria-mediated apoptosis by modulating Bcl-2 family proteins.

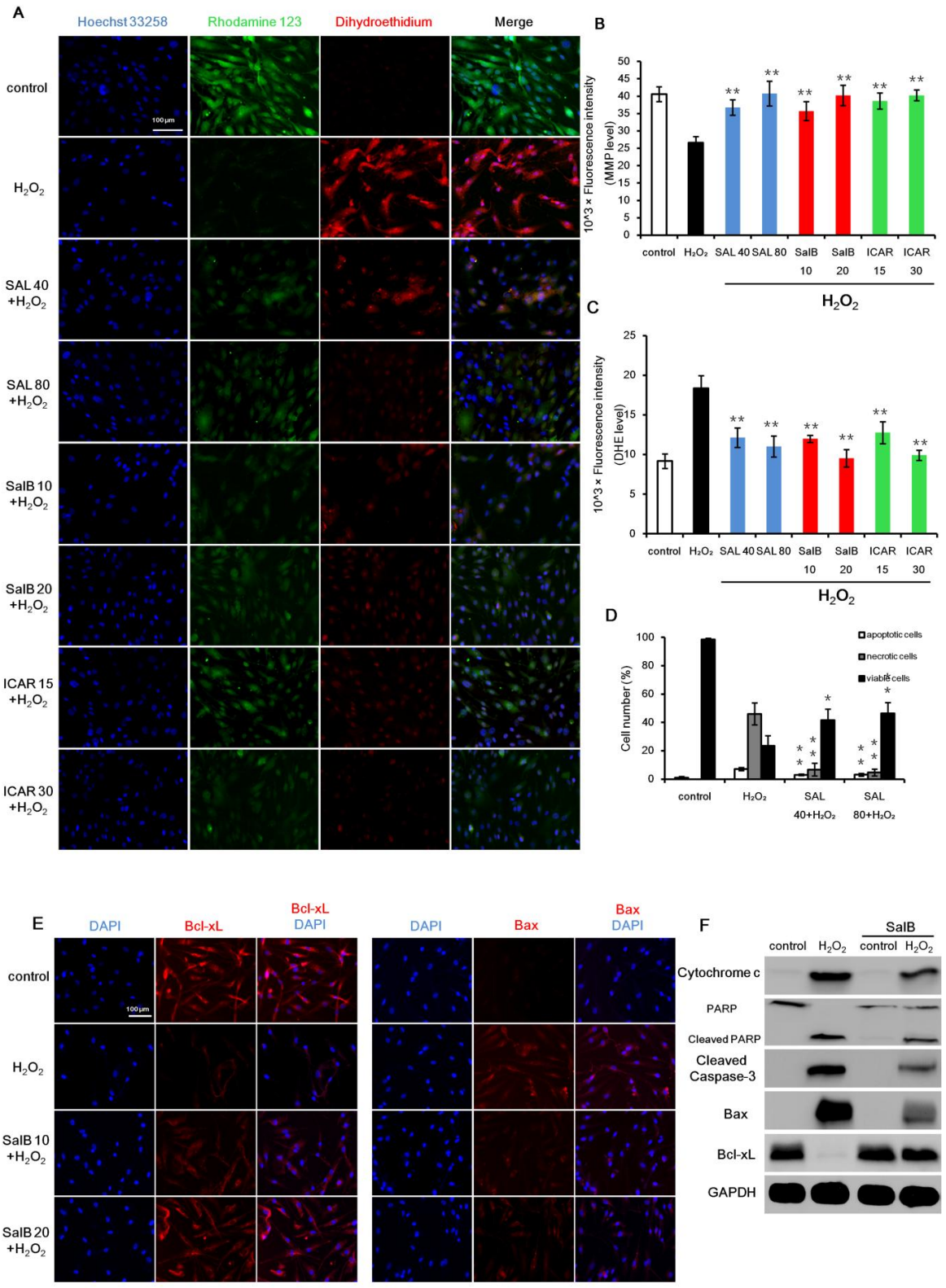

Figure 18. SAL, SalB and ICAR inhibit H_2O_2-induced cell apoptosis. BM-EPCs were pretreated with indicated concentrations of TCM extracts for 48 h and stressed by 1 mM H_2O_2. (A) Then cells were

labeled with the fluorescent dye Rhodamine 123, the superoxide indicator DHE and the nucleic acid stain Hoechst 33258, n=4. (B) BM-EPCs were loaded with 5 μM Rhodamine 123. After 20 min incubation in the dark, cells were washed twice with phosphate buffered saline, and the plates were immediately read using a fluorescent plate reader, n=5. (C) Cells were probed with 10 μM DHE for 30 min, fluorescence intensity was acquired using a fluorescent plate reader, n=4. (D) Cells were harvested and labeled with a combination of annexin V-FITC and PI. H_2O_2-induced apoptosis was determined by flow cytometry, n=3. (E) Immunofluorescence. Bcl-xL and Bax were stained with primary antibodies followed by staining with secondary Cy3-conjugated antibody. Cell nuclei were labeled with DAPI and immunofluorescence analysis was performed under the fluorescence microscope. (F) Relative changes in cytochrome c, PARP, cleaved caspase-3, Bax and Bcl-xL protein levels were analyzed by Western blot. GAPDH was used as a loading control. All data are expressed as mean ± SD, $^{*}P < 0.05$, $^{**}P < 0.01$ versus H_2O_2 group.

3.2.4 SAL protects BM-EPCs from H_2O_2-induced injury through JNK, p38 MAPK pathways and modulates the levels of Bcl-2 family proteins

In order to investigate the mechanisms underlying SALs protective effect towards oxidative stress, the expression of Nox4, STAT-3 as well as some endothelial genes was investigated. The results showed that Nox4 as well as STAT-3 expression was decreased considerably (Figure 19A). Compared to cells treated with H_2O_2, gene expression of VEGF of SAL-stimulated cells was increased to nearly the same level found in H_2O_2-untreated cells. BM-EPCs preincubated with SAL and treated with H_2O_2 also showed an enhanced KDR expression. Compared to untreated cells, H_2O_2-stimulated cells showed a significantly higher eNOS expression. However, pretreatment with SAL for 48 h attenuated this increase to a normal level (Figure 19A).

Since Bcl-2 family proteins play important roles in apoptosis by functioning as promoters or inhibitors of cell death processes, we next studied the changes in the levels of Bax/Bcl-xL in BM-EPCs after exposing to H_2O_2. Western blot analysis showed that 1 mM H_2O_2 caused a profound up-regulation of pro-apoptotic protein Bax and downregulation of

Bcl-xL, which strongly increased the ratio of Bax/Bcl-xL. But SAL preincubation reversed this high ratio of Bax/Bcl-xL notably by declining Bax and restoring Bcl-xL expression (Figure 19B). To further elucidate the underlying mechanisms of the protective effect of SAL, phosphorylation of JNK, p38 MAPK and ERK1/2 were determined. As shown in Figure 19B, stimulation of BM-EPCs with H_2O_2 induced the phosphorylation of all the three targets, whereas SAL pretreatment significantly inhibited the upregulation of both phosphorylated JNK and p38 MAPK, but not ERK1/2.

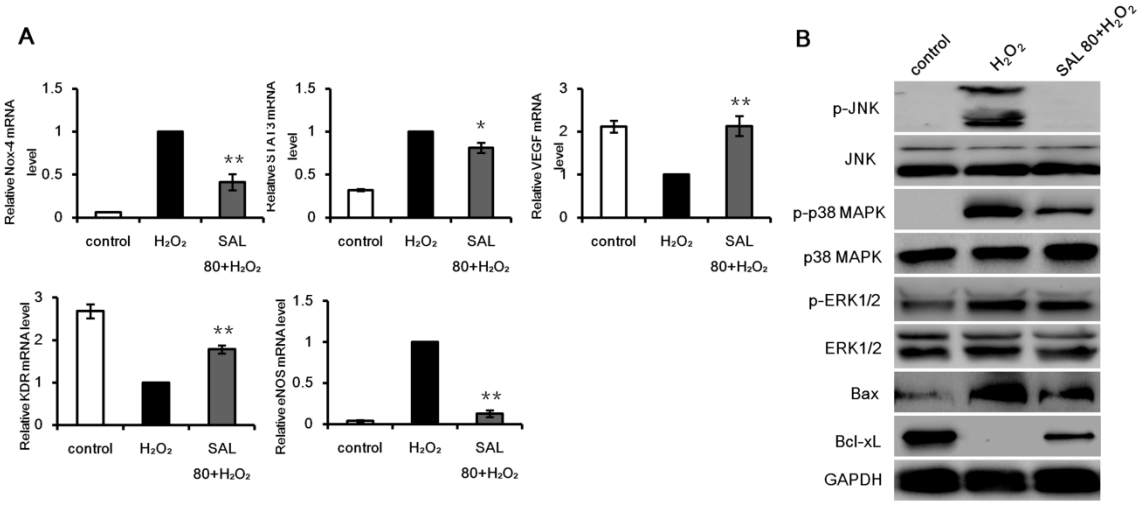

Figure 19. Gene expression and signal pathway analysis of SAL-treated BM-EPCs upon oxidative stress. (A) BM-EPCs were treated with 80 μM SAL for 2 d, then incubated with 1 mM H_2O_2 for 6 h and gene expression levels of Nox4, STAT3, VEGF, KDR, eNOS were determined, n=3. (B) Cells were incubated without or with 80 μM SAL for 48 h before stimulation with 1 mM H_2O_2. Total protein (30 μg) was isolated from the cells, applied to Western blot and probed with specific antibodies. The immunoblots shown here are representative of at least three independent experiments with similar results. All data are presented as mean ± SD. $^{*}P < 0.05$, $^{**}P < 0.01$ versus H_2O_2 group.

3.2.5 SalB exerts its cytoprotective potential via mTOR signaling pathway

Cellular proliferation and survival require the involvement of mTOR and phosphoinositide 3-kinase (PI3-K)/Akt pathways (Sato et al., 2010). Since SalB employs

mTOR to modulate the phosphorylation of p70S6K and 4EBP1, we assessed whether the cytoprotective effects SalB also involves the Akt/mTOR pathway. BM-EPCs were stressed by 1 mM H_2O_2 for 6 h prior to protein extraction and Western blot analysis. As shown in Figure 20A, H_2O_2 induction almost blocked the expression of p-mTOR, as well as p-p70S6K and p-4EBP1, while SalB (20 μM) significantly restored the expression of these proteins in the presence of H_2O_2. We hypothesized that mTOR/p70S6K/4EBP1 activation is responsible for the observed increased cell survival in response to H_2O_2 and thus performed inhibiting experiments by use of rapamycin. As shown in Figure 20B, rapamycin completely reversed SalB-mediated mTOR/p70S6K/4EBP1 phosphorylation in response to H_2O_2. Furthermore, increased expression of p-mTOR, p-p70S6K and p-4EBP1 by SalB during H_2O_2 exposure was blocked during application of the PI3-K inhibitor LY294002 (20 μM) (Figure 20C). In addition, a considerable decrease in cell survival rate was found when rapamycin (73.9% of SalB+H_2O_2 group, $P < 0.01$) or LY294002 (77.1% of SalB+H_2O_2 group, $P < 0.01$) were applied combined with SalB (Figure 20D). These results demonstrated that SalB exerted its cytoprotective potential via mTOR signaling pathway.

To further demonstrate the downstream protein that may regulate the effect of SalB, we used specific siRNA to silence the 4EBP1 expression in BM-EPCs. RT-PCR and Western blot analyses were performed to ensure adequate knocking down of 4EBP1 (Figure 20E). Consequently, cleaved caspase-3 and Bax induction by H_2O_2 were enhanced in 4EBP1 siRNA-transfected cells, whereas the Bcl-xL expression was declined (Figure 20F, 20G). More importantly, cell viability was significantly decreased while ROS production was considerably elevated during inhibition of 4EBP1, suggesting that the protection by SalB is significantly reduced in case of 4EBP1 knockdown (Figure 20H, 20I). Taken together, these observations demonstrate that the cytoprotective, antioxidative properties of SalB rely upon mTOR/4EBP1 to offer cellular protection during oxidant stress. Unexpectedly, both rapamycin treatment 4EBP1 and 4EBP1 knockdown activated phosphorylated p38 level, but did not facilitate the induced effect of H_2O_2 on p-ERK1/2 (Figure 20J, 20K). We hypothesize that oxidative stress induced activation of p38 MAPK suppresses the

physiological mTOR/4EBP1 activity of proliferating and differentiating cells and, in turn, this loss of mTOR activity sensitizes the BM-EPCs to p38 mediated apoptosis.

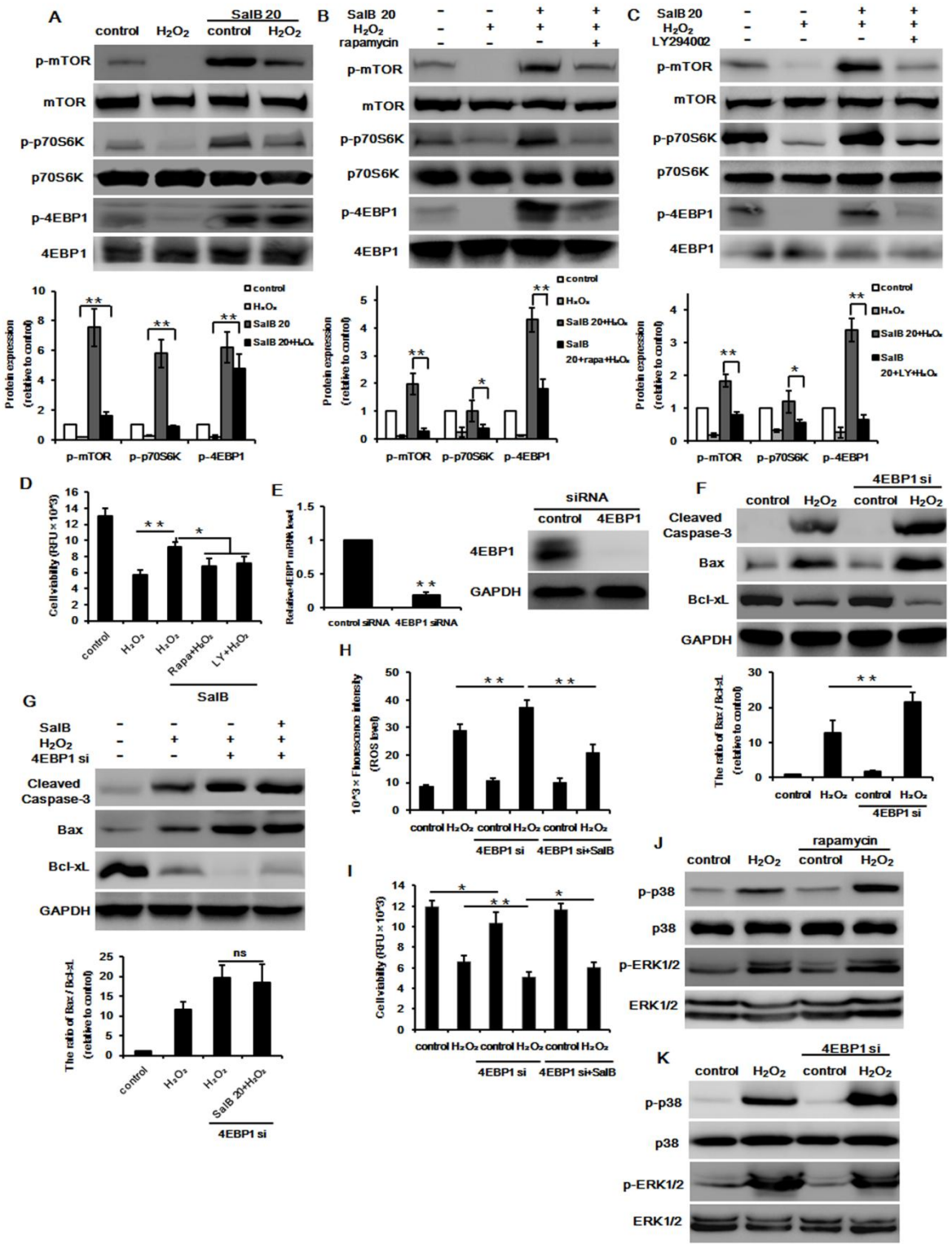

Figure 20. SalB provides cellular protection against oxidative stress in BM-EPCs through mTOR and its signaling pathways. (A) Cells were pretreated with 20 μM SalB for 48 h, and incubated with H_2O_2 for 6 h, Western blot analysis was used for determination of p-mTOR, p-p70S6K and p-4EBP1 levels. (B, C) SalB (20 μM) alone or combined with rapamycin (100 nM) or LY294002 (20 μM) were applied to BM-EPCs prior to H_2O_2 treatment, and Western blot analysis was performed. (D) in the presence of rapamycin or LY294002 in response to H_2O_2-stimulation for 6 h, Cellular survival rates were determined by quantification of DNA content, n=5. (E) BM-EPCs were transfected with 4EBP1-specific or non-specific siRNA. 48 h after transfection, mRNA and protein expression were measured to determine the efficiency of the silence. (F, G) BM-EPCs were incubated in the absence or presence of 4EBP1 siRNA for 48 h, then cells were treated by SalB and H_2O_2-stimulation, and indicated protein expressions were measured by Western blot. (H, I) Cellular viability and ROS generation were determined by quantification of DNA content (n=5) and by the amount of DCF formed (n=5) in cells in the presence or absence of 4EBP1 siRNA, in response to either SalB treatment or H_2O_2-stimulation. (J, K) p-p38 MAPK and p-ERK1/2 protein expression levels were detected in the presence of rapamycin or 4EBP1 siRNA in response to H_2O_2 stimulation for 6 h. The densitometric analysis of all Western blot band intensities were normalized to the total proteins or GAPDH. All data are expressed as mean ± SD, $^{*}P < 0.05$, $^{**}P < 0.01$. ns, not significant.

3.2.6 SalB inhibits activation of H_2O_2-induced MKK3/6-p38 MAPK-ATF2 pathways in BM-EPCs

MAPK signaling pathway is considered crucial for intracellular signal transduction events upon oxidative stress. In our study, H_2O_2 loading was associated with an increase in the phosphorylation of p38 MAPK, which was significantly inhibited by SalB pretreatment (Figure 21A). In considering the impact of SalB on signaling events both upstream and downstream of p38 MAPK, we assessed oxidative-dependent phosphorylation of the upstream kinase MKK3/6 and of the downstream effector ATF2. Notably, the markedly increased levels of MKK3/6 and ATF2 mediated by oxidative stress were suppressed by

SalB (Figure 21A). In contrast to upstream MKK-mediated p38 MAPK phosphorylation, autophosphorylation requires p38 MAPK intrinsic kinase activity. We therefore examined whether inhibition of p38 MAPK activity by SB203580 abolishes p38 MAPK phosphorylation induced by H_2O_2. As shown in Figure 21B, the enhancement of p38 MAPK phosphorylation by H_2O_2 treatment was significantly attenuated by the presence of SB203580 (10 μM). However, the baseline level of p38 phosphorylation was not changed by SB203580 suggesting that constitutive activation of MKK3/6 contributes to the baseline level of p38 MAPK activation that is independent of H_2O_2-triggered p38 MAPK phosphorylation. Furthermore, immunoblot analysis showed that the increase in caspase-3 activation and Bax/Bcl-xL ratio were prevented by treatment with SB203580 (Figure 21B). The presence of SB203580 significantly abolished the protective effect imposed by SalB, as observed in cell viability and ROS generation assays (Figure 21C, 21D). No influence of SB203580 on the expression levels of p-ERK1/2 or total ERK1/2 and p-JNK or total JNK was detected (data not shown). To further confirm the results derived from the cytotoxicity assay, we examined the protein levels of both cleaved caspase-3 and Bax/Bcl-xL in BM-EPCs and found that the inhibition of p38 significantly suppressed the induction of cleaved caspase-3 protein levels in BM-EPCs upon H_2O_2 treatment (Figure 21B). Strikingly, inhibition of p38 MAPK by SB203580 completely abolished the prevention by SalB on cleaved caspase-3 and Bax/Bcl-xL expression suggesting that inactivation of p38 MAPK pathway plays a critical role in SalB mediated protection against H_2O_2-induced oxidative stress in BM-EPCs.

To determine the role of ATF2 in the context of SalB-mediated cytoprotective effects, mRNA expression was determined by qRT-PCR. As shown in Figure 21E, the increase in ATF2 expression was prevented by treatment with SB203580. And the presence of SB203580 or U0126 all significantly suppressed ATF2 level induced by H_2O_2. After ATF2 was knocked down by siRNA, RT-PCR and Western blot analyses were performed to ensure adequate silencing (Figure 21F). ATF2 knockdown modestly decreased H_2O_2-stimulated phosphorylation of p38 MAPK compared with cells transfected with the

non-specific siRNA. H_2O_2-caused cleavage of caspase-3 and increased Bax/Bcl-xL ratio expression were largely inhibited when cells were silenced with ATF2 (Figure 21G, 21H). In addition, knockdown of ATF2 suppressed ROS production (53.5% of non-silenced H_2O_2 group, $P < 0.01$) and promoted cell survival (1.66-fold of non-silenced H_2O_2 group, $P < 0.01$) upon H_2O_2-induced oxidative stress in BM-EPCs (Figure 21I, 21J), illustrating that loss of ATF2 is protective during H_2O_2 exposure.

In summary, the combined data support a model in which oxidation triggers p38 activation, potentially via MKK3/6, which in turn induces the proapoptotic ATF2. Our data indicate that MKK3/6-p38 MAPK-ATF2 signaling are the principal target pathways of SalB.

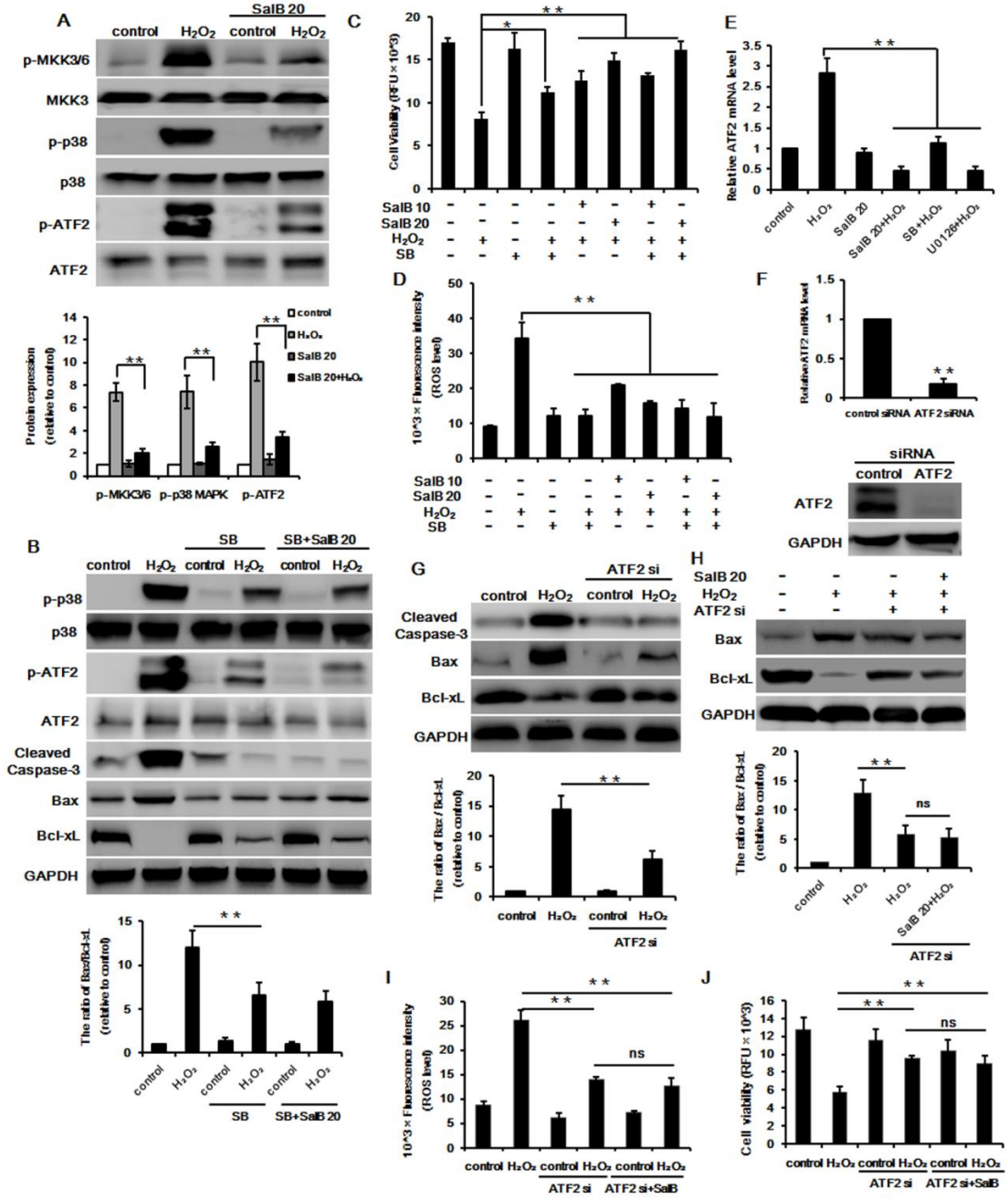

Figure 21. SalB inhibits H_2O_2-induced MKK3/6-p38 MAPK-ATF2 pathways in BM-EPCs. (A) BM-EPCs were treated with or without 20 μM SalB, then stimulated by 1 mM H_2O_2, MKK3/6, p38 MAPK, ATF2 were detected with phospho-specific antibodies by Western blot. (B) Forty-eight hours after SalB treatment BM-EPCs were further incubated with selective p38 MAPK inhibitor SB203580 (10 μM) and 1 mM H_2O_2, and protein expression was assessed by Western blot analysis. (C, D, E) Cellular viability, ROS generation and mRNA level of ATF2 were determined by quantification of DNA

content (n = 5), by the amount of cellular DCF synthesis (n=3), and by qRT-PCR (n=3) in the presence of SalB or SB203580 in response to H_2O_2-stimulation for 6 h. (F) BM-EPCs were transfected with ATF2-specific or non-specific siRNA. 48 h after transfection, mRNA and protein expression were measured to determine the efficiency of the silence. (G, H) BM-EPCs were incubated in the absence or presence of ATF2 siRNA for 48 h, then cells were treated by SalB and H_2O_2-stimulation, and protein expression was measured by Western blot. (I, J) Cellular viability and ROS generation were determined by quantification of DNA content and by the amount of cellular DCF formation in the presence or absence of ATF2 siRNA, in response to either SalB treatment or H_2O_2-stimulation, n=4. The densitometric analysis of all Western blot band intensities were normalized to the total proteins or GAPDH. All data are shown as mean ± SD. $^{*}P < 0.05$, $^{**}P < 0.01$. ns, not significant.

3.2,7 Inhibition of ERK1/2 by SalB prevents H_2O_2- mediated injury in BM-EPCs

ROS is known to be related with p38 MAPK (Jiang et al., 2011). In order to confirm that SalB inhibits H_2O_2-induced p38 MAPK phosphorylation via decreased ROS generation, DPI was added prior to H_2O_2 stimulation. As shown in Figure 22A, 22B, DPI treatment significantly attenuated H_2O_2-induced generation of ROS and cell death in BM-EPCs. Notably this effect was enhanced by 20 μM SalB. DPI partially inhibited phosphorylation of p38 MAPK during H_2O_2 stress and enhanced the inhibitory effect of SalB on p-p38 MAPK and p-ATF2 (Figure 22C, 22D). Furthermore, DPI strongly suppressed the H_2O_2-stimulated cleaved caspase-3 and Bax/Bcl-xL ratio, and enhanced the aforementioned suppressive effect of SalB on these proteins (Figure 22C, 22D). In summary, these findings suggest a positive feedback loop involving NADPH oxidase, H_2O_2, and p38 MAPK amplifying the signaling pathways related to oxidative stress-induced cell injury in BM-EPCs that can be modulated by SalB.

The ERK1/2 pathway is associated with protection against apoptosis. In our study, pretreatment with 20 μM SalB for 48 h prior to H_2O_2 exposure inhibited the H_2O_2-induced ERK1/2 activation, while total ERK1/2 expression was not altered in any treatment group

(Figure 22E). The NADPH oxidase inhibitor DPI treatment also showed an inhibition on H_2O_2-induced ERK1/2 phosphorylation (Figure 22F). To evaluate the putative role of ERK1/2 pathways on H_2O_2-induced apoptosis in the presence of SalB, cells were preincubated for 60 min with the selective MEK1 and MEK2 inhibitor U0126 (10 μM) prior to H_2O_2 (1 mM) addition. U0126 markedly reduced the phosphorylation of ERK1/2 and the abundance of Bax/Bcl-xL ratio, and enhanced the anti-apoptotic effect of SalB on H_2O_2-induced cell dysfunction in BM-EPCs (Figure 22F). In addition, phosphor-ATF2 stimulated by H_2O_2 was downregulated by U0126 (Figure 22F). Furthermore, inhibition of ERK1/2 by U0126 markedly prevented ROS production (60.7% of H_2O_2 group) and counteracted cell damage (1.45-fold of H_2O_2 group) imposed by H_2O_2, which showed an additive effect when combined with 20 μM SalB (Figure 22G, 22H). These data highlight the blockade of ERK1/2 by SalB plays a critical role in counteracting H_2O_2-induced oxidative stress and EPCs dysfunction.

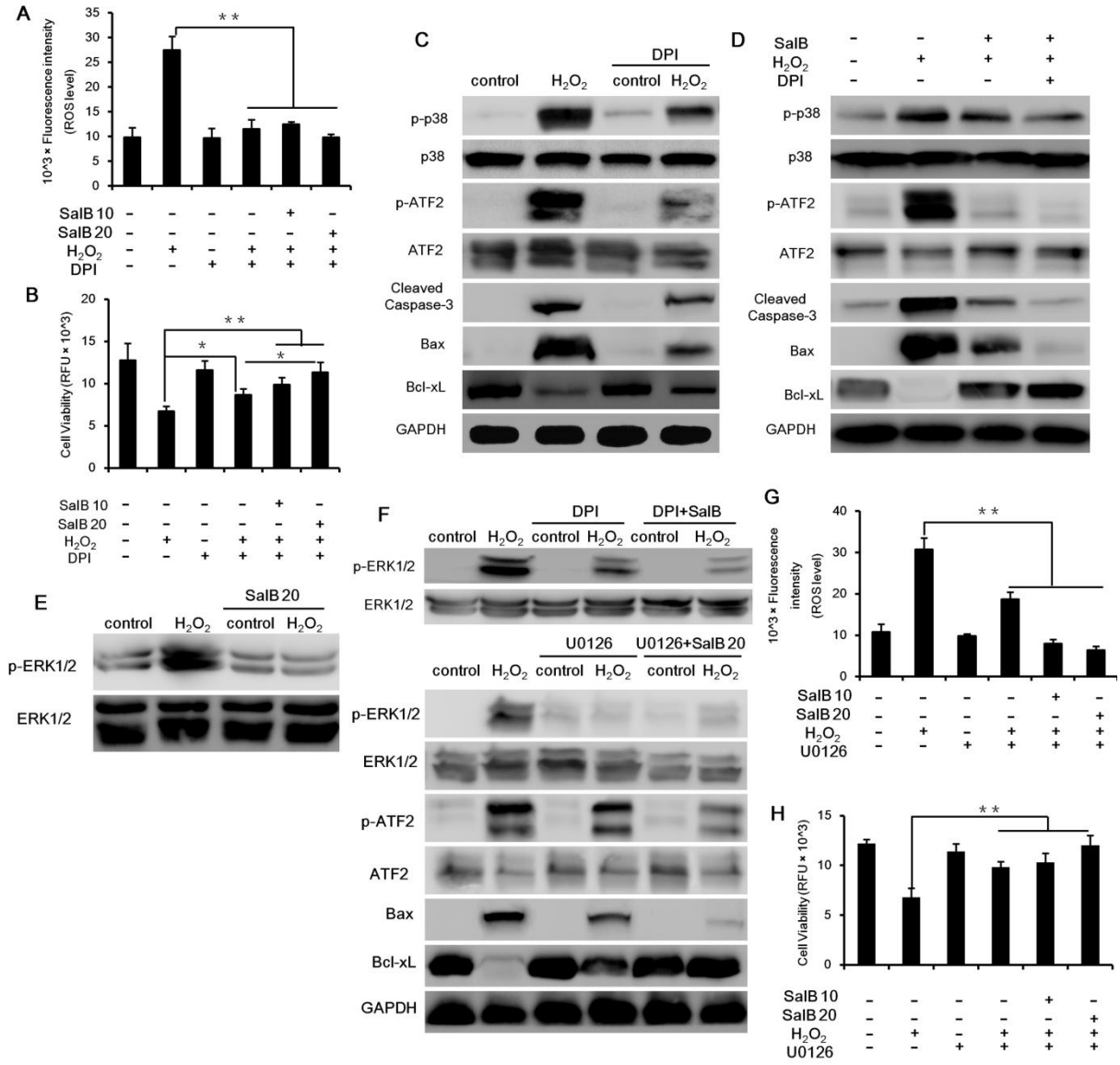

Figure 22. Inhibition of ERK1/2 by SalB prevents H_2O_2- mediated injury in BM-EPCs. (A, B) Forty-eight hours after SalB treatment, BM-EPCs were further incubated with 1 mM H_2O_2 alone or in combination with 10 μM of DPI, cellular viability and ROS generation were determined by quantification of DNA content and by the amount of cellular DCF formation, n=6. (C, D) Indicated protein expressions were detected by Western blot in the presence or absence of DPI, in response to SalB treatment (or not) and H_2O_2-stimulation. (E) Cells were pretreated with 20 μM SalB for 48 h, and incubated with H_2O_2 for 6 h, protein expression of p-ERK1/2 and total ERK1/2 were determined by Western blot. (F) Forty-eight hours after SalB treatment, BM-EPCs were further incubated with 1 mM H_2O_2 alone or in combination with 10 μM of DPI or 10 μM of U0126, and Western blot was performed to detect protein expression. (G,

H) ROS generation and cellular viability were determined by the amount of cellular DCF formation and quantification of DNA content in the presence of either SalB or U0126 in response to H_2O_2-stimulation for 6 h, n=4. Data are expressed as mean ± SD, $^{*}P < 0.05$, $^{**}P < 0.01$.

3.2.8 ICAR restores loss of mTOR phosphorylation induced by H_2O_2, which is associated with autophagy inhibition

Since ICAR employs mTOR to modulate cell angiogenic differentiation as described above, we assessed whether ICAR also relies upon the PI 3-K/Akt/mTOR pathway to protect cells. As showed in Figure 23A, H_2O_2 (1 mM) markedly decreased p-mTOR, p-p70S6K, as well as p-4EBP1 expression in BM-EPCs. Conversely, ICAR pretreatment restored p-mTOR protein expression and its two targets, p70S6K and 4EBP1 back to nearly baseline levels. We considered the possibility that the higher mTOR/p70S6K/4EBP1 activation in cells could be responsible for the increased survival in response to H_2O_2. Thus, we inhibited this pathway with rapamycin to evaluate it. As shown in Figure 23B -6D, treatment with rapamycin partly abolished mTOR/p70S6K/4EBP1 phosphorylation by ICAR in response to H_2O_2, and a considerable decrease in cell survival rate was found when rapamycin (73.9% of ICAR+H_2O_2 group, $P < 0.01$) was applied combined with ICAR. Moreover, ROS generation elevated significantly when mTOR was inhibited.

Compelling evidence demonstrates that the PI3-K/Akt/mTOR pathway is the major regulatory signal of autophagy. Inactivation of mTOR is considered as a key step in autophagy activation. We therefore investigated whether H_2O_2-mediated autophagy is occurring via an mTOR mediated pathway in our system. As shown in Figure 23E, H_2O_2-induced autophagic flux was observed at 3 h, and then was sustained at high levels during 12 h treatment indicated by increased processing of LC3B-I to LC3B-II. Sequestome-1 protein (p62/SQSTM1), which was implicated to directly degrade by autophagy, was reduced after 3 h in BM-EPCs in response to H_2O_2-indueced autophagy. However, ICAR pretreatment notably decreased LC3B-II/LC3B-I ratio, while restored

expression of p62/SQSTM1. Moreover, Beclin-1 protein expression, an upstream promoter of autophagic induced cell death pathways, was also attenuated by ICAR remarkably (Figure 23F). he suppression effect on cell autophagy was also evidenced by the decreased number of acridine orange-positive cells.

The canonical mTOR inhibitor rapamycin increased autophagic response of the cells under the induction by H_2O_2, which undermined the suppression effect of ICAR on it (Figure 23H). In order to examine whether the suppression of autophagy is related to oxidative stress-induced cell death, we pretreated BM-EPCs with autophagic inhibitor 3-methyladenine (3-MA). As shown in Figure 23I, 3-MA inhibited acridine orange-positive vacuole accumulation by H_2O_2, and H_2O_2-induced accumulation of LC3BII and decrease of p62. What's more, the ratio expression of Bax/Bcl-xL was significantly declined in the presence of 3-MA, and a reduced level of cell death was correlated with the observed decreased amount of ROS accumulation, further strengthening the association between autophagy, ROS, and cell death (Figure 23J-L).

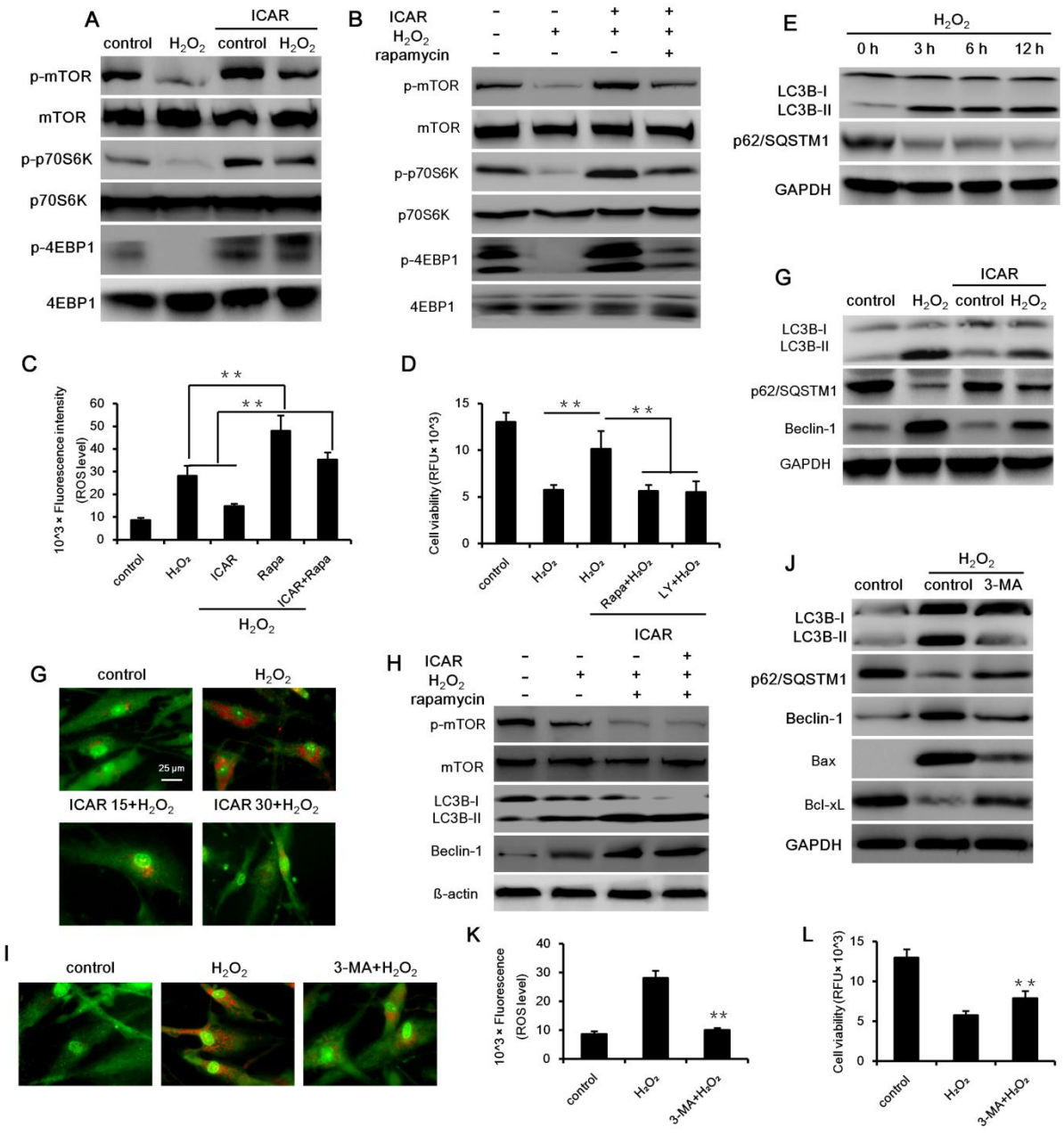

Figure 23. ICAR restores loss of mTOR phosphorylation induced by H_2O_2, which is associated with autophagy inhibition. (A) BM-EPCs were treated with or without 30 μM ICAR, then stimulated by 1 mM H_2O_2, mTOR, p70S6K and 4EBP1 were detected with phospho-specific antibodies by Western blot. (B) Indicated protein expressions were detected by Western blot in the presence or absence of rapamycin, in response to ICAR treatment (or not) and H_2O_2-stimulation. (C, D) ROS generation and cellular survival rates were determined by quantification of DCF formation and DNA content in the presence of rapamycin or LY294002 in response to H_2O_2-stimulation for 6 h, n=5. (E) Cells were treated without or

with H_2O_2 for 3, 6, and 12 h, protein expression were detected by Western blot. (F) Cells were treated without or with H_2O_2 for 6 h, acidic intracellular compartments were visualized by acridine orange staining. (G, H) BM-EPCs were treated with or without 30 μM ICAR in the presence of rapamycin in response to H_2O_2-stimulation, protein expression was detected by Western blot. (I, J) BM-EPCs were pretreated with 3-MA (5 mM), and stressed by H_2O_2 for 6 h, acidic intracellular compartments were visualized by acridine orange staining using fluorescence microscope and indicated protein expression was detected by Western blot. (K, L) BM-EPCs were pretreated with 3-MA (5 mM), and stressed by H_2O_2 for 6 h, ROS generation and cellular survival rates were determined by quantification of DCF formation and DNA content, n=4. Data are expressed as mean ± SD, $^{**}P < 0.01$.

3.2.9 Blockade of p38 MAPK/ATF2 attenuates H_2O_2 induced cell apoptosis and autophagy mediated by ICAR

It has been reported that an increase in p38 MAPK activation sensitizes cells to oxidation-induced apoptosis in several cell types. Consistent with previous reports, phospho-38 MAPK was rapidly upregulated in response to H_2O_2 stimulation in our study, but ICAR pretreatment significantly decreased the phospho-38 MAPK expression almost back to baseline (Figure 24A). ATF2 has been shown to be the downstream effector of p38, mediating its proapoptotic function. As shown in Figure 24A, the level of phospho-ATF2 was also blunted by ICAR pretreatment upon H_2O_2 induction. The attenuation of ATF2 by ICAR was also confirmed at mRNA levels (Figure 24B). To determine a possible role of p38 MAPK/ATF2 mediating cell apoptosis and autophagy upon oxidation, BM-EPCs were loaded with H_2O_2 in the absence or presence of the p38 MAPK inhibitor SB203580. As shown in Figure 24B and 24C, SB203580 profoundly abrogated H_2O_2-triggered mRNA level and phosphorylated protein expression of ATF2. The ratio expression of Bax/Bcl-xL and the cleavage of caspase-3 stimulated by oxidation were significantly prevented by the application of SB203580, suggesting that p38 MAPK activation was responsible for H_2O_2-mediated apoptosis in BM-EPCs. Furthermore, we have observed that SB203580

prevented the accumulation of LC3-II and restored the expression of p62/SQSTM1 in response to H_2O_2, suggesting that p38 MAPK is necessary for the activation of autophagy by oxidation (Figure 24D). No influence of SB203580 on the expression levels of p-ERK1/2 or total ERK1/2 and p-JNK or total JNK was detected (data not shown).

To assess the role of NADPH in the anti-injury effect exerted by ICAR, diphenyliodonium (DPI), a NADPH oxidase inhibitor, was added to the cells for 90 min prior to H_2O_2 stimulation. Treating cells with DPI effectively blocked the H_2O_2-induced activation of p38 MAPK and ATF2, and enhanced the inhibitory effect of ICAR on both of them (Figure 24E). DPI strongly suppressed the H_2O_2-stimulated cleaved caspase-3 and Bax/Bcl-xL ratio, and strengthened the suppression effect by ICAR with above proteins. More importantly, preincubation of BM-EPCs with DPI dramatically blocked H_2O_2-induced autophagy (Figure 24E). These results confirm the pro-apoptotic role of p38 MAPK and identify its novel effect on autophagy during oxidative stress.

To further investigate whether oxidative stress-induced activation of ATF2 plays a role in H_2O_2-induced autophagy, ATF2 was knocked down by siRNA transfection. Successful transfection was confirmed by RT-PCR and Western blot analysis (Figure 24F). As shown in the Figure 24G, ATF2 knockdown dramatically decreased numbers of acridine-orange positive cells in response to H_2O_2, and blunted the effect of ICAR. Moreover, H_2O_2-caused cleavage of PARP and caspase-3 were largely inhibited when cells were silenced with ATF2 (Figure 24H). Cells with low expression of ATF2 showed a reaccumulation of p62 and decrease in LC3B-II compared with cells treated with H_2O_2 alone (Figure 24H). Moreover, the knock down of ATF2 abolished the attenuated effect on Bax/Bcl-xL expression and autophagy by ICAR in response to H_2O_2 (Figure 24I). These findings suggest that p38 MAPK signaling appears to be upstream of autophagic signaling, and the reduction of ATF2 expression was an important step in H_2O_2-induced cell apoptosis that also contributed to autophagy suppression. In addition, knockdown of ATF2 suppressed ROS production (53.5% of non-silenced H_2O_2 group, $P < 0.01$) and promoted cell survival (1.66-fold of non-silenced H_2O_2 group, $P < 0.01$) upon H_2O_2-induced oxidative stress in BM-EPCs (Figure 24J, 24K).

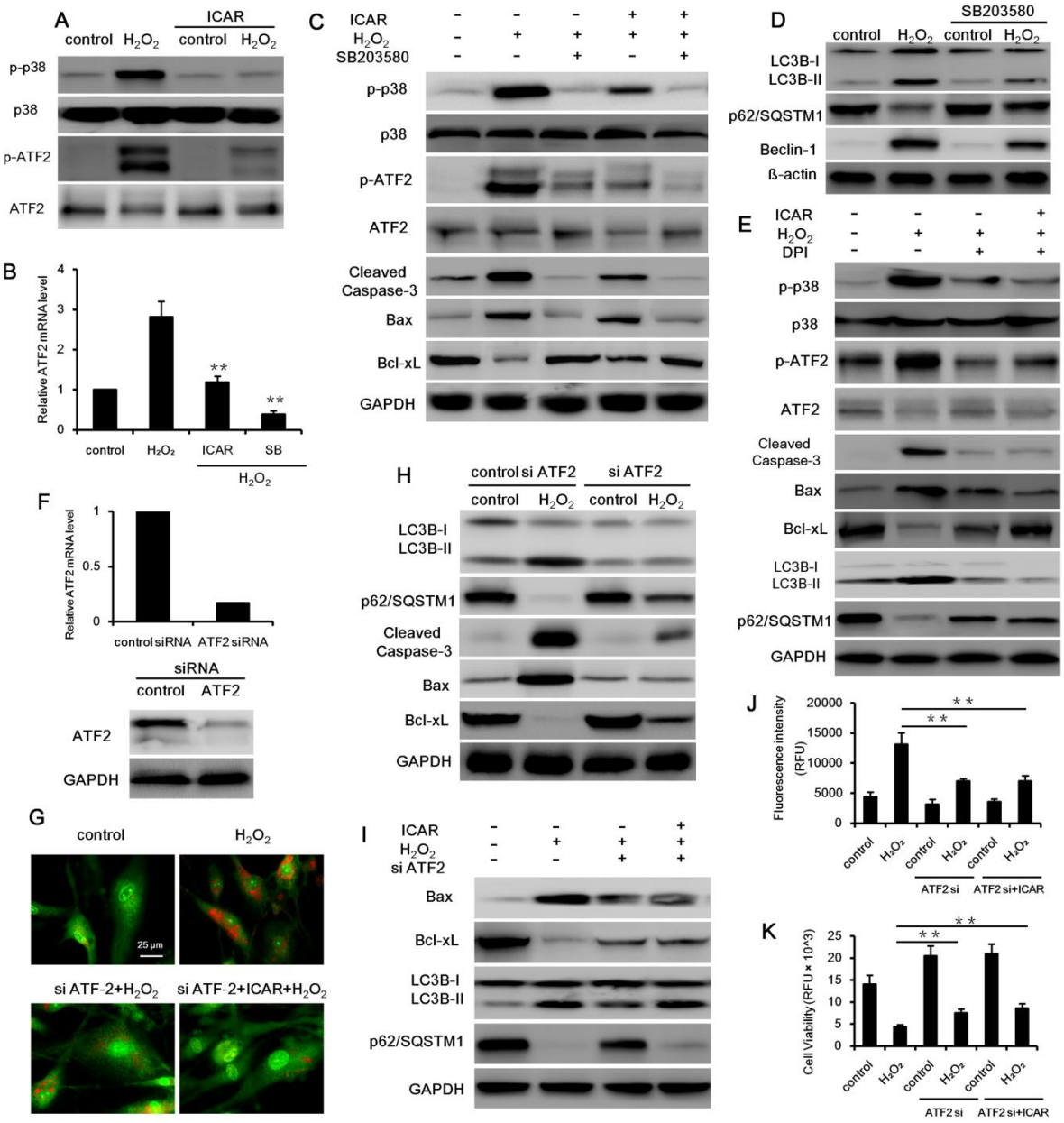

Figure 24. Blockade of p38 MAPK/ATF2 by ICAR attenuates H_2O_2 induced cell apoptosis and autophagy. (A) BM-EPCs were treated with or without 30 μM ICAR, then stimulated by 1 mM H_2O_2, expression of p38 and ATF2 were detected with phospho-specific antibodies by Western blot. (B) mRNA level of ATF2 was detected by qRT-PCR in the presence or absence of SB203580, in response to ICAR treatment (or not) and H_2O_2-stimulation, n=5. (C, D) BM-EPCs were pretreated with or without 30 μM ICAR in the presence or absence of SB203580, then stimulated by 1 mM H_2O_2, protein expression was detected by Western blot. (E) Indicated protein expressions were detected by Western blot in the presence or absence of DPI, in response to ICAR treatment (or not) and H_2O_2-stimulation. (F) BM-EPCs were

transfected with ATF2-specific or non-specific siRNA. 48 h after transfection, mRNA and protein expression were measured to determine the efficiency of the silence. (G) BM-EPCs were incubated in the absence or presence of ATF2 siRNA for 48 h, then cells were treated by ICAR and H_2O_2-stimulation, acidic intracellular compartments were visualized by acridine orange staining using fluorescence microscope. (H, I) BM-EPCs were incubated in the absence or presence of ATF2 siRNA for 48 h, then cells were treated by ICAR (or not) and H_2O_2-stimulation, protein expression was measured by Western blot. (J, K) BM-EPCs were incubated in the absence or presence of ATF2 siRNA for 48 h, then cells were treated by ICAR and H_2O_2-stimulation, cellular viability and ROS generation were determined by quantification of DNA content and by the amount of cellular DCF formation, n=6. Data are expressed as mean ± SD, $^{**}P < 0.01$.

3.2.10 ERK1/2 and p38 MAPK are required for mTOR phosphorylation in H_2O_2-induced autophagy

In general ERK is believed to activate mTOR; however mTOR inhibition has been associated with increased ERK activity in response to non-starvation stress. Since H_2O_2-induced LC3B-II upregulation was found to be accompanied by an increase in ERK1/2 phosphorylation, we sought to investigate the role of ERK1/2 pathway in H_2O_2 induced autophagy using the MEK1/2 inhibitor U0126. As shown in Figure 25A, H_2O_2 loading was associated with an increase in the phosphorylation of ERK1/2, which was significantly inhibited by ICAR pretreatment. Moreover, H_2O_2-induced autophagic responses were attenuated when ERK1/2 activity was suppressed by pharmacologic inhibitor U0126, suggesting ERK activation is required for autophagy induced by H_2O_2 in BM-EPCs (Figure 25B). What's more, H_2O_2 (1mM) reduced phospho-mTOR protein expression, while pretreatment with U0126 partially restored phospho-mTOR expression, implying that an ERK-mTOR pathway is at least partially involved in H_2O_2-mediated autophagy. Moreover, the ERK inhibition enhanced the suppressive effect of ICAR on autophagic response to H_2O_2 in BM-EPCs (Figure 25C).

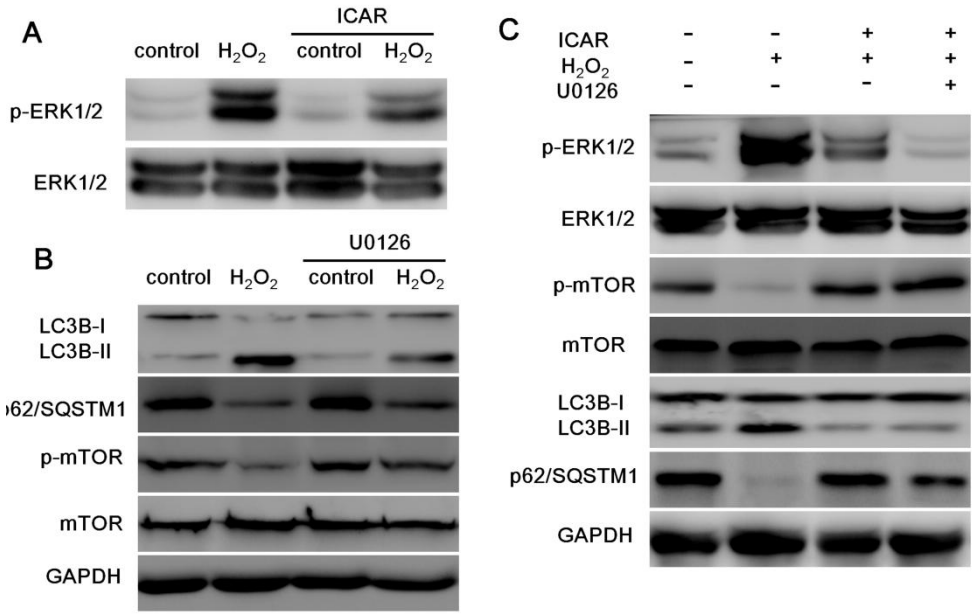

Figure 25. The role of ERK1/2 and p38 MAPK in mTOR phosphorylation upon H_2O_2-induced autophagy. (A) Forty-eight hours after ICAR treatment, BM-EPCs were further incubated with 1 mM H_2O_2, protein expression of p-ERK1/2 and total ERK1/2 were determined by western blot. (B, C) Indicated protein expressions were detected by Western blot in the presence or absence of U0126, in response to ICAR treatment (or not) and H_2O_2 stimulation.

3.2.11 p38 MAPK activation lies eNOS activation to induce apoptotic and autophagic cell death

The mTOR integrates the input from several upstream pathways by sensing the nutrient levels, bioenergetic status, and redox state of the cell. We hypothesized that mTOR signaling was involved in the p38 MAPK-mediated induction of autophagy. Therefore we examined phosphorylation status of p38 MAPK and mTOR after H_2O_2 and rapamycin treatment. Induction of autophagy by rapamycin significantly increased oxidative stress-induced apoptosis evidenced by cleavage of caspase 3 and PARP, and increased LC3B-II levels with upregulating p38 MAPK phosphorylation, but this effect was all largely reversed by the p38 pathway inhibitor SB203580 (Figure 26A). Thus, we concluded that

H_2O_2 induced autophagy via activation of p38 MAPK, which functions through the downstream inhibition of the mTOR signaling pathway.

Since H_2O_2 exposure induces the upregulation of eNOS, leading to increased free radical NO generation. And ICAR administration could counteract these effects significantly as shown in Figure 26B, 26C. Further study found that the inhibition of p38 MAPK activity by SB203580 also attenuated the NO production and eNOS expression induced by H_2O_2. We reasoned that eNOS may also be involved in H_2O_2 signaling to induce cell injury and autophagy. Therefore, we examined the effect of the eNOS inhibitor L-NAME on H_2O_2-induced autophagy in BM-EPCs. Cells were pretreated for 2 h with L-NAME and then exposed to H_2O_2 for 6 h. As shown in Figure 26D-F, pretreatment with 10 μM L-NAME significantly reduced H_2O_2-mediated ROS accumulation and autophagy in BM-EPCs. We postulated that p38 MAPK activation lies eNOS activation to induce apoptotic and autophagic cell death.

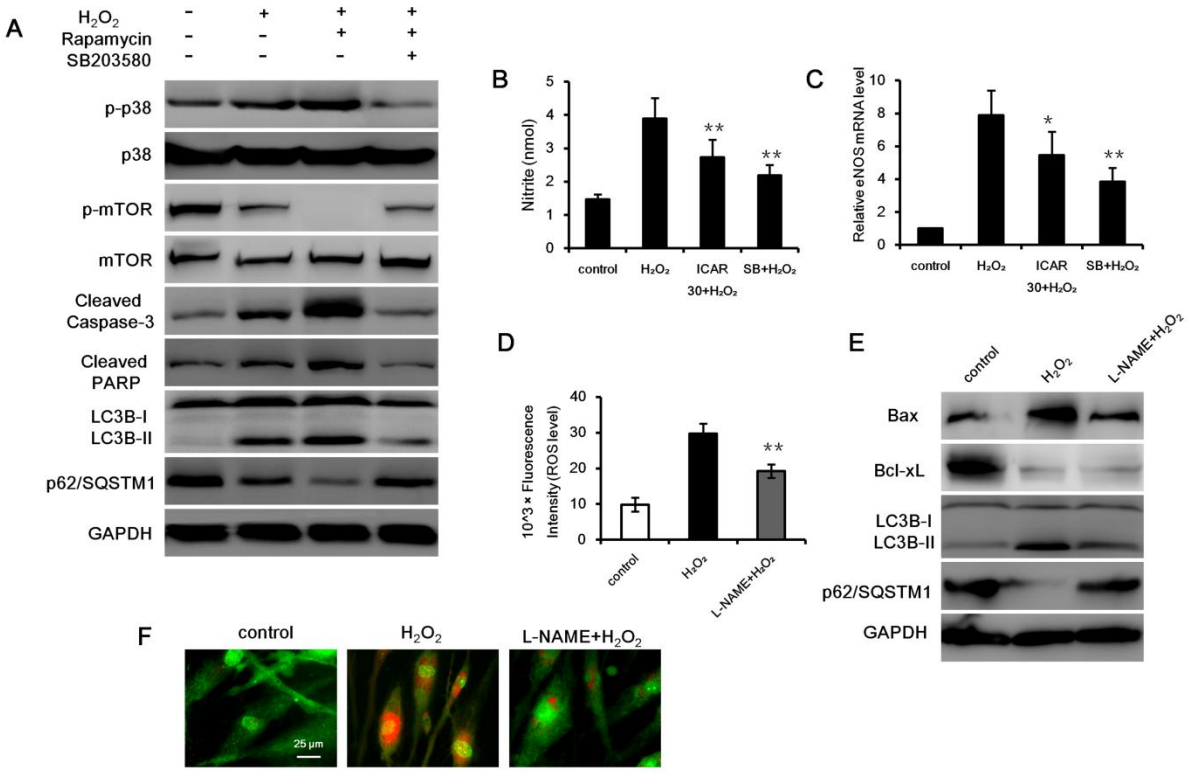

Figure 26. p38 MAPK activation lies eNOS activation to induce apoptotic and autophagic cell death. (A) Indicated protein expressions were detected by Western blot in the presence or absence of rapamycin or SB203580, in response to H_2O_2-stimulation. (B, C) BM-EPCs were treated with ICAR or SB203580 prior to be stimulated by 1 mM H_2O_2, cell culture supernatants were collected and analyzed by Griess assay, n=3; mRNA level of eNOS was detected by qRT-PCR, n=3. (D-F) BM-EPCs were preincubated in the absence or presence of L-NAME for 3 h, then cells were treated by H_2O_2, ROS generation was quantified by the amount of cellular DCF formation (n=4), indicated protein expressions were detected by Western blot, and acidic intracellular compartments were visualized by acridine orange staining using fluorescence microscopy. Data are expressed as mean ± SD, $^{*}P < 0.05$, $^{**}P < 0.01$.

4. DISCUSSION

Research using immortalized cells has a number of limitations with respect to a complete understanding of biological systems *in vivo*. Primary cells, however, are valuable tools enabling the study of a variety of cellular and biochemical functions under tightly controlled experimental conditions. *In vitro* vascularization is an upcoming strategy to solve the problem of insufficient blood supply upon construct implantation. Although recent publications show promising results, these studies were generally performed with endothelial cell model systems not enabling translational conclusions (Verseijden et al., 2010; Verseijden et al., 2012). To effectively facilitate bone defects repair with tissue engineering and treatment of ischemia disease, there is an urgent need for developing safe and cost effective drugs that can substitute or cooperate with growth factors for angiogenesis promotion. The evaluation of naturally occurring dietary compounds may indicate novel approaches for the bone repair. In the present study, we demonstrate the effects of TCM extracts (at a near medical applied dose) on the proliferation and differentiation of human BM-EPCs, and the underlying mechanisms. We found that TCM extracts acted on human BM-EPCs by promoting cellular proliferation, as well as enhancing key functional activities including migration, cell-matrix adhesion and tube formation. Moreover, TCM extracts initiated a significant increase in VEGF secretion and NO production, and exerted a considerable cytoprotective effect upon oxidative stress.

Although the proportional contribution of angiogenesis and vasculogenesis to neovascularization of adult tissue remains to be determined, it has been shown, either by mobilization of EPCs or by injection of *in vitro*-cultured hematopoietic stem cells, that EPCs improved neovascularization of the hind limb and cardiac function (Kalka et al., 2000; Murohara, 2003). However, defining EPC is an ongoing debate in the scientific community. Different culturing methods (e.g. using early-adherent or non-adherent mononuclear cells) and detection of various combinations of surface antigens (e.g. CD14, CD45, and eNOS) were reported for the characterization of EPC. Although different morphological and

survival features exist to distinguish between early- and late-outgrowth EPCs, these cell classes showed comparable *in vivo* vasculogenic capacity (Hur et al., 2004). The early EPCs contribute to neovasculogenesis mainly by secreting angiogenic cytokines, whereas late EPCs enhance neovasculogenesis by providing a sufficient number of endothelial cells based on their high proliferation potency. Yoon and colleagues reported that mixed transplantation of these two types of cells results in synergistic neovascularization through cytokines and matrix metalloproteinases (Yoon et al., 2005).

In order to characterize the EPCs in the present study, immunofluorescence staining and flow cytometry were performed. We observed double-uptake of Dil-ac-LDL and FITC-UEA-I after 10 d cultivation accompanied by high expression of VEGFR-2 (79.2%), E-selectin (46.4), vWF (35.4%), and relatively low expression of CD133 (3.8%), along with negative expression of CD45 (Figure 7). Moreover, the appearance of well-circumscribed colonies was monitored daily. We found that endothelial colony cannot be efficiently obtained from all donors (colonies were generated from 5 donors of the 8 donors), indicating a function of donor age. However, the *in vitro* tubular formation capacities between colony-forming cells and non-colony-forming cells did not differ significantly, suggesting colony forming ability is not essentially associated with tube formation capacity of the cells *in vitro*. All cells used in the present study were cultivated with EGM-2 at passages 3 to 5 and can be categorized as late-outgrowth EPCs according to the previous reports (Kalka et al., 2000; Reinisch et al., 2009).

Angiogenesis is a complex process requiring multiple sequential steps including interplay between cells, soluble factors, and ECM components. Vascular endothelium proliferation is the first step in angiogenesis, including processes like migration, differentiation, survival and death. Under the conditions used in the present study, ICAR and PUER show significantly enhancing effect on cell proliferation, but SAL significantly, yet non-dose-dependently, promoted proliferation of BM-EPCs at 20, 40, and 80 μM (Figure 8). A possible explanation for this finding may be a saturation of the cell receptors involved in cell proliferation by SAL at concentrations exceeding 20 μM. Furthermore the

absence of a time-dependent effect of SAL on EPCs proliferation at the early time point of 24 h cultivation can be explained as follows. Firstly, the effect of SAL on cell proliferation is indirect via activation of the secretion of cytokines and may therefore be associated with a time delay. Secondly, the cells are metabolically more active and thus more responsive to the drug after 48 h adherence to the tissue culture polystyrene plate. Thirdly, as we used serum-free medium for the proliferation assay to reduce any potential bias on cellular function exerted by growth factors, cells grew slowly and thus the time window for observing potential proliferative effects by SAL may have been extended. The lack of an observed proliferative effect on EPC by SAL at 96 h can be at least partly explained by a reduced drug efficacy over time due to a comparatively short half-life of SAL as known from *in vivo* studies.

Homing and incorporation of EPCs to the sites of revascularization probably are determined not only by the number of circulating EPCs, but also by the motility of the cells. The present study provides evidence that SAL and ICAR not only increases the chemotactic response of BM-EPCs but SAL per se can trigger the cells' innate chemoattractive potency (Figure 9).

VEGF is one of the most potent angiogenic cytokines and promotes proliferation of vascular cells. Interestingly, there are several reports describing that VEGF increases vascular permeability and endothelial cell survival in quiescent vessels, and the cellular responses to these effectors involve disruption of the VE-cadherin-based adherent junction (Gavard and Gutkind, 2006; Mura et al., 2006; Wong et al., 2009). In our study, SAL and ICAR stimulated EPCs tubule formation (Figure 11) *in vitro* accompanied by enhanced mRNA expression and protein secretion of VEGF (Figure 12, 13). Additionally, the mRNA expression of VEGF receptor KDR, eNOS, vWF, and PECAM1 were upregulated by SAL and ICAR, which in turn promoted EPCs mobilization and differentiation.

Cell-cell adhesion ensures tight contacts between neighbouring cells, which is necessary for cell segregation, as well as for the morphological and functional

differentiation of different tissues. Evidently there are cell-cell recognition systems that make cells of the same type preferentially adherent to one another. Several studies have shown that cell-cell adhesions inhibit cell migration which finally lead to the inability to assemble new capillary blood vessels (Lamalice et al., 2007). Homotypic cell adhesion plays an important role in mediating a range of physiological processes such as cell survival, migration and invasion. Thus in the present study we selected two populations of EPCs to investigate the possible effect of TCM extracts on homotypic cell adhesion. Many angiogenic factors can destabilize the organization of intercellular junctions, causing endothelial barrier opening (Gavard and Gutkind, 2006). VE-cadherin is a transmembrane or membrane-associated glycoprotein that mediates specific cell-cell adhesion in a Ca^{2+}-dependent manner (Egami et al., 2005; Montero-Balaguer et al., 2009). VE-cadherin knockdown in HUVEC resulted in increased tubule formation indicating that it is loss of VE-cadherin that leads to increased angiogenesis (Mavria et al., 2006). In the present study, the low expression of VE-cadherin after SAL and ICAR treatment suggests decreased cell-cell adhesion that may contribute to the enhanced angiogenic effect exerted by them (Figure 10).

The role of NO as a major regulator of cell migration and angiogenesis is suggested by the observation that it is produced by eNOS following its activation downstream of the VEGFR-2/PI3-K/Akt-PKB axis in endothelial cells activated by VEGF (Williams et al., 2000). Endothelial-derived NO is essential in the maintenance of vascular homeostasis (Drummond et al., 2000; Matz et al., 2000; Murohara and Asahara, 2002). Our results reveal a continuously increasing production of NO over time exerted by SAL and ICAR treatment. However, inhibition of NO synthesis by L-NAME considerably attenuated the promotion effect of SAL on cell migration and tubular formation, implying that NO essentially participates in the angiogenic events (Figure 12).

mTOR functions as a multichannel processor in a cellular nutrient-sensing network by receiving multiple inputs derived from distinct environmental cues and directing different outputs to appropriate downstream effectors. Several studies have shown the roles of

VEGF/Akt/mTOR in potentiating pro-angiogenesis (Fan et al., 2012) and p70S6K, a direct downstream target of the mTORC1 (mTOR, GβL, and raptor) in modulating cell migration (Berven et al., 2004; Qiu et al., 2004). Of note, it seems that the primary pathway by which most growth factors and cytokines activate mTOR and its downstream targets is the PI3-K/Akt (Fingar and Blenis, 2004; Li et al., 1999). MAPK signaling is critical during the endothelial differentiation of vascular progenitor cell (Takahashi et al., 2012). In our study, treatment with SAL showed a marked increase in the phosphorylation of mTOR, p70S6K, and its upstream kinase Akt (Figure 14). Moreover, the phosphorylation level of ERK1/2 was increased significantly upon SAL stimulation. In further blocking experiments we observed that LY294002 and U0126 significantly inhibited phosphorylated Akt/mTOR and ERK1/2, and consequently led to a decrease in cell migration and tube formation capacity in BM-EPCs. The application of rapamycin also showed a suppressive effect on the phosphorylation of Akt/mTOR/4EBP1, and remarkably inhibited the promoting effect of ICAR on cell mobility and tube formation (Figure 14). What's more, the results from 4EBP1-knockdown cells imply distinct role of 4EBP1 in the cell motility and tube formation (Figure 14), could be due to the various subcellular localizations 4EBP1 resides in, responding to different upstream signals which would result in distinct outcomes. In summary, these data suggest that SAL and ICAR promotes proliferation and differentiation of EPCs and enhances their functions via activation of the Akt/mTOR/p70S6K/4EBP1 and ERK1/2 pathways.

The development of a microvasculature and microcirculation is critical for the homeostasis and regeneration of living bone, without which, the tissue would simply degenerate and die. In our preliminary animal study using immunodeficient mice, we found that SAL could significantly augment the total bone growth after 6 weeks in a femoral critical-size bone defect model (Figure 15). Further studies, however, are necessary to assess the potential TCM extracts on EPCs differentiation into neovessels and their integration with the host vasculature.

Evidence of *in vivo* exposure to oxidative stress is observed in several diseases or with risk factors associated with enhanced vascular pathologies, e.g. atherosclerosis, hypertension, diabetes, and heart failure (Cai and Harrison, 2000; Davi and Falco, 2005; Leopold and Loscalzo, 2005). A growing body of evidence suggests that oxidative stress due to excessive production of ROS is associated with endothelial dysfunction (Harrison et al., 2003). Interestingly, cellular oxidant damage is detected before clinically significant vascular disease, which support the concept that increased endogenous oxidant stress promotes the development of vasculopathies. Strategies to decrease intracellular ROS levels have shown therapeutic potential for patients suffering from cardiovascular and metabolic disorders and related complications (Li et al., 2009; Virdis et al., 2004). Usually the imbalance caused by oxidative stress is derived either from an increase in ROS production or from a decreased level of ROS scavenging proteins. ROS-induced stimulation of protein phosphorylation pathways modulates transcription factor activities and gene expression, which results in a variety of responses such as cell necrosis or apoptosis. Here, H_2O_2-induced oxidative stress was found to be dependent on a significant production of ROS in EPCs which in turn was associated with an upregulation of Nox4, STAT-3, and eNOS. SAL significantly increased cell viability and declined cell death in EPCs subjected to H_2O_2-induced oxidative stress by reducing ROS formation and attenuating the increased expression of Nox4, STAT-3, and eNOS (Figure 19). NADPH oxidase is one of the most prominent sources of vascular ROS being expressed in a variety of vascular cells. The importance of NADPH oxidase in both vascular physiology and pathophysiology has been emphasized extensively (Frey et al., 2009; Li and Shah, 2003). Among other catalytic NADPH oxidase (Nox) homologues, Nox4 is abundantly expressed in ECs and functions as a key endothelial NADPH oxidase membrane component which is involved in the regulation of cell growth and cell survival in ECs (Ago et al., 2004). Nox4 is the major source of evoked $O_2^{\bullet-}$ that triggers apoptosis in cerebral vascular ECs (Basuroy et al., 2009). Upregulation of Nox4 may have a direct influence on mitochondrial oxidative stress increase along with consequent mitochondrial dysfunction and cell death. In this regard, the

present data show that SAL and SalB attenuates the upregulation of NADPH oxidase and Nox4 expression (Figure 17, 19). The NADPH oxidase inhibitor DPI at least partially mediated the suppression of ROS and restored the cell survival rate by downregulating the cleaved caspase-3 and Bax/Bcl-xL protein expression (Figure 17). This suggests that the inhibition of ROS production and the subsequent protective effect of SAL and SalB against oxidation is likely to be related to the suppression of NADPH oxidase. Furthermore, cell apoptosis was suppressed by SAL and SalB after H_2O_2 provocation, which was evidenced by preventing the loss of MMP and maintaining the integrity of the plasma membrane (Figure 18).

Members of the Bcl-2 family of proteins have a central role in controlling the apoptotic pathway. Some proteins within this family, including Bcl-2 and Bcl-xL, suppress apoptosis, while others such as Bax and Bak promote apoptosis. Hence, alterations in the levels of anti- and pro-apoptotic Bcl-2 family proteins are critical for the induction of apoptosis. We found that H_2O_2 stress resulted in an increased expression of Bax protein and a decreased expression of Bcl-xL. Pretreatment with SAL or ICAR reversed this effect thereby decreasing the Bax/Bcl-xL ratio (Figure 19). Therefore, it is conclusive to postulate that downregulation of Bax and upregulation of Bcl-xL may be responsible for the observed anti-apoptotic effect of them. Xu and co-workers found that SAL is capable of protecting HUVECs against H_2O_2-induced apoptosis by inhibiting ROS production and by activating the PI3-K/Akt/mTOR-dependent pathway (Xu et al., 2013). Dai et al. observed that the reduction of oxidative stress enhances ECs survival thereby facilitating ischemia-mediated angiogenesis (Dai et al., 2009). Taken together, it is likely that the antioxidative effect of SAL contributes to an increased angiogenic ability in BM-EPCs.

On the one side, NO is beneficial as a messenger or modulator of angiogeneic events, however, on the other side it is potentially toxic under conditions of oxidative stress (Colasanti and Suzuki, 2000). The toxic effects of NO may be attributed to its free radical character, which makes NO react with superoxide (O_2^-) to produce a strong oxidant,

peroxynitrite ($ONOO^-$), that may mediate much of the NO toxicity. In the present study, we showed that H_2O_2 induced the production of NO and that the expression of eNOS protein was restored by SalB to baseline level (Figure 17). Interestingly, NADPH oxidase inhibitor fully abrogated the increase in ROS generation as well as eNOS uncoupling triggered by H_2O_2, and abolished the effect of SalB, suggesting that NADPH functions upstream of eNOS underlying the action of SalB. The oxidative-mediated autophagy was alleviated when eNOS was inhibited, indicating that elevated levels of 'uncoupled eNOS' derived from over-oxidation contributes to an increased generation of superoxide anions representing a critical step during the initiation of endothelial dysfunction.

Prior studies have shown that the mTOR pathway plays a key role in the regulation of both resting oxygen consumption and oxidative capacity, and mTOR-raptor complex formation is tightly correlated with mitochondrial metabolism (Schieke et al., 2006). Oxidative stress can block the activity of mTOR signaling pathways to reverse cell metabolism and longevity leading to cell death (Andreucci et al., 2009; Chen et al., 2010). In contrast, activation of mTOR during oxidative stress can result in cytoprotection (Chen et al., 2010). We show that administration of both rapamycin and LY294002 during SalB application significantly prevented cellular protection by SalB illustrating that SalB relies upon the activation of mTOR to protect BM-EPCs against oxidative stress (Figure 20). Moreover, we provide evidence that loss of 4EBP1 significantly elevates cell apoptosis after H_2O_2 exposure, and abolishes the protection by SalB, suggesting that 4EBP1 controls caspase activation and modulates the proteins of the Bcl-2 family thereby mediating the ability of SalB to resist to oxidative injury.

Exogenous H_2O_2 mimics the effect of endogenous receptor-induced H_2O_2 and activates multiple kinases (Konishi et al., 1997; Sun et al., 2000). MAPK signaling pathways are well known to be affected by receptor ligand interactions, as well as by different stimuli placed on the cell (Sun et al., 2001). The well-characterized MAPK family members p38 MAPK, ERK1/2, and JNK play important roles in the coordination of cellular stress responses towards oxidation (Aggeli et al., 2006; Gutierrez-Uzquiza et al., 2012).

Each MAPK is activated by phosphorylation by specific upstream MAPK kinases (MKKs) as part of a three-tiered cascade of kinases (MAPK kinase kinase (MAPKKK)/MKK/MAPK) in response to a wide range of physiological and pathological stimuli. Mitochondrial dysfunction could result in cell death by release of mitochondrial proteins into the cytosol and subsequent activation of cell death execution molecules. Activation of MAPKs signaling pathways in response to a variety of stressors such as oxidative stress, also leads to apoptosis via the mitochondria-dependent pathway (Chen et al., 2013; Ghosh et al., 2011). To elucidate the mechanism underlying the cytoprotective effect of TCM extracts we investigated potentially relevant signaling pathways. Loss of MMP ($\Delta\psi m$), release of cytochrome c from mitochondria and subsequent activation of caspase-3 and cleavage of PARP are key steps in the mitochondrion-dependent apoptotic cell death pathway. Treatment with SalB and ICAR prior to H_2O_2 stress, however, counteracted mitochondrion-mediated apoptosis. It is known that SB203580 exerts its inhibitory effect by binding to the ATP binding pocket of p38 MAPK, thus inhibiting its ability to undergo autophosphorylation, but not affecting the capacity of p38 MAPK to be phosphorylated by upstream MAPKK, MKK3/6 (Figure 21). We found that H_2O_2-induced p38 phosphorylation was SB203580-sensitive, suggesting that the p38 MAPK autophosphorylation triggers cell apoptosis by differentially regulating the expression and/or activities of pro-and anti-apoptotic Bcl-2 family proteins. Moreover, we found that SalB-mediated attenuation of stress-stimulated p38 MAPK signaling includes the inhibition of phosphorylation of MKK3/6, its direct upstream activating kinases indicating that SalB regulates signaling events upstream of MAPKKs resulting in p38 MAPK activation. Unexpectedly, the phosphorylation of p38 MAPK was supported by inhibition of mTOR and by knockdown of 4EBP1, resulting in subsequent enhanced cell injury (Figure 21). We hypothesize that oxidative stress induced activation of p38 MAPK suppresses the physiological mTOR/4EBP1 activity of proliferating and differentiating cells and, in turn, this loss of mTOR activity sensitizes the BM-EPCs to p38 mediated apoptosis.

ATF2 has been implicated in a large set of cellular stress responses, such as those exposed to proinflammatory cytokines, ultraviolet irradiation, DNA damage, change in ROS, and as a primary downstream target of p38 involved in the control of cell cycle progression (Bhoumik et al., 2007; Hayakawa et al., 2004; Lewis et al., 2005). In the present study, we have identified a novel role for ATF2 as an essential target of oxidative stress-dependent endothelial injury that mediate the stress-counteraction of SalB. ERK1/2 has been shown to have proliferative and protective effects on cells exposed to oxidative stress. Low and adequate concentrations of H_2O_2 is mitogenic, being partly due to activation of ERK1/2 (Burdon, 1995). However recently, ERK1/2 was reported to exert a pro-apoptotic role depended on oxidative stress (Lee et al., 2006; Leong et al., 2011). The present findings suggest that blockade of H_2O_2-induced ERK1/2 by U0126 conveys survival signals as observed by enhanced cellular resistance towards oxidative stress accompanied by a decreased Bax/Bcl-xL ratio. Moreover, the possible downstream effector phosphorylated ATF2 was repressed by ERK1/2 inhibition (Figure 22).

Autophagy occurs at basal level in most cells and contributes to the turnover of long-lived proteins and organelles to maintain intracellular homeostasis. In response to cellular stress, autophagy is upregulated and can provide an adaptive strategy for cell survival, but excessive autophagy causes cellular destruction and is referred to as type-II cell death. Thus a full understanding of the signaling pathways that regulate autophagy will allow the development of new therapies to treat diseases in which this process is implicated. The microtubule-associated protein LC3 is an autophagosome ortholog of yeast Atg8, which is associated with autophagosome membranes after processing, and is modified via an ubiquitination-like system. The LC3 is now widely used to monitor autophagy that is a tipical early marker for the formation of autophagosomes. There are two cellular forms of the LC3 protein. One is LC3-I (18 kDa), a cytoplasmic form of LC3, and another one is LC3-II (16 kDa), a cleavage form of LC3, which is associated with the autophagosomal membrane. Thus, the increased expression of LC3-II is associated with autophagy induction. In addition, the protein p62 SQSTM1 has been reported to interact with the

autophagic effector protein LC3 and is degraded through an autophagy-lysosome pathway. Beclin 1, the mammalian orthologue of yeast Atg6, can interacts with several cofactors (Atg14L, UVRAG, Bif-1, Rubicon, surviving, etc) to regulate the lipid kinase Vps-34 protein and promote formation of Beclin 1-Vps34-Vps15 core complexes, thereby inducing autophagy (He and Levine, 2010).

Worthy of note, investigators have demonstrated that oxidative stress could induce autophagy *in vitro*. Bhogal and colleagues reported that oxidative stress increases hepatocyte autophagy in a ROS-dependent manner, and mitochondrial ROS and NADPH are found to be key regulators of autophagy (Bhogal et al., 2012). Consistent with prior reports, our results show that pathophysiological concentrations of H_2O_2 induces autophagosome formation in cultured human BM-EPCs. However, co-treatment of ICAR reduced H_2O_2-induced autophagy as indicated by multiple independent approaches that either revealed the formation of autophagic vacuoles or the expression of autophagy specific proteins (Figure 23).

Numerous autophagic pathways converge at the mTOR, which when phosphorylated becomes a potent inhibitor of autophagy. Silencing of mTOR using siRNA transfection was known to enhance rapamycin-induced autophagy (Ravikumar et al., 2004). Interestingly, we found that p-mTOR expression was reduced but LC3-II expression was elevated by oxidative stress; however, such effect was notably attenuated by ICAR. To further test the involvement of mTOR-dependent pathway in this protective process, we applied rapamycin, a specific inhibitor of mTOR, to the cells before administration of H_2O_2 or ICAR. We found that p-mTOR was significantly inhibited by H_2O_2 in the presence of rapamycin, and ICAR-induced suppression of LC3-II expression was partially blocked by pretreated with rapamycin. Moreover, ICAR-induced suppression of autophagy was partially blocked by pretreated with rapamycin. In our system, the autophagy inhibitor 3-MA suppressed the oxidative stress induced-cell death, further strengthening the association between autophagy, ROS, and cell death (Figure 23).

There are many reports on the effect of p38 MAPK in autophagy. However, depending on the stimulus and the cell type, p38MAPK has been described to act either as a positive or as a negative regulator of this process. For example, it has been described that LPS (lipopolysaccharide) and interferon-γ activate p38 MAPK inducing autophagy (Doyle et al., 2011; Matsuzawa et al., 2012). In contrast, Webber and co-workers showed that in full medium p38 MAPK is phosphorylated and inhibits autophagy by sequestering p38-IP (p38-interacting protein) (Webber and Tooze, 2010). In the present study, we have observed that p38 MAPK phosphorylation is induced under oxidative conditions and that inhibition of p38 MAPK by SB203580 prevents the accumulation of LC3-II, suggesting that p38 MAPK is necessary for the activation of autophagy by H_2O_2 (Figure 24). The substrates of p38 MAPK, ATF2 was also phosphorylated after the addition of H_2O_2. When ATF2 was knocked down, a reduced level of cell death was correlated with the observed decreased amount of ROS accumulation, and the H_2O_2-induced autophagy. Since p38 MAPK also translocates to the nucleus after H_2O_2 treatment, it is tempting to hypothesize that this activates some transcription factors, e.g. ATF2, that will drive the expression of genes implicated in autophagy induction. Furthermore, when examined the phosphorylation status of p38 MAPK and mTOR after H_2O_2 and rapamycin treatment, we found that induction of autophagy by rapamycin significantly increased oxidative stress-induced apoptosis which was all largely reversed by SB203580 (Figure 26). Thus, we concluded that H_2O_2 induced autophagy via activation of p38 MAPK, which functions through the downstream inhibition of the mTOR signaling pathway.

Here, we also present evidence supporting that the ROS-dependent ERK activation by oxidation plays an important role in autophagy induction. ERK activation appears to have divergent roles in autophagy in different cell types. ERK upregulates starvation-induced autophagy by down-regulating Akt/mTOR/S6K (Shinojima et al., 2007). Wang and co-workers proposed that a non-canonical MEK/ERK module regulates autophagy by modulating Beclin 1 level through an AMPK-MEK/ERK-TSC-mTOR signaling pathway (Wang et al., 2009). In our study pathophysiological levels of H_2O_2 induces an autophagic

phenotype that is also mediated by ERK activation in addition to mTOR signaling pathway (Figure 25). These findings suggest that the regulation of autophagy by ROS involves multiple kinase signaling pathways, and underlining a possible universal mechanism in autophagy regulation through mTOR.

The mechanisms of apoptosis and autophagy are different, and involve fundamentally distinct sets of regulatory and executioner molecules. Although autophagy is independent of apoptosis, it could act in conjunction with apoptosis to induce neurotoxic cell death (Nopparat et al., 2010). In our study, both autophagy and apoptosis are involved in protection of ICAR against H_2O_2-induced injury in BM-EPCs. We hypothesized that MAPK/P38 MAPK signaling, which is induced by ROS accumulation, downregulates mTOR function and subsequently activates the apoptosis and autophagy pathway.

Taken together, the present study demonstrated that SAL, ICAR and PUER promote cell growth, cell migration, cell-matrix and capillary-like tube formation of BM-EPCs. The results provide mechanistic evidence that activation of the mTOR/p70S6K/4EBP1 pathways is required for both SAL and ICAR-mediated pro-proliferative and pro-angionenic effects in BM-EPCs. In addition, SAL, SalB and ICAR attenuate the cytotoxic and pro-apoptotic effect of H_2O_2 *in vitro*. Suppression of MKK3/6-p38 MAPK-ATF2 and ERK1/2 signaling pathways, and maintenance of mTOR/4EBP1 activity are associated with the reduction of oxidative stress-induced intracellular ROS levels and apoptosis mediated by SalB and ICAR. The investigation also found that ICAR owns the ability to inhibit apoptotic and autophagic programmed cell death via restoring the loss of mTOR and attenuation of ATF2 activity upon oxidative stress. Based on the outcomes of the present work, we propose SAL, SalB and ICAR as novel proanigiogenic and cytoprotective therapeutic agents with potential applications in the fields of systemic and site-specific tissue regeneration including ischaemic disease and extended musculoskeletal tissue defects.

REFERENCES

Adams, R.H., and Alitalo, K. (2007). Molecular regulation of angiogenesis and lymphangiogenesis. Nature reviews Molecular cell biology *8*, 464-478.

Aggeli, I.K., Gaitanaki, C., and Beis, I. (2006). Involvement of JNKs and p38-MAPK/MSK1 pathways in H2O2-induced upregulation of heme oxygenase-1 mRNA in H9c2 cells. Cellular signalling *18*, 1801-1812.

Ago, T., Kitazono, T., Ooboshi, H., Iyama, T., Han, Y.H., Takada, J., Wakisaka, M., Ibayashi, S., Utsumi, H., and Iida, M. (2004). Nox4 as the major catalytic component of an endothelial NAD(P)H oxidase. Circulation *109*, 227-233.

Albrecht-Schgoer, K., Schgoer, W., Holfeld, J., Theurl, M., Wiedemann, D., Steger, C., Gupta, R., Semsroth, S., Fischer-Colbrie, R., Beer, A.G.*, et al.* (2012). The angiogenic factor secretoneurin induces coronary angiogenesis in a model of myocardial infarction by stimulation of vascular endothelial growth factor signaling in endothelial cells. Circulation *126*, 2491-2501.

Alliston, T., Choy, L., Ducy, P., Karsenty, G., and Derynck, R. (2001). TGF-beta-induced repression of CBFA1 by Smad3 decreases cbfa1 and osteocalcin expression and inhibits osteoblast differentiation. The EMBO journal *20*, 2254-2272.

Anderson, T.J., Gerhard, M.D., Meredith, I.T., Charbonneau, F., Delagrange, D., Creager, M.A., Selwyn, A.P., and Ganz, P. (1995). Systemic nature of endothelial dysfunction in atherosclerosis. The American journal of cardiology *75*, 71B-74B.

Andreucci, M., Fuiano, G., Presta, P., Lucisano, G., Leone, F., Fuiano, L., Bisesti, V., Esposito, P., Russo, D., Memoli, B.*, et al.* (2009). Downregulation of cell survival signalling pathways and increased cell damage in hydrogen peroxide-treated human renal proximal tubular cells by alpha-erythropoietin. Cell proliferation *42*, 554-561.

Asahara, T., Masuda, H., Takahashi, T., Kalka, C., Pastore, C., Silver, M., Kearne, M., Magner, M., and Isner, J.M. (1999). Bone marrow origin of endothelial progenitor cells responsible for postnatal vasculogenesis in physiological and pathological neovascularization. Circulation research *85*, 221-228.

Asahara, T., Murohara, T., Sullivan, A., Silver, M., van der Zee, R., Li, T., Witzenbichler, B., Schatteman, G., and Isner, J.M. (1997). Isolation of putative progenitor endothelial cells for angiogenesis. Science *275*, 964-967.

Axe, E.L., Walker, S.A., Manifava, M., Chandra, P., Roderick, H.L., Habermann, A., Griffiths, G., and Ktistakis, N.T. (2008). Autophagosome formation from membrane compartments enriched in

phosphatidylinositol 3-phosphate and dynamically connected to the endoplasmic reticulum. The Journal of cell biology *182*, 685-701.

Baehrecke, E.H. (2005). Autophagy: dual roles in life and death? Nature reviews Molecular cell biology *6*, 505-510.

Ballinger, S.W., Patterson, C., Knight-Lozano, C.A., Burow, D.L., Conklin, C.A., Hu, Z., Reuf, J., Horaist, C., Lebovitz, R., Hunter, G.C*., et al.* (2002). Mitochondrial integrity and function in atherogenesis. Circulation *106*, 544-549.

Barnes, G.L., Kostenuik, P.J., Gerstenfeld, L.C., and Einhorn, T.A. (1999). Growth factor regulation of fracture repair. Journal of bone and mineral research : the official journal of the American Society for Bone and Mineral Research *14*, 1805-1815.

Basuroy, S., Bhattacharya, S., Leffler, C.W., and Parfenova, H. (2009). Nox4 NADPH oxidase mediates oxidative stress and apoptosis caused by TNF-alpha in cerebral vascular endothelial cells. American journal of physiology Cell physiology *296*, C422-432.

Basuroy, S., Leffler, C.W., and Parfenova, H. (2013). CORM-A1 prevents blood-brain barrier dysfunction caused by ionotropic glutamate receptor-mediated endothelial oxidative stress and apoptosis. American journal of physiology Cell physiology *304*, C1105-1115.

Bax, B.E., Wozney, J.M., and Ashhurst, D.E. (1999). Bone morphogenetic protein-2 increases the rate of callus formation after fracture of the rabbit tibia. Calcified tissue international *65*, 83-89.

Beenken, A., and Mohammadi, M. (2009). The FGF family: biology, pathophysiology and therapy. Nature reviews Drug discovery *8*, 235-253.

Bernales, S., McDonald, K.L., and Walter, P. (2006). Autophagy counterbalances endoplasmic reticulum expansion during the unfolded protein response. PLoS biology *4*, e423.

Berven, L.A., Willard, F.S., and Crouch, M.F. (2004). Role of the p70(S6K) pathway in regulating the actin cytoskeleton and cell migration. Experimental cell research *296*, 183-195.

Beswick, R.A., Zhang, H., Marable, D., Catravas, J.D., Hill, W.D., and Webb, R.C. (2001). Long-term antioxidant administration attenuates mineralocorticoid hypertension and renal inflammatory response. Hypertension *37*, 781-786.

Betin, V.M., and Lane, J.D. (2009). Caspase cleavage of Atg4D stimulates GABARAP-L1 processing and triggers mitochondrial targeting and apoptosis. Journal of cell science *122*, 2554-2566.

Bhattacharya, V., McSweeney, P.A., Shi, Q., Bruno, B., Ishida, A., Nash, R., Storb, R.F., Sauvage, L.R., Hammond, W.P., and Wu, M.H. (2000). Enhanced endothelialization and microvessel formation in polyester grafts seeded with CD34(+) bone marrow cells. Blood *95*, 581-585.

Bhogal, R.H., Weston, C.J., Curbishley, S.M., Adams, D.H., and Afford, S.C. (2012). Autophagy: a cyto-protective mechanism which prevents primary human hepatocyte apoptosis during oxidative stress. Autophagy *8*, 545-558.

Bhoumik, A., Lopez-Bergami, P., and Ronai, Z. (2007). ATF2 on the double - activating transcription factor and DNA damage response protein. Pigment cell research / sponsored by the European Society for Pigment Cell Research and the International Pigment Cell Society *20*, 498-506.

Bialik, S., and Kimchi, A. (2010). Lethal weapons: DAP-kinase, autophagy and cell death: DAP-kinase regulates autophagy. Current opinion in cell biology *22*, 199-205.

Bordenave, L., Georges, A., Bareille, R., Conrad, V., Villars, F., and Amedee, J. (2002). Human bone marrow endothelial cells: a new identified source of B-type natriuretic peptide. Peptides *23*, 935-940.

Bouxsein, M.L., Turek, T.J., Blake, C.A., D'Augusta, D., Li, X., Stevens, M., Seeherman, H.J., and Wozney, J.M. (2001). Recombinant human bone morphogenetic protein-2 accelerates healing in a rabbit ulnar osteotomy model. The Journal of bone and joint surgery American volume *83-A*, 1219-1230.

Bowie, A., and O'Neill, L.A. (2000). Oxidative stress and nuclear factor-kappaB activation: a reassessment of the evidence in the light of recent discoveries. Biochemical pharmacology *59*, 13-23.

Brandi, M.L., and Collin-Osdoby, P. (2006). Vascular biology and the skeleton. Journal of bone and mineral research : the official journal of the American Society for Bone and Mineral Research *21*, 183-192.

Brunner, H., Cockcroft, J.R., Deanfield, J., Donald, A., Ferrannini, E., Halcox, J., Kiowski, W., Luscher, T.F., Mancia, G., Natali, A*., et al.* (2005). Endothelial function and dysfunction. Part II: Association with cardiovascular risk factors and diseases. A statement by the Working Group on Endothelins and Endothelial Factors of the European Society of Hypertension. Journal of hypertension *23*, 233-246.

Burdon, R.H. (1995). Superoxide and hydrogen peroxide in relation to mammalian cell proliferation. Free radical biology & medicine *18*, 775-794.

Burkhardt, R., Kettner, G., Bohm, W., Schmidmeier, M., Schlag, R., Frisch, B., Mallmann, B., Eisenmenger, W., and Gilg, T. (1987). Changes in trabecular bone, hematopoiesis and bone marrow

vessels in aplastic anemia, primary osteoporosis, and old age: a comparative histomorphometric study. Bone *8*, 157-164.

Cai, H., and Harrison, D.G. (2000). Endothelial dysfunction in cardiovascular diseases: the role of oxidant stress. Circulation research *87*, 840-844.

Canu, N., Tufi, R., Serafino, A.L., Amadoro, G., Ciotti, M.T., and Calissano, P. (2005). Role of the autophagic-lysosomal system on low potassium-induced apoptosis in cultured cerebellar granule cells. Journal of neurochemistry *92*, 1228-1242.

Carano, R.A., and Filvaroff, E.H. (2003). Angiogenesis and bone repair. Drug discovery today *8*, 980-989.

Chen, C.H., Chen, S.J., Su, C.C., Yen, C.C., Tseng, T.J., Jinn, T.R., Tang, F.C., Chen, K.L., Su, Y.C., Lee k, I.*, et al.* (2013). Chloroacetic acid induced neuronal cells death through oxidative stress-mediated p38-MAPK activation pathway regulated mitochondria-dependent apoptotic signals. Toxicology *303*, 72-82.

Chen, D., Harris, M.A., Rossini, G., Dunstan, C.R., Dallas, S.L., Feng, J.Q., Mundy, G.R., and Harris, S.E. (1997). Bone morphogenetic protein 2 (BMP-2) enhances BMP-3, BMP-4, and bone cell differentiation marker gene expression during the induction of mineralized bone matrix formation in cultures of fetal rat calvarial osteoblasts. Calcified tissue international *60*, 283-290.

Chen, L., Xu, B., Liu, L., Luo, Y., Yin, J., Zhou, H., Chen, W., Shen, T., Han, X., and Huang, S. (2010). Hydrogen peroxide inhibits mTOR signaling by activation of AMPKalpha leading to apoptosis of neuronal cells. Laboratory investigation; a journal of technical methods and pathology *90*, 762-773.

Chen, S.C., Lin, Y.L., Huang, B., Wang, D.L., and Cheng, J.J. (2011). Salvianolic acid B suppresses IFN-gamma-induced JAK/STAT1 activation in endothelial cells. Thrombosis research *128*, 560-564.

Chen, Y.H., Du, G.H., and Zhang, J.T. (2000). Salvianolic acid B protects brain against injuries caused by ischemia-reperfusion in rats. Acta pharmacologica Sinica *21*, 463-466.

Cho, T.J., Gerstenfeld, L.C., and Einhorn, T.A. (2002). Differential temporal expression of members of the transforming growth factor beta superfamily during murine fracture healing. Journal of bone and mineral research : the official journal of the American Society for Bone and Mineral Research *17*, 513-520.

Colasanti, M., and Suzuki, H. (2000). The dual personality of NO. Trends in pharmacological sciences *21*, 249-252.

Colnot, C., Romero, D.M., Huang, S., and Helms, J.A. (2005). Mechanisms of action of demineralized bone matrix in the repair of cortical bone defects. Clinical orthopaedics and related research, 69-78.

Dai, S., He, Y., Zhang, H., Yu, L., Wan, T., Xu, Z., Jones, D., Chen, H., and Min, W. (2009). Endothelial-specific expression of mitochondrial thioredoxin promotes ischemia-mediated arteriogenesis and angiogenesis. Arteriosclerosis, thrombosis, and vascular biology *29*, 495-502.

Dailey, L., Ambrosetti, D., Mansukhani, A., and Basilico, C. (2005). Mechanisms underlying differential responses to FGF signaling. Cytokine & growth factor reviews *16*, 233-247.

Darbinyan, V., Kteyan, A., Panossian, A., Gabrielian, E., Wikman, G., and Wagner, H. (2000). Rhodiola rosea in stress induced fatigue--a double blind cross-over study of a standardized extract SHR-5 with a repeated low-dose regimen on the mental performance of healthy physicians during night duty. Phytomedicine : international journal of phytotherapy and phytopharmacology *7*, 365-371.

Davi, G., and Falco, A. (2005). Oxidant stress, inflammation and atherogenesis. Lupus *14*, 760-764.

De Bock, K., Eijnde, B.O., Ramaekers, M., and Hespel, P. (2004). Acute Rhodiola rosea intake can improve endurance exercise performance. International journal of sport nutrition and exercise metabolism *14*, 298-307.

De Vriese, A.S., Verbeuren, T.J., Van de Voorde, J., Lameire, N.H., and Vanhoutte, P.M. (2000). Endothelial dysfunction in diabetes. British journal of pharmacology *130*, 963-974.

Dickinson, R.J., Williams, D.J., Slack, D.N., Williamson, J., Seternes, O.M., and Keyse, S.M. (2002). Characterization of a murine gene encoding a developmentally regulated cytoplasmic dual-specificity mitogen-activated protein kinase phosphatase. The Biochemical journal *364*, 145-155.

Dimitriou, R., Jones, E., McGonagle, D., and Giannoudis, P.V. (2011). Bone regeneration: current concepts and future directions. BMC medicine *9*, 66.

Dimmeler, S., and Zeiher, A.M. (2004). Vascular repair by circulating endothelial progenitor cells: the missing link in atherosclerosis? Journal of molecular medicine *82*, 671-677.

Ding, D.C., Shyu, W.C., Lin, S.Z., and Li, H. (2007). The role of endothelial progenitor cells in ischemic cerebral and heart diseases. Cell transplantation *16*, 273-284.

Djavaheri-Mergny, M., Amelotti, M., Mathieu, J., Besancon, F., Bauvy, C., and Codogno, P. (2007). Regulation of autophagy by NFkappaB transcription factor and reactives oxygen species. Autophagy *3*, 390-392.

Djavaheri-Mergny, M., Maiuri, M.C., and Kroemer, G. (2010). Cross talk between apoptosis and autophagy by caspase-mediated cleavage of Beclin 1. Oncogene *29*, 1717-1719.

Donati, A., Cavallini, G., Paradiso, C., Vittorini, S., Pollera, M., Gori, Z., and Bergamini, E. (2001). Age-related changes in the autophagic proteolysis of rat isolated liver cells: effects of antiaging dietary restrictions. The journals of gerontology Series A, Biological sciences and medical sciences *56*, B375-383.

Doyle, A., Zhang, G., Abdel Fattah, E.A., Eissa, N.T., and Li, Y.P. (2011). Toll-like receptor 4 mediates lipopolysaccharide-induced muscle catabolism via coordinate activation of ubiquitin-proteasome and autophagy-lysosome pathways. Faseb J *25*, 99-110.

Drummond, G.R., Cai, H., Davis, M.E., Ramasamy, S., and Harrison, D.G. (2000). Transcriptional and posttranscriptional regulation of endothelial nitric oxide synthase expression by hydrogen peroxide. Circulation research *86*, 347-354.

Edelberg, J.M., Tang, L., Hattori, K., Lyden, D., and Rafii, S. (2002). Young adult bone marrow-derived endothelial precursor cells restore aging-impaired cardiac angiogenic function. Circulation research *90*, E89-93.

Egami, R., Tanaka, Y., Nozaki, M., Koera, K., Okuma, A., and Nakano, H. (2005). Chronic treatment with 17beta-estradiol increases susceptibility of smooth muscle cells to nitric oxide. European journal of pharmacology *520*, 142-149.

Egermann, M., Lill, C.A., Griesbeck, K., Evans, C.H., Robbins, P.D., Schneider, E., and Baltzer, A.W. (2006). Effect of BMP-2 gene transfer on bone healing in sheep. Gene therapy *13*, 1290-1299.

Einhorn, T.A. (1995). Enhancement of fracture-healing. The Journal of bone and joint surgery American volume *77*, 940-956.

Einhorn, T.A. (1998). The cell and molecular biology of fracture healing. Clinical orthopaedics and related research, S7-21.

Eisenberg-Lerner, A., Bialik, S., Simon, H.U., and Kimchi, A. (2009). Life and death partners: apoptosis, autophagy and the cross-talk between them. Cell death and differentiation *16*, 966-975.

Fan, W., Sun, D., Liu, J., Liang, D., Wang, Y., Narsinh, K.H., Li, Y., Qin, X., Liang, J., Tian, J.*, et al.* (2012). Adipose stromal cells amplify angiogenic signaling via the VEGF/mTOR/Akt pathway in a murine hindlimb ischemia model: a 3D multimodality imaging study. PloS one *7*, e45621.

Fantz, D.A., Jacobs, D., Glossip, D., and Kornfeld, K. (2001). Docking sites on substrate proteins direct extracellular signal-regulated kinase to phosphorylate specific residues. The Journal of biological chemistry *276*, 27256-27265.

Farre, J.C., and Subramani, S. (2004). Peroxisome turnover by micropexophagy: an autophagy-related process. Trends in cell biology *14*, 515-523.

Fimia, G.M., and Piacentini, M. (2010). Regulation of autophagy in mammals and its interplay with apoptosis. Cellular and molecular life sciences : CMLS *67*, 1581-1588.

Fingar, D.C., and Blenis, J. (2004). Target of rapamycin (TOR): an integrator of nutrient and growth factor signals and coordinator of cell growth and cell cycle progression. Oncogene *23*, 3151-3171.

Fleury, C., Mignotte, B., and Vayssiere, J.L. (2002). Mitochondrial reactive oxygen species in cell death signaling. Biochimie *84*, 131-141.

Frey, R.S., Ushio-Fukai, M., and Malik, A.B. (2009). NADPH oxidase-dependent signaling in endothelial cells: role in physiology and pathophysiology. Antioxidants & redox signaling *11*, 791-810.

Gallagher, K.A., Liu, Z.J., Xiao, M., Chen, H., Goldstein, L.J., Buerk, D.G., Nedeau, A., Thom, S.R., and Velazquez, O.C. (2007). Diabetic impairments in NO-mediated endothelial progenitor cell mobilization and homing are reversed by hyperoxia and SDF-1 alpha. The Journal of clinical investigation *117*, 1249-1259.

Gao, L., Ji, X., Song, J., Liu, P., Yan, F., Gong, W., Dang, S., and Luo, Y. (2009). Puerarin protects against ischemic brain injury in a rat model of transient focal ischemia. Neurological research *31*, 402-406.

Garmy-Susini, B., and Varner, J.A. (2005). Circulating endothelial progenitor cells. British journal of cancer *93*, 855-858.

Gavard, J., and Gutkind, J.S. (2006). VEGF controls endothelial-cell permeability by promoting the beta-arrestin-dependent endocytosis of VE-cadherin. Nature cell biology *8*, 1223-1234.

Gerber, H.P., Vu, T.H., Ryan, A.M., Kowalski, J., Werb, Z., and Ferrara, N. (1999). VEGF couples hypertrophic cartilage remodeling, ossification and angiogenesis during endochondral bone formation. Nature medicine *5*, 623-628.

Ghosh, M., Manna, P., and Sil, P.C. (2011). Protective role of a coumarin-derived schiff base scaffold against tertiary butyl hydroperoxide (TBHP)-induced oxidative impairment and cell death via MAPKs, NF-kappaB and mitochondria-dependent pathways. Free radical research *45*, 620-637.

Giannoudis, P.V., Einhorn, T.A., and Marsh, D. (2007). Fracture healing: the diamond concept. Injury *38 Suppl 4*, S3-6.

Gill, M., Dias, S., Hattori, K., Rivera, M.L., Hicklin, D., Witte, L., Girardi, L., Yurt, R., Himel, H., and Rafii, S. (2001). Vascular trauma induces rapid but transient mobilization of VEGFR2(+)AC133(+) endothelial precursor cells. Circulation research *88*, 167-174.

Glowacki, J. (1998). Angiogenesis in fracture repair. Clinical orthopaedics and related research, S82-89.

Grellier, M., Bordenave, L., and Amedee, J. (2009). Cell-to-cell communication between osteogenic and endothelial lineages: implications for tissue engineering. Trends in biotechnology *27*, 562-571.

Gunsilius, E., Petzer, A.L., Duba, H.C., Kahler, C.M., and Gastl, G. (2001). Circulating endothelial cells after transplantation. Lancet *357*, 1449-1450.

Gutierrez-Uzquiza, A., Arechederra, M., Bragado, P., Aguirre-Ghiso, J.A., and Porras, A. (2012). p38alpha mediates cell survival in response to oxidative stress via induction of antioxidant genes: effect on the p70S6K pathway. The Journal of biological chemistry *287*, 2632-2642.

Haigh, J.J., Gerber, H.P., Ferrara, N., and Wagner, E.F. (2000). Conditional inactivation of VEGF-A in areas of collagen2a1 expression results in embryonic lethality in the heterozygous state. Development *127*, 1445-1453.

Hamacher-Brady, A., Brady, N.R., and Gottlieb, R.A. (2006). Enhancing macroautophagy protects against ischemia/reperfusion injury in cardiac myocytes. The Journal of biological chemistry *281*, 29776-29787.

Harris, G.M., Rutledge, K., Cheng, Q., Blanchette, J., and Jabbarzadeh, E. (2013). Strategies to direct angiogenesis within scaffolds for bone tissue engineering. Current pharmaceutical design *19*, 3456-3465.

Harrison, D., Griendling, K.K., Landmesser, U., Hornig, B., and Drexler, H. (2003). Role of oxidative stress in atherosclerosis. The American journal of cardiology *91*, 7A-11A.

Hayakawa, J., Mittal, S., Wang, Y., Korkmaz, K.S., Adamson, E., English, C., Ohmichi, M., McClelland, M., and Mercola, D. (2004). Identification of promoters bound by c-Jun/ATF2 during rapid large-scale gene activation following genotoxic stress. Molecular cell *16*, 521-535.

He, C., and Levine, B. (2010). The Beclin 1 interactome. Current opinion in cell biology *22*, 140-149.

He, H., Shi, M., Zeng, X., Yang, J., Li, Y., Wu, L., and Li, L. (2008). Cardioprotective effect of salvianolic acid B on large myocardial infarction mediated by reversing upregulation of leptin,

endothelin pathways, and abnormal expression of SERCA2a, phospholamban in rats. Journal of ethnopharmacology *118*, 35-45.

He, W., Sun, H., Yang, B., Zhang, D., and Kabelitz, D. (1995). Immunoregulatory effects of the herba Epimediia glycoside icariin. Arzneimittel-Forschung *45*, 910-913.

Hoetzer, G.L., Van Guilder, G.P., Irmiger, H.M., Keith, R.S., Stauffer, B.L., and DeSouza, C.A. (2007). Aging, exercise, and endothelial progenitor cell clonogenic and migratory capacity in men. Journal of applied physiology *102*, 847-852.

Hristov, M., and Weber, C. (2004). Endothelial progenitor cells: characterization, pathophysiology, and possible clinical relevance. Journal of cellular and molecular medicine *8*, 498-508.

Hsu, F.L., Liu, I.M., Kuo, D.H., Chen, W.C., Su, H.C., and Cheng, J.T. (2003). Antihyperglycemic effect of puerarin in streptozotocin-induced diabetic rats. Journal of natural products *66*, 788-792.

Hu, W., Zhang, Q., Yang, X., Wang, Y., and Sun, L. (2010). Puerarin inhibits adhesion molecule expression in tnf-alpha-stimulated human endothelial cells via modulation of the nuclear factor kappaB pathway. Pharmacology *85*, 27-35.

Huang, C., Li, J., Ding, M., Leonard, S.S., Wang, L., Castranova, V., Vallyathan, V., and Shi, X. (2001). UV Induces phosphorylation of protein kinase B (Akt) at Ser-473 and Thr-308 in mouse epidermal Cl 41 cells through hydrogen peroxide. The Journal of biological chemistry *276*, 40234-40240.

Hur, J., Yoon, C.H., Kim, H.S., Choi, J.H., Kang, H.J., Hwang, K.K., Oh, B.H., Lee, M.M., and Park, Y.B. (2004). Characterization of two types of endothelial progenitor cells and their different contributions to neovasculogenesis. Arteriosclerosis, thrombosis, and vascular biology *24*, 288-293.
Ichimura, Y., Kirisako, T., Takao, T., Satomi, Y., Shimonishi, Y., Ishihara, N., Mizushima, N., Tanida, I.,

Kominami, E., Ohsumi, M.*, et al.* (2000). A ubiquitin-like system mediates protein lipidation. Nature *408*, 488-492.

Imai, K., Kobayashi, M., Wang, J., Shinobu, N., Yoshida, H., Hamada, J., Shindo, M., Higashino, F., Tanaka, J., Asaka, M.*, et al.* (1999). Selective secretion of chemoattractants for haemopoietic progenitor cells by bone marrow endothelial cells: a possible role in homing of haemopoietic progenitor cells to bone marrow. British journal of haematology *106*, 905-911.

Imhof, B.A., and Dunon, D. (1997). Basic mechanism of leukocyte migration. Hormone and metabolic research = Hormon- und Stoffwechselforschung = Hormones et metabolisme *29*, 614-621.

Iwaguro, H., Yamaguchi, J., Kalka, C., Murasawa, S., Masuda, H., Hayashi, S., Silver, M., Li, T., Isner, J.M., and Asahara, T. (2002). Endothelial progenitor cell vascular endothelial growth factor gene transfer for vascular regeneration. Circulation *105*, 732-738.

Iwami, Y., Masuda, H., and Asahara, T. (2004). Endothelial progenitor cells: past, state of the art, and future. Journal of cellular and molecular medicine *8*, 488-497.

Jain, R.K. (2003). Molecular regulation of vessel maturation. Nature medicine *9*, 685-693.
Janssens, K., ten Dijke, P., Janssens, S., and Van Hul, W. (2005). Transforming growth factor-beta1 to the bone. Endocrine reviews *26*, 743-774.

Jiang, F., Zhang, Y., and Dusting, G.J. (2011). NADPH oxidase-mediated redox signaling: roles in cellular stress response, stress tolerance, and tissue repair. Pharmacological reviews *63*, 218-242.

Jimi, E., Hirata, S., Osawa, K., Terashita, M., Kitamura, C., and Fukushima, H. (2012). The current and future therapies of bone regeneration to repair bone defects. International journal of dentistry *2012*, 148261.

Kaigler, D., Krebsbach, P.H., Wang, Z., West, E.R., Horger, K., and Mooney, D.J. (2006). Transplanted endothelial cells enhance orthotopic bone regeneration. Journal of dental research *85*, 633-637.

Kaigler, D., Krebsbach, P.H., West, E.R., Horger, K., Huang, Y.C., and Mooney, D.J. (2005). Endothelial cell modulation of bone marrow stromal cell osteogenic potential. Faseb J *19*, 665-667.

Kalka, C., Masuda, H., Takahashi, T., Kalka-Moll, W.M., Silver, M., Kearney, M., Li, T., Isner, J.M., and Asahara, T. (2000). Transplantation of ex vivo expanded endothelial progenitor cells for therapeutic neovascularization. Proceedings of the National Academy of Sciences of the United States of America *97*, 3422-3427.

Kanczler, J.M., and Oreffo, R.O. (2008). Osteogenesis and angiogenesis: the potential for engineering bone. European cells & materials *15*, 100-114.

Kawamoto, A., and Asahara, T. (2007). Role of progenitor endothelial cells in cardiovascular disease and upcoming therapies. Catheterization and cardiovascular interventions : official journal of the Society for Cardiac Angiography & Interventions *70*, 477-484.

Keaney, J.F., Jr. (2005). Oxidative stress and the vascular wall: NADPH oxidases take center stage. Circulation *112*, 2585-2588.

Keramaris, N.C., Calori, G.M., Nikolaou, V.S., Schemitsch, E.H., and Giannoudis, P.V. (2008). Fracture vascularity and bone healing: a systematic review of the role of VEGF. Injury *39 Suppl 2*, S45-57.

Kim, K.M., Pae, H.O., Zheng, M., Park, R., Kim, Y.M., and Chung, H.T. (2007). Carbon monoxide induces heme oxygenase-1 via activation of protein kinase R-like endoplasmic reticulum kinase and inhibits endothelial cell apoptosis triggered by endoplasmic reticulum stress. Circulation research *101*, 919-927.

Klinkner, D.B., Densmore, J.C., Kaul, S., Noll, L., Lim, H.J., Weihrauch, D., Pritchard, K.A., Jr., Oldham, K.T., and Sander, T.L. (2006). Endothelium-derived microparticles inhibit human cardiac valve endothelial cell function. Shock *25*, 575-580.

Klionsky, D.J., Meijer, A.J., and Codogno, P. (2005). Autophagy and p70S6 kinase. Autophagy *1*, 59-60; discussion 60-51.

Kneser, U., Kaufmann, P.M., Fiegel, H.C., Pollok, J.M., Kluth, D., Herbst, H., and Rogiers, X. (1999). Long-term differentiated function of heterotopically transplanted hepatocytes on three-dimensional polymer matrices. Journal of biomedical materials research *47*, 494-503.

Kneser, U., Schaefer, D.J., Polykandriotis, E., and Horch, R.E. (2006). Tissue engineering of bone: the reconstructive surgeon's point of view. Journal of cellular and molecular medicine *10*, 7-19.

Knight-Lozano, C.A., Young, C.G., Burow, D.L., Hu, Z.Y., Uyeminami, D., Pinkerton, K.E., Ischiropoulos, H., and Ballinger, S.W. (2002). Cigarette smoke exposure and hypercholesterolemia increase mitochondrial damage in cardiovascular tissues. Circulation *105*, 849-854.

Kondo, Y., Kanzawa, T., Sawaya, R., and Kondo, S. (2005). The role of autophagy in cancer development and response to therapy. Nature reviews Cancer *5*, 726-734.

Konishi, H., Matsuzaki, H., Tanaka, M., Takemura, Y., Kuroda, S., Ono, Y., and Kikkawa, U. (1997). Activation of protein kinase B (Akt/RAC-protein kinase) by cellular stress and its association with heat shock protein Hsp27. FEBS letters *410*, 493-498.

Kruse, K.B., Brodsky, J.L., and McCracken, A.A. (2006). Characterization of an ERAD gene as VPS30/ATG6 reveals two alternative and functionally distinct protein quality control pathways: one for soluble Z variant of human alpha-1 proteinase inhibitor (A1PiZ) and another for aggregates of A1PiZ. Mol Biol Cell *17*, 203-212.

Kushner, E.J., Van Guilder, G.P., Maceneaney, O.J., Cech, J.N., Stauffer, B.L., and DeSouza, C.A. (2009). Aging and endothelial progenitor cell telomere length in healthy men. Clinical chemistry and laboratory medicine : CCLM / FESCC *47*, 47-50.

Lamalice, L., Le Boeuf, F., and Huot, J. (2007). Endothelial cell migration during angiogenesis. Circulation research *100*, 782-794.

Lee, H.S., Namkoong, K., Kim, D.H., Kim, K.J., Cheong, Y.H., Kim, S.S., Lee, W.B., and Kim, K.Y. (2004). Hydrogen peroxide-induced alterations of tight junction proteins in bovine brain microvascular endothelial cells. Microvascular research *68*, 231-238.

Lee, J.S., Kim, S.Y., Kwon, C.H., and Kim, Y.K. (2006). EGFR-dependent ERK activation triggers hydrogen peroxide-induced apoptosis in OK renal epithelial cells. Archives of toxicology *80*, 337-346.

Lemasters, J.J. (2005). Selective mitochondrial autophagy, or mitophagy, as a targeted defense against oxidative stress, mitochondrial dysfunction, and aging. Rejuvenation research *8*, 3-5.

Leong, P.K., Chiu, P.Y., Chen, N., Leung, H., and Ko, K.M. (2011). Schisandrin B elicits a glutathione antioxidant response and protects against apoptosis via the redox-sensitive ERK/Nrf2 pathway in AML12 hepatocytes. Free radical research *45*, 483-495.

Leopold, J.A., and Loscalzo, J. (2005). Oxidative enzymopathies and vascular disease. Arteriosclerosis, thrombosis, and vascular biology *25*, 1332-1340.

Lewis, J.S., Vijayanathan, V., Thomas, T.J., Pestell, R.G., Albanese, C., Gallo, M.A., and Thomas, T. (2005). Activation of cyclin D1 by estradiol and spermine in MCF-7 breast cancer cells: a mechanism involving the p38 MAP kinase and phosphorylation of ATF-2. Oncology research *15*, 113-128.

Li, J., DeFea, K., and Roth, R.A. (1999). Modulation of insulin receptor substrate-1 tyrosine phosphorylation by an Akt/phosphatidylinositol 3-kinase pathway. The Journal of biological chemistry *274*, 9351-9356.

Li, J.M., and Shah, A.M. (2003). Mechanism of endothelial cell NADPH oxidase activation by angiotensin II. Role of the p47phox subunit. The Journal of biological chemistry *278*, 12094-12100.

Li, M., Zhao, C., Wong, R.N., Goto, S., Wang, Z., and Liao, F. (2004). Inhibition of shear-induced platelet aggregation in rat by tetramethylpyrazine and salvianolic acid B. Clinical hemorheology and microcirculation *31*, 97-103.

Li, X.N., Song, J., Zhang, L., LeMaire, S.A., Hou, X., Zhang, C., Coselli, J.S., Chen, L., Wang, X.L., Zhang, Y.*, et al.* (2009). Activation of the AMPK-FOXO3 pathway reduces fatty acid-induced increase in intracellular reactive oxygen species by upregulating thioredoxin. Diabetes *58*, 2246-2257.

Liang, X.H., Jackson, S., Seaman, M., Brown, K., Kempkes, B., Hibshoosh, H., and Levine, B. (1999). Induction of autophagy and inhibition of tumorigenesis by beclin 1. Nature *402*, 672-676.

Libby, P. (2001). Current concepts of the pathogenesis of the acute coronary syndromes. Circulation *104*, 365-372.

Lieberman, J.R., Daluiski, A., and Einhorn, T.A. (2002). The role of growth factors in the repair of bone. Biology and clinical applications. The Journal of bone and joint surgery American volume *84-A*, 1032-1044.

Lin, Y., Weisdorf, D.J., Solovey, A., and Hebbel, R.P. (2000). Origins of circulating endothelial cells and endothelial outgrowth from blood. The Journal of clinical investigation *105*, 71-77.

Lipinski, M.M., Zheng, B., Lu, T., Yan, Z., Py, B.F., Ng, A., Xavier, R.J., Li, C., Yankner, B.A., Scherzer, C.R.*, et al.* (2010). Genome-wide analysis reveals mechanisms modulating autophagy in normal brain aging and in Alzheimer's disease. Proceedings of the National Academy of Sciences of the United States of America *107*, 14164-14169.

Ludmer, P.L., Selwyn, A.P., Shook, T.L., Wayne, R.R., Mudge, G.H., Alexander, R.W., and Ganz, P. (1986). Paradoxical vasoconstriction induced by acetylcholine in atherosclerotic coronary arteries. The New England journal of medicine *315*, 1046-1051.

Luo, S., and Rubinsztein, D.C. (2010). Apoptosis blocks Beclin 1-dependent autophagosome synthesis: an effect rescued by Bcl-xL. Cell death and differentiation *17*, 268-277.

Luppen, C.A., Blake, C.A., Ammirati, K.M., Stevens, M.L., Seeherman, H.J., Wozney, J.M., and Bouxsein, M.L. (2002). Recombinant human bone morphogenetic protein-2 enhances osteotomy healing in glucocorticoid-treated rabbits. Journal of bone and mineral research : the official journal of the American Society for Bone and Mineral Research *17*, 301-310.

Maeda, S., Hayashi, M., Komiya, S., Imamura, T., and Miyazono, K. (2004). Endogenous TGF-beta signaling suppresses maturation of osteoblastic mesenchymal cells. The EMBO journal *23*, 552-563.

Maiuri, M.C., Zalckvar, E., Kimchi, A., and Kroemer, G. (2007). Self-eating and self-killing: crosstalk between autophagy and apoptosis. Nature reviews Molecular cell biology *8*, 741-752.

Marie, P.J. (2003). Fibroblast growth factor signaling controlling osteoblast differentiation. Gene *316*, 23-32.

Maslov, L.N., Lishmanov, Y.B., Arbuzov, A.G., Krylatov, A.V., Budankova, E.V., Konkovskaya, Y.N., Burkova, V.N., and Severova, E.A. (2009). Antiarrhythmic activity of phytoadaptogens in short-term ischemia-reperfusion of the heart and postinfarction cardiosclerosis. Bulletin of experimental biology and medicine *147*, 331-334.

Massey, A., Kiffin, R., and Cuervo, A.M. (2004). Pathophysiology of chaperone-mediated autophagy. The international journal of biochemistry & cell biology *36*, 2420-2434.

Matsushita, E., Asai, N., Enomoto, A., Kawamoto, Y., Kato, T., Mii, S., Maeda, K., Shibata, R., Hattori, S., Hagikura, M.*, et al.* (2011). Protective role of Gipie, a Girdin family protein, in endoplasmic reticulum stress responses in endothelial cells. Mol Biol Cell *22*, 736-747.

Matsuzawa, A., and Ichijo, H. (2008). Redox control of cell fate by MAP kinase: physiological roles of ASK1-MAP kinase pathway in stress signaling. Biochimica et biophysica acta *1780*, 1325-1336.

Matsuzawa, T., Kim, B.H., Shenoy, A.R., Kamitani, S., Miyake, M., and Macmicking, J.D. (2012). IFN-gamma elicits macrophage autophagy via the p38 MAPK signaling pathway. Journal of immunology *189*, 813-818.

Matz, R.L., de Sotomayor, M.A., Schott, C., Stoclet, J.C., and Andriantsitohaina, R. (2000). Vascular bed heterogeneity in age-related endothelial dysfunction with respect to NO and eicosanoids. British journal of pharmacology *131*, 303-311.

Mavria, G., Vercoulen, Y., Yeo, M., Paterson, H., Karasarides, M., Marais, R., Bird, D., and Marshall, C.J. (2006). ERK-MAPK signaling opposes Rho-kinase to promote endothelial cell survival and sprouting during angiogenesis. Cancer cell *9*, 33-44.

McCarthy, I. (2006). The physiology of bone blood flow: a review. The Journal of bone and joint surgery American volume *88 Suppl 3*, 4-9.

Mercer, J.R., Cheng, K.K., Figg, N., Gorenne, I., Mahmoudi, M., Griffin, J., Vidal-Puig, A., Logan, A., Murphy, M.P., and Bennett, M. (2010). DNA damage links mitochondrial dysfunction to atherosclerosis and the metabolic syndrome. Circulation research *107*, 1021-1031.

Michaud, S.E., Dussault, S., Haddad, P., Groleau, J., and Rivard, A. (2006). Circulating endothelial progenitor cells from healthy smokers exhibit impaired functional activities. Atherosclerosis *187*, 423-432.

Milkiewicz, M., Hudlicka, O., Shiner, R., Egginton, S., and Brown, M.D. (2006). Vascular endothelial growth factor mRNA and protein do not change in parallel during non-inflammatory skeletal muscle ischaemia in rat. The Journal of physiology *577*, 671-678.

Mizushima, N. (2007). Autophagy: process and function. Genes & development *21*, 2861-2873.

Mobasheri, A. (2013). The future of osteoarthritis therapeutics: emerging biological therapy. Current rheumatology reports *15*, 385.

Montero-Balaguer, M., Swirsding, K., Orsenigo, F., Cotelli, F., Mione, M., and Dejana, E. (2009). Stable vascular connections and remodeling require full expression of VE-cadherin in zebrafish embryos. PloS one *4*, e5772.

Mundy, G.R. (1996). Regulation of bone formation by bone morphogenetic proteins and other growth factors. Clinical orthopaedics and related research, 24-28.

Mura, M., Han, B., Andrade, C.F., Seth, R., Hwang, D., Waddell, T.K., Keshavjee, S., and Liu, M. (2006). The early responses of VEGF and its receptors during acute lung injury: implication of VEGF in alveolar epithelial cell survival. Critical care *10*, R130.

Murohara, T. (2003). Angiogenesis and vasculogenesis for therapeutic neovascularization. Nagoya journal of medical science *66*, 1-7.

Murohara, T., and Asahara, T. (2002). Nitric oxide and angiogenesis in cardiovascular disease. Antioxidants & redox signaling *4*, 825-831.

Murohara, T., Ikeda, H., Duan, J., Shintani, S., Sasaki, K., Eguchi, H., Onitsuka, I., Matsui, K., and Imaizumi, T. (2000). Transplanted cord blood-derived endothelial precursor cells augment postnatal neovascularization. The Journal of clinical investigation *105*, 1527-1536.

Nakamura, T., Hara, Y., Tagawa, M., Tamura, M., Yuge, T., Fukuda, H., and Nigi, H. (1998). Recombinant human basic fibroblast growth factor accelerates fracture healing by enhancing callus remodeling in experimental dog tibial fracture. Journal of bone and mineral research : the official journal of the American Society for Bone and Mineral Research *13*, 942-949.

Nieda, M., Nicol, A., Denning-Kendall, P., Sweetenham, J., Bradley, B., and Hows, J. (1997). Endothelial cell precursors are normal components of human umbilical cord blood. British journal of haematology *98*, 775-777.

Nishikawa, T., Edelstein, D., Du, X.L., Yamagishi, S., Matsumura, T., Kaneda, Y., Yorek, M.A., Beebe, D., Oates, P.J., Hammes, H.P*., et al.* (2000). Normalizing mitochondrial superoxide production blocks three pathways of hyperglycaemic damage. Nature *404*, 787-790.

Nopparat, C., Porter, J.E., Ebadi, M., and Govitrapong, P. (2010). The mechanism for the neuroprotective effect of melatonin against methamphetamine-induced autophagy. Journal of pineal research *49*, 382-389.

Ornitz, D.M. (2005). FGF signaling in the developing endochondral skeleton. Cytokine & growth factor reviews *16*, 205-213.

Orr, A.W., Stockton, R., Simmers, M.B., Sanders, J.M., Sarembock, I.J., Blackman, B.R., and Schwartz, M.A. (2007). Matrix-specific p21-activated kinase activation regulates vascular permeability in atherogenesis. The Journal of cell biology *176*, 719-727.

Paleolog, E. (2005). It's all in the blood: circulating endothelial progenitor cells link synovial vascularity with cardiovascular mortality in rheumatoid arthritis? Arthritis research & therapy *7*, 270-272.

Pan, C., Lou, L., Huo, Y., Singh, G., Chen, M., Zhang, D., Wu, A., Zhao, M., Wang, S., and Li, J. (2011). Salvianolic acid B and tanshinone IIA attenuate myocardial ischemia injury in mice by NO production through multiple pathways. Therapeutic advances in cardiovascular disease *5*, 99-111.

Pan, C.H., Chen, C.W., Sheu, M.J., and Wu, C.H. (2012). Salvianolic acid B inhibits SDF-1alpha-stimulated cell proliferation and migration of vascular smooth muscle cells by suppressing CXCR4 receptor. Vascular pharmacology *56*, 98-105.

Parfitt, A.M. (2000). The mechanism of coupling: a role for the vasculature. Bone *26*, 319-323.

Pattingre, S., Tassa, A., Qu, X., Garuti, R., Liang, X.H., Mizushima, N., Packer, M., Schneider, M.D., and Levine, B. (2005). Bcl-2 antiapoptotic proteins inhibit Beclin 1-dependent autophagy. Cell *122*, 927-939.

Peichev, M., Naiyer, A.J., Pereira, D., Zhu, Z., Lane, W.J., Williams, M., Oz, M.C., Hicklin, D.J., Witte, L., Moore, M.A.*, et al.* (2000). Expression of VEGFR-2 and AC133 by circulating human CD34(+) cells identifies a population of functional endothelial precursors. Blood *95*, 952-958.

Pelicano, H., Carney, D., and Huang, P. (2004). ROS stress in cancer cells and therapeutic implications. Drug resistance updates : reviews and commentaries in antimicrobial and anticancer chemotherapy *7*, 97-110.

Platini, F., Perez-Tomas, R., Ambrosio, S., and Tessitore, L. (2010). Understanding autophagy in cell death control. Current pharmaceutical design *16*, 101-113.

Qiu, Q., Yang, M., Tsang, B.K., and Gruslin, A. (2004). Both mitogen-activated protein kinase and phosphatidylinositol 3-kinase signalling are required in epidermal growth factor-induced human trophoblast migration. Molecular human reproduction *10*, 677-684.

Qu, Z.Q., Zhou, Y., Zeng, Y.S., Lin, Y.K., Li, Y., Zhong, Z.Q., and Chan, W.Y. (2012). Protective effects of a Rhodiola crenulata extract and salidroside on hippocampal neurogenesis against streptozotocin-induced neural injury in the rat. PloS one *7*, e29641.

Ravikumar, B., Vacher, C., Berger, Z., Davies, J.E., Luo, S., Oroz, L.G., Scaravilli, F., Easton, D.F., Duden, R., O'Kane, C.J.*, et al.* (2004). Inhibition of mTOR induces autophagy and reduces toxicity of polyglutamine expansions in fly and mouse models of Huntington disease. Nature genetics *36*, 585-595.

Reddi, A.H. (2001). Bone morphogenetic proteins: from basic science to clinical applications. The Journal of bone and joint surgery American volume *83-A Suppl 1*, S1-6.

Reinisch, A., Hofmann, N.A., Obenauf, A.C., Kashofer, K., Rohde, E., Schallmoser, K., Flicker, K., Lanzer, G., Linkesch, W., Speicher, M.R.*, et al.* (2009). Humanized large-scale expanded endothelial colony-forming cells function in vitro and in vivo. Blood *113*, 6716-6725.

Rhee, S.G., Bae, Y.S., Lee, S.R., and Kwon, J. (2000). Hydrogen peroxide: a key messenger that modulates protein phosphorylation through cysteine oxidation. Science's STKE : signal transduction knowledge environment *2000*, pe1.

Risau, W. (1997). Mechanisms of angiogenesis. Nature *386*, 671-674.

Rouwkema, J., de Boer, J., and Van Blitterswijk, C.A. (2006). Endothelial cells assemble into a 3-dimensional prevascular network in a bone tissue engineering construct. Tissue engineering *12*, 2685-2693.

Ryan, A.M. (1999). Commentary: role of the pathologist in the identification and characterization of therapeutic molecules. Toxicologic pathology *27*, 474-476.

Saeki, K., Yuo, A., Okuma, E., Yazaki, Y., Susin, S.A., Kroemer, G., and Takaku, F. (2000). Bcl-2 down-regulation causes autophagy in a caspase-independent manner in human leukemic HL60 cells. Cell death and differentiation *7*, 1263-1269.

Saitoh, M., Nishitoh, H., Fujii, M., Takeda, K., Tobiume, K., Sawada, Y., Kawabata, M., Miyazono, K., and Ichijo, H. (1998). Mammalian thioredoxin is a direct inhibitor of apoptosis signal-regulating kinase (ASK) 1. The EMBO journal *17*, 2596-2606.

Salsman, S., Felts, N., Pye, Q.N., Floyd, R.A., and Hensley, K. (2001). Induction of Akt phosphorylation in rat primary astrocytes by H2O2 occurs upstream of phosphatidylinositol 3-kinase: no evidence for oxidative inhibition of PTEN. Archives of biochemistry and biophysics *386*, 275-280.

Sandberg, M.M., Aro, H.T., and Vuorio, E.I. (1993). Gene expression during bone repair. Clinical orthopaedics and related research, 292-312.

Sato, A., Sunayama, J., Matsuda, K., Tachibana, K., Sakurada, K., Tomiyama, A., Kayama, T., and Kitanaka, C. (2010). Regulation of neural stem/progenitor cell maintenance by PI3K and mTOR. Neuroscience letters *470*, 115-120.

Scheubel, R.J., Zorn, H., Silber, R.E., Kuss, O., Morawietz, H., Holtz, J., and Simm, A. (2003). Age-dependent depression in circulating endothelial progenitor cells in patients undergoing coronary artery bypass grafting. Journal of the American College of Cardiology *42*, 2073-2080.

Schieke, S.M., Phillips, D., McCoy, J.P., Jr., Aponte, A.M., Shen, R.F., Balaban, R.S., and Finkel, T. (2006). The mammalian target of rapamycin (mTOR) pathway regulates mitochondrial oxygen consumption and oxidative capacity. The Journal of biological chemistry *281*, 27643-27652.

Shantsila, E., Watson, T., and Lip, G.Y. (2007). Endothelial progenitor cells in cardiovascular disorders. Journal of the American College of Cardiology *49*, 741-752.

Shevtsov, V.A., Zholus, B.I., Shervarly, V.I., Vol'skij, V.B., Korovin, Y.P., Khristich, M.P., Roslyakova, N.A., and Wikman, G. (2003). A randomized trial of two different doses of a SHR-5 Rhodiola rosea extract versus placebo and control of capacity for mental work. Phytomedicine : international journal of phytotherapy and phytopharmacology *10*, 95-105.

Shi, Q., Rafii, S., Wu, M.H., Wijelath, E.S., Yu, C., Ishida, A., Fujita, Y., Kothari, S., Mohle, R., Sauvage, L.R.*, et al.* (1998). Evidence for circulating bone marrow-derived endothelial cells. Blood *92*, 362-367.

Shi, T.Y., Feng, S.F., Xing, J.H., Wu, Y.M., Li, X.Q., Zhang, N., Tian, Z., Liu, S.B., and Zhao, M.G. (2012). Neuroprotective effects of Salidroside and its analogue tyrosol galactoside against focal cerebral ischemia in vivo and H2O2-induced neurotoxicity in vitro. Neurotoxicity research *21*, 358-367.

Shimizu, S., Kanaseki, T., Mizushima, N., Mizuta, T., Arakawa-Kobayashi, S., Thompson, C.B., and Tsujimoto, Y. (2004). Role of Bcl-2 family proteins in a non-apoptotic programmed cell death dependent on autophagy genes. Nature cell biology *6*, 1221-1228.

Shinojima, N., Yokoyama, T., Kondo, Y., and Kondo, S. (2007). Roles of the Akt/mTOR/p70S6K and ERK1/2 signaling pathways in curcumin-induced autophagy. Autophagy *3*, 635-637.

Shintani, S., Murohara, T., Ikeda, H., Ueno, T., Honma, T., Katoh, A., Sasaki, K., Shimada, T., Oike, Y., and Imaizumi, T. (2001). Mobilization of endothelial progenitor cells in patients with acute myocardial infarction. Circulation *103*, 2776-2779.

Shou, Q., Pan, Y., Xu, X., Xu, J., Wang, D., Ling, Y., and Chen, M. (2012). Salvianolic acid B possesses vasodilation potential through NO and its related signals in rabbit thoracic aortic rings. European journal of pharmacology *697*, 81-87.

Shu, H., Arita, H., Hayashida, M., Zhang, L., An, K., Huang, W., and Hanaoka, K. (2010). Anti-hypersensitivity effects of Shu-jing-huo-xue-tang, a Chinese herbal medicine, in CCI-neuropathic rats. Journal of ethnopharmacology *131*, 464-470.

Simonsen, A., and Tooze, S.A. (2009). Coordination of membrane events during autophagy by multiple class III PI3-kinase complexes. The Journal of cell biology *186*, 773-782.

Sirker, A.A., Astroulakis, Z.M., and Hill, J.M. (2009). Vascular progenitor cells and translational research: the role of endothelial and smooth muscle progenitor cells in endogenous arterial remodelling in the adult. Clinical science *116*, 283-299.

Sorescu, D., Weiss, D., Lassegue, B., Clempus, R.E., Szocs, K., Sorescu, G.P., Valppu, L., Quinn, M.T., Lambeth, J.D., Vega, J.D*., et al.* (2002). Superoxide production and expression of nox family proteins in human atherosclerosis. Circulation *105*, 1429-1435.

Spasov, A.A., Wikman, G.K., Mandrikov, V.B., Mironova, I.A., and Neumoin, V.V. (2000). A double-blind, placebo-controlled pilot study of the stimulating and adaptogenic effect of Rhodiola rosea SHR-5 extract on the fatigue of students caused by stress during an examination period with a repeated low-dose regimen. Phytomedicine : international journal of phytotherapy and phytopharmacology *7*, 85-89.

Street, J., Bao, M., deGuzman, L., Bunting, S., Peale, F.V., Jr., Ferrara, N., Steinmetz, H., Hoeffel, J., Cleland, J.L., Daugherty, A*., et al.* (2002). Vascular endothelial growth factor stimulates bone repair by promoting angiogenesis and bone turnover. Proceedings of the National Academy of Sciences of the United States of America *99*, 9656-9661.

Streeten, E.A., and Brandi, M.L. (1990). Biology of bone endothelial cells. Bone and mineral *10*, 85-94.

Streeten, E.A., Ornberg, R., Curcio, F., Sakaguchi, K., Marx, S., Aurbach, G.D., and Brandi, M.L. (1989). Cloned endothelial cells from fetal bovine bone. Proceedings of the National Academy of Sciences of the United States of America *86*, 916-920.

Sun, L., Isaak, C.K., Zhou, Y., Petkau, J.C., O, K., Liu, Y., and Siow, Y.L. (2012). Salidroside and tyrosol from Rhodiola protect H9c2 cells from ischemia/reperfusion-induced apoptosis. Life sciences *91*, 151-158.

Sun, W., Kesavan, K., Schaefer, B.C., Garrington, T.P., Ware, M., Johnson, N.L., Gelfand, E.W., and Johnson, G.L. (2001). MEKK2 associates with the adapter protein Lad/RIBP and regulates the MEK5-BMK1/ERK5 pathway. The Journal of biological chemistry *276*, 5093-5100.

Sun, X., Wu, F., Datta, R., Kharbanda, S., and Kufe, D. (2000). Interaction between protein kinase C delta and the c-Abl tyrosine kinase in the cellular response to oxidative stress. The Journal of biological chemistry *275*, 7470-7473.

Suzaki, Y., Yoshizumi, M., Kagami, S., Koyama, A.H., Taketani, Y., Houchi, H., Tsuchiya, K., Takeda, E., and Tamaki, T. (2002). Hydrogen peroxide stimulates c-Src-mediated big mitogen-activated protein kinase 1 (BMK1) and the MEF2C signaling pathway in PC12 cells: potential role in cell survival following oxidative insults. The Journal of biological chemistry *277*, 9614-9621.

Takahashi, M., Okubo, N., Chosa, N., Takahashi, N., Ibi, M., Kamo, M., Mizuki, H., Ishisaki, A., and Kyakumoto, S. (2012). Fibroblast growth factor-1-induced ERK1/2 signaling reciprocally regulates proliferation and smooth muscle cell differentiation of ligament-derived endothelial progenitor cell-like cells. International journal of molecular medicine *29*, 357-364.

Tang, M.K., Ren, D.C., Zhang, J.T., and Du, G.H. (2002). Effect of salvianolic acids from Radix Salviae miltiorrhizae on regional cerebral blood flow and platelet aggregation in rats. Phytomedicine : international journal of phytotherapy and phytopharmacology *9*, 405-409.

Tang, Y., Huang, B., Sun, L., Peng, X., Chen, X., and Zou, X. (2011). Ginkgolide B promotes proliferation and functional activities of bone marrow-derived endothelial progenitor cells: involvement of Akt/eNOS and MAPK/p38 signaling pathways. European cells & materials *21*, 459-469.

Tang, Y., Wu, X., Lei, W., Pang, L., Wan, C., Shi, Z., Zhao, L., Nagy, T.R., Peng, X., Hu, J.*, et al.* (2009). TGF-beta1-induced migration of bone mesenchymal stem cells couples bone resorption with formation. Nature medicine *15*, 757-765.

Trueta, J., and Buhr, A.J. (1963). The Vascular Contribution to Osteogenesis. V. The Vasculature Supplying the Epiphysial Cartilage in Rachitic Rats. The Journal of bone and joint surgery British volume *45*, 572-581.

Unger, R.E., Sartoris, A., Peters, K., Motta, A., Migliaresi, C., Kunkel, M., Bulnheim, U., Rychly, J., and Kirkpatrick, C.J. (2007). Tissue-like self-assembly in cocultures of endothelial cells and osteoblasts and the formation of microcapillary-like structures on three-dimensional porous biomaterials. Biomaterials *28*, 3965-3976.

Vane, J.R., Anggard, E.E., and Botting, R.M. (1990). Regulatory functions of the vascular endothelium. The New England journal of medicine *323*, 27-36.

Vasa, M., Fichtlscherer, S., Aicher, A., Adler, K., Urbich, C., Martin, H., Zeiher, A.M., and Dimmeler, S. (2001). Number and migratory activity of circulating endothelial progenitor cells inversely correlate with risk factors for coronary artery disease. Circulation research *89*, E1-7.

Venkatesh, S., Deecaraman, M., Kumar, R., Shamsi, M.B., and Dada, R. (2009). Role of reactive oxygen species in the pathogenesis of mitochondrial DNA (mtDNA) mutations in male infertility. The Indian journal of medical research *129*, 127-137.

Verseijden, F., Posthumus-van Sluijs, S.J., Farrell, E., van Neck, J.W., Hovius, S.E., Hofer, S.O., and van Osch, G.J. (2010). Prevascular structures promote vascularization in engineered human adipose tissue constructs upon implantation. Cell transplantation *19*, 1007-1020.

Verseijden, F., Posthumus-van Sluijs, S.J., van Neck, J.W., Hofer, S.O., Hovius, S.E., and van Osch, G.J. (2012). Vascularization of prevascularized and non-prevascularized fibrin-based human adipose tissue constructs after implantation in nude mice. Journal of tissue engineering and regenerative medicine *6*, 169-178.

Virdis, A., Neves, M.F., Amiri, F., Touyz, R.M., and Schiffrin, E.L. (2004). Role of NAD(P)H oxidase on vascular alterations in angiotensin II-infused mice. Journal of hypertension *22*, 535-542.

Wang, J., Whiteman, M.W., Lian, H., Wang, G., Singh, A., Huang, D., and Denmark, T. (2009). A non-canonical MEK/ERK signaling pathway regulates autophagy via regulating Beclin 1. The Journal of biological chemistry *284*, 21412-21424.

Wang, Y., Wan, C., Deng, L., Liu, X., Cao, X., Gilbert, S.R., Bouxsein, M.L., Faugere, M.C., Guldberg, R.E., Gerstenfeld, L.C*., et al.* (2007). The hypoxia-inducible factor alpha pathway couples angiogenesis to osteogenesis during skeletal development. The Journal of clinical investigation *117*, 1616-1626.

Wang, Y.K., and Huang, Z.Q. (2005). Protective effects of icariin on human umbilical vein endothelial cell injury induced by H2O2 in vitro. Pharmacological research : the official journal of the Italian Pharmacological Society *52*, 174-182.

Webber, J.L., and Tooze, S.A. (2010). Coordinated regulation of autophagy by p38alpha MAPK through mAtg9 and p38IP. The EMBO journal *29*, 27-40.

Williams, J.L., Cartland, D., Hussain, A., and Egginton, S. (2006). A differential role for nitric oxide in two forms of physiological angiogenesis in mouse. The Journal of physiology *570*, 445-454.

Williams, M.R., Arthur, J.S., Balendran, A., van der Kaay, J., Poli, V., Cohen, P., and Alessi, D.R. (2000). The role of 3-phosphoinositide-dependent protein kinase 1 in activating AGC kinases defined in embryonic stem cells. Current biology : CB *10*, 439-448.

Wirawan, E., Vande Walle, L., Kersse, K., Cornelis, S., Claerhout, S., Vanoverberghe, I., Roelandt, R., De Rycke, R., Verspurten, J., Declercq, W*., et al.* (2010). Caspase-mediated cleavage of Beclin-1 inactivates Beclin-1-induced autophagy and enhances apoptosis by promoting the release of proapoptotic factors from mitochondria. Cell death & disease *1*, e18.

Wong, B.W., Rahmani, M., Luo, Z., Yanagawa, B., Wong, D., Luo, H., and McManus, B.M. (2009). Vascular endothelial growth factor increases human cardiac microvascular endothelial cell permeability to low-density lipoproteins. The Journal of heart and lung transplantation : the official publication of the International Society for Heart Transplantation *28*, 950-957.

Xiao, C., Li, J., Dong, X., He, X., Niu, X., Liu, C., Zhong, G., Bauer, R., Yang, D., and Lu, A. (2011). Anti-oxidative and TNF-alpha suppressive activities of puerarin derivative (4AC) in RAW264.7 cells and collagen-induced arthritic rats. European journal of pharmacology *666*, 242-250.

Xin, Z.C., Kim, E.K., Lin, C.S., Liu, W.J., Tian, L., Yuan, Y.M., and Fu, J. (2003). Effects of icariin on cGMP-specific PDE5 and cAMP-specific PDE4 activities. Asian journal of andrology *5*, 15-18.

Xu, M.C., Shi, H.M., Wang, H., and Gao, X.F. (2013). Salidroside protects against hydrogen peroxide-induced injury in HUVECs via the regulation of REDD1 and mTOR activation. Molecular medicine reports *8*, 147-153.

Xu, Y., Kim, S.O., Li, Y., and Han, J. (2006). Autophagy contributes to caspase-independent macrophage cell death. The Journal of biological chemistry *281*, 19179-19187.

Yamada, T., Egashira, N., Imuta, M., Yano, T., Yamauchi, Y., Watanabe, H., and Oishi, R. (2010). Role of oxidative stress in vinorelbine-induced vascular endothelial cell injury. Free radical biology & medicine *48*, 120-127.

Yamamoto, M., Yang, G., Hong, C., Liu, J., Holle, E., Yu, X., Wagner, T., Vatner, S.F., and Sadoshima, J. (2003). Inhibition of endogenous thioredoxin in the heart increases oxidative stress and cardiac hypertrophy. The Journal of clinical investigation *112*, 1395-1406.

Yan, L.P., Chan, S.W., Chan, A.S., Chen, S.L., Ma, X.J., and Xu, H.X. (2006). Puerarin decreases serum total cholesterol and enhances thoracic aorta endothelial nitric oxide synthase expression in diet-induced hypercholesterolemic rats. Life sciences *79*, 324-330.

Yang, J., Wu, L.J., Tashino, S., Onodera, S., and Ikejima, T. (2008). Reactive oxygen species and nitric oxide regulate mitochondria-dependent apoptosis and autophagy in evodiamine-treated human cervix carcinoma HeLa cells. Free radical research *42*, 492-504.

Yang, X., Hu, W., Zhang, Q., Wang, Y., and Sun, L. (2010). Puerarin inhibits C-reactive protein expression via suppression of nuclear factor kappaB activation in lipopolysaccharide-induced peripheral blood mononuclear cells of patients with stable angina pectoris. Basic & clinical pharmacology & toxicology *107*, 637-642.

Yao, X.J., Yin, J.A., Xia, Y.F., Wei, Z.F., Luo, Y.B., Liu, M., Feleder, C., and Dai, Y. (2012). Puerarin exerts antipyretic effect on lipopolysaccharide-induced fever in rats involving inhibition of pyrogen production from macrophages. Journal of ethnopharmacology *141*, 322-330.

Yin, X.X., Chen, Z.Q., Dang, G.T., Ma, Q.J., and Liu, Z.J. (2005). [Effects of Epimedium pubescens icariine on proliferation and differentiation of human osteoblasts]. Zhongguo Zhong yao za zhi = Zhongguo zhongyao zazhi = China journal of Chinese materia medica *30*, 289-291.

Yoon, C.H., Hur, J., Park, K.W., Kim, J.H., Lee, C.S., Oh, I.Y., Kim, T.Y., Cho, H.J., Kang, H.J., Chae, I.H., *et al.* (2005). Synergistic neovascularization by mixed transplantation of early endothelial progenitor cells and late outgrowth endothelial cells: the role of angiogenic cytokines and matrix metalloproteinases. Circulation *112*, 1618-1627.

Zelzer, E., McLean, W., Ng, Y.S., Fukai, N., Reginato, A.M., Lovejoy, S., D'Amore, P.A., and Olsen, B.R. (2002). Skeletal defects in VEGF(120/120) mice reveal multiple roles for VEGF in skeletogenesis. Development *129*, 1893-1904.

Zhai, Z., Li, H., Liu, G., Qu, X., Tian, B., Yan, W., Lin, Z., Tang, T., Qin, A., and Dai, K. (2013). Andrographolide suppresses RANKL-induced osteoclastogenesis in vitro and prevents inflammatory bone loss in vivo. British journal of pharmacology.

Zhang, H., Zhang, L., Zhang, Q., Yang, X., Yu, J., Shun, S., Wu, Y., Zeng, Q., and Wang, T. (2011a). Puerarin: a novel antagonist to inward rectifier potassium channel (IK1). Molecular and cellular biochemistry *352*, 117-123.

Zhang, H.S., and Wang, S.Q. (2006). Salvianolic acid B from Salvia miltiorrhiza inhibits tumor necrosis factor-alpha (TNF-alpha)-induced MMP-2 upregulation in human aortic smooth muscle cells via suppression of NAD(P)H oxidase-derived reactive oxygen species. Journal of molecular and cellular cardiology *41*, 138-148.

Zhang, L., Yang, R., and Han, Z.C. (2006a). Transplantation of umbilical cord blood-derived endothelial progenitor cells: a promising method of therapeutic revascularisation. European journal of haematology *76*, 1-8.

Zhang, N.B., Huang, Z.G., Cui, W.D., and Ding, B.P. (2011b). Effects of puerarin on expression of cardiac Smad3 and Smad7 mRNA in spontaneously hypertensive rat. Journal of ethnopharmacology *138*, 737-740.

Zhang, S., Chen, S., Shen, Y., Yang, D., Liu, X., Sun-Chi, A.C., and Xu, H. (2006b). Puerarin induces angiogenesis in myocardium of rat with myocardial infarction. Biological & pharmaceutical bulletin *29*, 945-950.

Zhang, Y.W., Morita, I., Shao, G., Yao, X.S., and Murota, S. (2000). Screening of anti-hypoxia/reoxygenation agents by an in vitro model. Part 1: Natural inhibitors for protein tyrosine kinase activated by hypoxia/reoxygenation in cultured human umbilical vein endothelial cells. Planta medica *66*, 114-118.

Zhong, H., Xin, H., Wu, L.X., and Zhu, Y.Z. (2010). Salidroside attenuates apoptosis in ischemic cardiomyocytes: a mechanism through a mitochondria-dependent pathway. Journal of pharmacological sciences *114*, 399-408.

1. Human endothelial progenitor cells were successfully isolated and induced from bone marrow-derived mononuclear cells, which exhibiting prominent proliferative and capillary-like tube formation capacities, as well as the ability to differentiate towards mature endothelial cells.

2. SAL, SalB, ICAR and PUER show promoting effects on cell angiogenic abilities, including cell chemotaxis, cell-matrix adhesion, and capillary-like tube formation *in vitro*.

3. SAL and ICAR suppress cell-cell adhesion of BM-EPCs, elevate the secretion level of VEGF and NO, and regulate endothelial marker gene expression.

4. Akt/mTOR/p70S6K/4EBP1 and ERK1/2 signaling pathways are involved in the angiogenic effects of SAL and ICAR.

5. SAL, SalB and ICAR substantially abrogate H_2O_2-induced cell injury on BM-EPCs, contributing to their increased angiogenic ability.

6. SAL, SalB and ICAR suppress H_2O_2-provoked generation of ROS and expression of NADPH, and downregulate gene expression levels of Nox4 and eNOS. Furthermore, NADPH functions upstream of eNOS underlying the action of SalB.

7. Constitutive activation of MKK3/6 contributes to the baseline level of p38 MAPK activation that is independent of H_2O_2-triggered p38 MAPK phosphorylation in BM-EPCs.

8. SAL, SalB and ICAR protect mitochondrial function and inhibit mitochondrion-mediated apoptosis by decreasing cytochrome c release, inhibiting the cleavage of PARP, inactivating of caspase 3, and downregulating Bax/Bcl-xL ratio.

9. Maintenance of mTOR kinase and its downstream target 4EBP1 are responsible for the protective potential of ICAR on oxidation stressed-BM-EPCs. The loss of mTOR /4EBP1activity sensitizes BM-EPCs to p38 MAPK mediated apoptosis.

10. 4EBP1 controls caspase activation and modulates the proteins of Bcl-2 family thereby mediating the ability of SalB to block cell-injury activity caused by oxidative stress.

11. Elevated levels of 'uncoupled eNOS' derived from over-oxidation contributes to an increased degree of apoptotic and autophagic programmed cell death.

12. ICAR restores loss of mTOR/4EBP1 activity upon oxidative stress, which is associated with cell autophagy inhibition.

13. mTOR inhibition is associated with increased ERK1/2 activity in response to oxidative stress that mediats H_2O_2-induced autophagy.

14. p38 MAPK/ATF2 acts as a negative upstream signal pathway regulating mTOR-mediated apoptosis and autophagy during ROS accumulation. And p38 MAPK activation lies eNOS activity to induce apoptotic and autophagic cell death.

1. **Tang Y**; Huang B; Sun L; Peng X; Chen X; Zou X. Ginkgolide B promotes proliferation and functional activities of bone marrow-derived endothelial progenitor cells: involvement of Akt/eNOS and MAPK/p38 signaling pathways. Eur Cell Mater. 2011 May 28; 21: 459-69.

2. Huang S; **Tang Y (co-first author)**; Cai X; Peng X; Liu X; Zhang L; Xiang Y; Wang D; Wang X; Pan T. Celastrol inhibits vasculogenesis by suppressing the VEGF-induced functional activity of bone marrow-derived endothelial progenitor cells. Biochem Biophys Res Commun. 2012. 423(3): 467-72.

3. Huang S; Guo W; **Tang Y**; Ren D; Zou X; Peng X. miR-143 and miR-145 inhibit stem cell characteristics of PC-3 prostate cancer cells. Oncol Rep. 2012. 28(5): 1831-7.

4. Huang S; Peng L; **Tang Y**; Zhang L; Guo W; Zou X, Peng X. Hypoxia of PC-3 Prostate Cancer Cells Enhances Migration and Vasculogenesis *in vitro* of Bone Marrow-Derived Endothelial Progenitor Cells by Secretion of Cytokines. Oncol Rep. 2013. 29(6): 2369-2377.

5. Peng X; Guo W; Liu T; Wang X; Tu X; Xiong D; Chen S; Lai Y; Du H; Chen G; Liu G; **Tang Y**; Huang S; Zou X. Identification of miRs-143 and -145 that is associated with bone metastasis of prostate cancer and involved in the regulation of EMT. PLOS ONE. 2011. 6(5): e20341.

6. **Tang Y**, Vater C, Jacobi A, Liebers C, Zou X, Stiehler M. Salidroside exerts angiogenic and cytoprotective effects towards human bone marrow derived endothelial progenitor cells via Akt/mTOR/p70S6K and MAPK signaling pathways. Br J Pharmacology. 2014 May;171(9):2440-56.

7. **Tang Y**, Jacobi A, Vater C, Zou X, Stiehler M. Salvianolic acid B protects human endothelial progenitor cells against oxidative stress-mediated dysfunction by modulating Akt/mTOR/4EBP1, p38 MAPK/ATF2, and ERK1/2 signaling pathways. Biochemical pharmacology. 2014 Apr 26. [Epub ahead of print]

8. **Tang Y**; He P; Chen X; Zou X; Xu D; Huang S; Zhang L; Peng X; Huang S. Acidic Extracellular promotes metastasis of PC-3 cell and partly reduces PC-3 cell induced-vasculogenesis of EPC in vitro at a Tumor-Like Low pH. International journal of biochemistry & cell biology. Under review.

9. **Tang Y**, Jacobi A, Vater C, Stiehler M. Icariin prevents hydrogen peroxide-induced cellular dysfunction and autophagy in human endothelial progenitor cells: involvement of p38 MAPK/ATF2 and mTOR/4EBP1 signaling pathways. (In preparation)

Communication to scientific conferences:

1. Sixth SICOT (International Society of Orthopaedic Surgery and Traumatology)/SIROT Annual International Conference. Pattaya, Thailand, 2009. Number and functional activity of bone-marrow derived endothelial progenitor cells inversely correlate with degree of intervertebral disc degeneration. (Poster presentation)

2. SICOT Triennial World Congress. Prague, Czech Republic, 2011. The role of Akt/eNOS and MAPK/p38 signaling pathways in the proliferation and functional activities of bone marrow-derived endothelial progenitor cells. (selected for an oral presentation)

3. Symposium "Modern Application of Biotechnology". Dresden, Germany, 2013. Functionalization of CBA scaffolds / biomaterials with biomolecules by poly-L-lysine / hyaluronate. (selected for an oral presentation)

4. TERMIS (Tissue Engineering and Regenerative Medicine International Society). Istanbul, Turkey, 2013. Salidroside induces angiogenic differentiation and protects against oxidative stress in bone marrow derived-endothelial progenitor cells via Akt/mTOR/p70S6K and ERK1/2 pathways. (selected for an oral presentation)

Acknowledgements

Firstly, I would like to thank Prof. Klaus-Peter Günther and Prof. Michael Gelinsky for the revision of my thesis.

Many thanks to Dr. Maik Stiehler for the allocation of the topic, for the support, for the many possibilities he offered and for the nice informal atmosphere he created in the group.

I would like to express my deep gratitude to Dr. Angela Jacobi, for her supervision of my whole PhD study, for her constant support, illuminating instructions and great advices during my research work, and her helpful comments on my thesis.

I am really happy I could share my days in the lab with all the members of our group, Corina, Falk, Juline, Theresa, Conny, Shosha, it was a pleasure to work together!

I would like to thank my TFO members, for the nice suggestions and interest they showed to my projects.

I would like to thank the staff of the imaging facility of BIOTEC for being always ready to help.

I have a special thanks for all of you that, starting as colleagues, became my friends.
You made me feel that coming to the lab was always fun…and leave it even more!

Finally, I am deeply indebted to my husband, my parents, my whole family and my friends, for their constant support, loving considerations and great confidence in me all through these years.

Declaration

Declaration according to §8 Para. 7

I hereby declare that I have produced this paper without the prohibited assistance of third parties and without making use of aids other than those specified; notions taken over directly or indirectly from other sources have been identified as such. This paper has not previously been presented in identical or similar form to any other German or foreign examination board. The thesis work was conducted from April 2011 to May 2014, under the supervision of Dr. Angela Jacobi and Dr. Maik Stiehler at Medizinisch Theoretisches Zentrum in Dresden. I declare that I have not undertaken any previous unsuccessful doctorate proceedings.

Deklaration gemäß §8 Abs. 7

Hiermit versichere ich, dass ich die vorliegende Arbeit ohne unzulässige Hilfe Dritter und ohne Benutzung anderer als der angegebenen Hilfsmittel angefertigt habe; die aus fremden Quellen direkt oder indirekt übernommenen Gedanken sind als solche kenntlich gemacht. Die Arbeit wurde bisher weder im Inland noch im Ausland in gleicher oder ähnlicher Form einer anderen Prüfungsbehörde vorgelegt. Die Dissertation wurde von Dr. Angela Jacobi und Dr. Maik Stiehler, Medizinisch Theoretisches Zentrum Dresden betreut und im Zeitraum vom April 2011 bis Mai 2014, verfasst. Weiterhin erkläre ich, dass ich keine vorangegangenen erfolglosen Promotionsversuche unternommen habe.

Ort, Datum

Unterschrift des Doktoranden

Technische Universität Dresden
Medizinische Fakultät Carl Gustav Carus
Promotionsordnung vom 24. Juli 2011

Erklärungen zur Eröffnung des Promotionsverfahrens

1. Hiermit versichere ich, dass ich die vorliegende Arbeit ohne unzulässige Hilfe Dritter und ohne Benutzung anderer als der angegebenen Hilfsmittel angefertigt habe; die aus fremden Quellen direkt oder indirekt übernommenen Gedanken sind als solche kenntlich gemacht.

2. Bei der Auswahl und Auswertung des Materials sowie bei der Herstellung des Manuskripts habe ich Unterstützungsleistungen von folgenden Personen erhalten: Dr. Angela Jacobi, Dr. Maik Stiehler.

3. Weitere Personen waren an der geistigen Herstellung der vorliegenden Arbeit nicht beteiligt. Insbesondere habe ich nicht die Hilfe eines kommerziellen Promotionsberaters in Anspruch genommen. Dritte haben von mir weder unmittelbar noch mittelbar geldwerte Leistungen für Arbeiten erhalten, die im Zusammenhang mit dem Inhalt der vorgelegten Dissertation stehen.

4. Die Arbeit wurde bisher weder im Inland noch im Ausland in gleicher oder ähnlicher Form einer anderen Prüfungsbehörde vorgelegt.

5. Die Inhalte dieser Dissertation wurden in folgender Form veröffentlicht:
Tang Y; Huang B; Sun L; Peng X; Chen X; Zou X. Ginkgolide B promotes proliferation and functional activities of bone marrow-derived endothelial progenitor cells: involvement of Akt/eNOS and MAPK/p38 signaling pathways. Eur Cell Mater. 2011 May 28; 21: 459-69.

Tang Y, Vater C, Jacobi A, Liebers C, Zou X, Stiehler M. Salidroside exerts angiogenic and cytoprotective effects towards human bone marrow derived endothelial progenitor cells via Akt/mTOR/p70S6K and MAPK signaling pathways. Br J Pharmacology. 2014 May; 171(9): 2440-56.

Tang Y, Jacobi A, Vater C, Zou X, Stiehler M. Salvianolic acid B protects human endothelial progenitor cells against oxidative stress-mediated dysfunction by modulating Akt/mTOR/4EBP1, p38 MAPK/ATF2, and ERK1/2 signaling pathways. 2014 Apr 26. [Epub ahead of print]

6. Ich bestätige, dass es keine zurückliegenden erfolglosen Promotionsverfahren gab.

7. Ich bestätige, dass ich die Promotionsordnung der Medizinischen Fakultät der Technischen Universität Dresden anerkenne.

8. Ich habe die Zitierrichtlinien für Dissertationen an der Medizinischen Fakultät der Technischen Universität Dresden zur Kenntnis genommen und befolgt.

9. Ich bin mit dem Kodex für gute wissenschaftliche Praxis und den Umgang bei wissenschaftlichem Fehlverhalten einverstanden. Die Gremien der Medizinischen Fakultät behalten sich vor, stichpunktartige Kontrollen der Dissertation vorzunehmen.

Ort, Datum
Unterschrift des Doktoranden

Hiermit bestätige ich die Einhaltung der folgenden aktuellen gesetzlichen Vorgaben im Rahmen meiner Dissertation

- ☐ das zustimmende Votum der Ethikkommission bei Klinischen Studien, epidemiologischen Untersuchungen mit Personenbezug oder Sachverhalten, die das Medizinproduktegesetz betreffen
  Aktenzeichen der zuständigen Ethikkommission: EK263122004.

- ☐ die Einhaltung der Bestimmungen des Tierschutzgesetzes
  Aktenzeichen der Genehmigungsbehörde zum Vorhaben/zur Mitwirkung:

  Protocol no. 24-9168.11-1/2010-29

- ☐ die Einhaltung des Gentechnikgesetzes
  Projektnummer

- ☐ die Einhaltung von Datenschutzbestimmungen der Medizinischen Fakultät und des Universitätsklinikums Carl Gustav Carus.

Ort, Datum

Unterschrift des Doktoranden